



## **DOTTORATO DI RICERCA IN CHIMICA**

**Convenzione tra  
UNIVERSITÀ DEGLI STUDI DI TRIESTE  
e  
UNIVERSITÀ CA' FOSCARI DI VENEZIA**

**CICLO XXXV**

**New insights in the enzymatic upgrade of lignin: from  
added value compounds to tunable nanoparticles**

Settore scientifico-disciplinare: **CHIMICA GENERALE E INORGANICA (CHIM/03)**

**DOTTORANDO  
NICOLÒ PAJER**

**COORDINATORE  
PROF. ENZO ALESSIO**

**SUPERVISORE DI TESI  
PROF. CLAUDIA CRESTINI**

**ANNO ACCADEMICO 2021/2022**



*“... col sangue sulle mani scalerò tutte le vette,  
voglio arrivare dove l’occhio umano si interrompe...”*  
(Måneskin, “Torna a casa”)

# Index

<b>A note on the nomenclature of lignin .....</b>	<b>5</b>
<b>1. Lignins: an overview on their chemistry, laccase-catalysed modification, and potential applications .....</b>	<b>6</b>
<b><i>1.1. Wood constitution and composition .....</i></b>	<b>6</b>
1.1.1 Cellulose: a crystalline cellobiose-based homopolymer .....	7
1.1.2 Hemicelluloses: hetero-polymeric sugars .....	9
1.1.3 Lignin: the most abundant aromatic biopolymer .....	12
<b><i>1.2. Lignin isolation from wood.....</i></b>	<b>20</b>
<b><i>1.3. Methods for structural elucidation of lignin.....</i></b>	<b>25</b>
1.3.1 Nitrobenzene oxidation .....	26
1.3.2 Permanganate oxidation.....	28
1.3.3 Acidolysis and thioacidolysis.....	30
1.3.4 Spectroscopic techniques in lignin chemistry .....	33
1.3.4.1 Traditional NMR analyses in lignin.....	34
1.3.4.2 2D NMR analyses .....	38
1.3.4.3 <sup>31</sup> P NMR: the key for the fast and reliable analysis of reactive groups in lignin.....	40
<b><i>1.4. Kraft lignin: a focus on the chemistry of the most important technical lignin .....</i></b>	<b>43</b>
1.4.1 Reactions occurring during pulping .....	43
1.4.2 On the structure of Kraft lignin.....	47
<b><i>1.5. On the actual promising pathways for the valorisation of lignin .....</i></b>	<b>50</b>
<b><i>1.6. Lignin nanoparticles: small size, high-value applications .....</i></b>	<b>51</b>
<b><i>1.7. Tailoring the properties of lignin preparations via the use of laccases. An evergreen in lignin chemistry.....</i></b>	<b>53</b>
1.7.1 Which are the lignin degrading microorganisms and what do they have in common? ....	54
1.7.2 On the structure of laccase .....	56

1.7.3 On the action of laccase on phenolic substrates.....	57
1.7.4 Laccase redox-mediators: overcoming the energetic barrier to oxidise non-phenolic substrates.....	60
<b>2. Aim of the research .....</b>	<b>64</b>
<b>3. How do laccases modify the structure of technical lignins? .....</b>	<b>65</b>
<b>3.1. Introduction.....</b>	<b>65</b>
<b>3.2. Results and discussion .....</b>	<b>66</b>
3.2.1 Fractionation of technical lignins.....	66
3.2.2 Identification of the optimum pH for ABTS test .....	70
3.2.3 Evaluation of the role of pH on the conversion of lignin model compounds .....	75
3.2.4 Set up of the enzymatic reactions: general assumptions, calculations, and considerations .....	78
3.2.5 Characterisation of low molecular weight lignin oxidation products .....	80
3.2.6 Residual lignin after laccase treatments: structural characterization .....	88
<b>3.3. Experimental part.....</b>	<b>100</b>
3.3.1 Lignin fractionation.....	100
3.3.2 Spectrophotometric determinations of laccase activity via ABTS .....	100
3.3.3 Preparation of apocynol 4-(1-hydroxyethyl)-2-methoxyphenol.....	101
3.3.4 Preparation of 4-(1-hydroxyethyl)-2,6-dimethoxyphenol.....	101
3.3.5 Laccase test of lignin model compounds .....	102
3.3.6 Enzymatic treatments of lignins.....	102
3.3.7 GC-MS analyses of low molecular weight compounds from lignin enzymatic oxidation .....	103
3.3.8 <sup>31</sup> P NMR analyses of the laccase modified lignins .....	103
3.3.9 GPC analyses of the enzymatically modified lignin .....	103
<b>3.4. Conclusions .....</b>	<b>104</b>
<b>4. Combined lignin fractionation/laccase modification in the development of with tailored size and hydrophobicity.....</b>	<b>106</b>

<b>4.1 Introduction</b> .....	106
<b>4.2 Results and discussion</b> .....	107
4.2.1 Design of a stream for tailoring lignin nanoparticles properties.....	107
4.2.2 Lignin fractionation.....	108
4.2.3 Preparation of AKL KLNPs.....	112
4.2.3 On the effect of the tandem system on KLNPs size .....	114
<b>4.3. Experimental part</b> .....	118
4.3.1 Isolation of lignin fractions .....	119
4.3.2 Enzymatic modification of lignin preparations.....	119
4.3.3 Characterisation of lignin preparations .....	119
4.3.4 Preparation of KLNPs via the hydrotropic method .....	119
4.3.5 Characterisation of lignins after fractionation and enzymatic modification.....	120
4.3.6 Dynamic light scattering analyses (DLS) .....	120
4.3.7 Zeta-potential analyses ( $\zeta$ -potential) .....	120
<b>4.4 Conclusions</b> .....	121
<b>5. Creating new networks with laccase: enzymatic deposition of angiosperm Kraft lignin nanoparticles on lignin-rich nanofibrillated cellulose</b> .....	<b>122</b>
<b>5.1. Introduction</b> .....	122
<b>5.2. Results and discussion</b> .....	123
5.2.1 Evaluation of KLNPs pH-stability.....	123
5.2.2 Preparation of CNFs from unbleached pulp and optimisation of the casting process for the preparation of films .....	124
5.2.3 Preparation of CNFs from unbleached pulp and optimisation of the casting process for the preparation of films .....	125
5.2.4 Laccase-mediated deposition of KLNPs.....	131
5.2.5 Preparation of CNFs from unbleached pulp with enzymatically deposited KLNPs.....	133
5.2.6 On the plasticity of unbleached CNFs films with enzymatically deposited KLNPs .....	137

<b>5.3. Experimental part</b> .....	139
5.3.1 Preparation of AKL KLNPs.....	139
5.3.2 Preparation of CNFs from unbleached pulp via ultra-grinding .....	139
5.3.3 Casting operation of CNFs films with deposited AKL KLNPs.....	139
5.3.4 Casting operation of CNFs films with enzymatically deposited AKL KLNPs .....	140
5.3.5 Thermogravimetric analyses of CNFs films with AKL KLNPs.....	140
5.3.6 Tensile tests for CNFs films with AKL KLNPs .....	140
<b>5.4. Conclusions</b> .....	141
<b>References</b> .....	<b>143</b>

## A note on the nomenclature of lignin

Lignin structure is commonly simplified by the use of models. In general, these simplifications contain aliphatic and aromatic domains. From one side, the aliphatic part is frequently schematised by the use of an substituted propanoic structure. From the other side, the aromatic domain is represented by an aromatic ring adorned with at least one oxygen atom (as a free hydroxyl group or as part of an ether bond); additional methoxy groups can appear too in the aromatic ring.

With regards to the nomenclature/numeration of the carbons constituting these models, and more generally lignin-like compounds, two systems have been devised, as summarised in Fig.0.1.

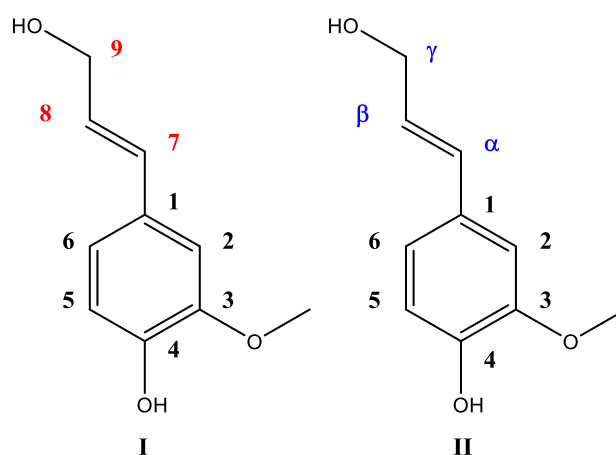


Figure 0.1. Nomenclature/numeration systems used in Lignin Chemistry applied to coniferyl alcohol structure.

IUPAC system recommends the use of number to refer to either the aliphatic or the aromatic domains (Fig. 0.1 I). In particular, C1 atom is associated with the aromatic carbon atom linked with the aliphatic chain; the atoms constituting the latter are indicated as C7, C8, and C9. Lignin community prefers the use of the traditional system (Fig. 0.1 II), which was strongly recommended by *Karl Freudenberg*, the founder of modern Lignin Chemistry.<sup>1</sup> The traditional system relies on the usage of Greek letters for aliphatic carbons, while Arabic numerals are applied to refer to atoms constituting the aromatic ring. In particular, with regard to the aliphatic domain, C7, C8, and C9 are indicated as C $\alpha$ , C $\beta$ , and C $\gamma$ .

In this thesis, the traditional nomenclature (Fig. 0.1 II) is followed.



# 1. Lignins: an overview on their chemistry, laccase-catalysed modification, and potential applications

*In this Chapter an introduction on the chemistry of lignin is provided. A general introduction on the relevant features of the three most abundant biopolymers constituting woody biomass is provided with a specific focus on lignin and its structure. The various methodology to isolate lignin from wood, as well as review of the traditional techniques to study its structure are then mentioned. A description of the nature of Kraft lignin is then provided, with regards on both its structure and the chemistry of Kraft pulping. Then, an overview of the most promising applications for technical lignins is depicted, with specific regard to lignin nanoparticles. Finally, the importance of tailoring the property of lignin prior to its nanosizing is discussed, and the use of laccases in view of that is critically discussed.*

## 1.1. Wood constitution and composition

Lignocellulosic biomass is primarily constituted by three polymers, cellulose, hemicelluloses, and lignin. Depending on the nature of the biomass, the composition in terms of these polymers varies as shown in Table 1.1. Not only the *clade* affect the composition of lignocellulosic; in fact, also the *family* and the *genus*, as well as the harvesting period and the geographical localisation of the cultivation contribute to the variability. Moreover, for both dicotyledon angiosperms and gymnosperms, the most abundant constituent is represented by cellulose, followed by lignin.

*Table 1.1* Ranges of chemical composition of dicotyledon angiosperms and gymnosperms. By referring to holocellulose, the sum of both cellulose and hemicelluloses is considered.<sup>2</sup>

	<i>Holocellulose</i> (%)	<i>Cellulose</i> (%)	<i>Pentosans</i> (%)	<i>Lignin</i> (%)	<i>Ashes</i> (%)
<i>Dicotyledon angiosperms</i>	71.7±5.7	45.4±3.5	19.3±2.2	23.0±3.0	0.5±0.3
<i>Gymnosperms</i>	64.5±4.6	43.7±2.6	9.8±2.2	28.8±2.6	0.3±0.1

The heterogeneity in composition coupled with the intrinsic variability of lignocellulosic biomass represent two critical point limiting the use of wood as a source of fine chemicals.

Wood has been considered as a energy source for the human from the very beginning of humanity, moreover the first examples of paper production, the nowadays most important wood-derivative,

seem to date to the 1<sup>st</sup> Century BC. Those were just the rudiments of the pulping industry; in fact, only during the 19<sup>th</sup> Century chemical and mechanical pulping industries started appearing in Europe. In perspective, it can be considered that the rise of pulping industry was the result of the coupling of empirical knowledges on wood with the then current spread of chemical engineering and organic chemistry.

If at the beginning of the pulping industry cellulose was the only interesting product from wood, nowadays the reality has drastically changed. In fact, today lignocellulosic biomass is considered not only as a cellulose-related products sources, but also as a starting point for the production of high-value low molecular weight products, which can be obtained via fermentative (e.g. ethanol) or catalytic depolymerisation (e.g. vanillin), or for preparation of energy feedstocks (e.g. pyrolysis oils). In order to provide an overview of the properties of the polymers constituting lignocellulosic biomass, and especially wood, a brief description on their chemistry and reactivity is provided in the following paragraphs.

### **1.1.1 Cellulose: a cellobiose-based homopolymer**

Cellulose is undoubtedly the most important wood-derived polymer and its potential has been being widely exploited. In fact, owing to its chemical and physical properties, cellulose has been applied not only for the fabrication of paper and its derivatives, but also, more recently, for the production of plastics (e.g. cellulose acetate), synthetic fibres (e.g. cuprammonium rayon), or technological materials replacing oil-based products (e.g. packaging foams).

From a chemical point of view, cellulose is the polycondensation product of cellobiose. Cellobiose is a disaccharide originated from the condensation of two glucopyranosidic units; the monosaccharidic units are bonded together via an ether bond. This bond is referred as glycosidic bond and derives from the hydroxyl groups in position C1 and C4 of two different glucopyranosidic units.

An interesting feature of cellulose is represented by its crystallinity. This property was firstly postulated by *Nägeli* during the 19<sup>th</sup> Century. Almost one century before, due to the development of X-ray crystallography, *Meyer* validated the *Nägeli* hypothesis on cellulose cristallinity.<sup>3,4</sup> Interestingly, not only one crystallographic form of cellulose exists. In fact, as of now seven polymorphs of cellulose have been identified and fully characterised.<sup>5</sup> Of them, only two allotropes can be found in nature, respectively  $I_{\alpha}$  and  $I_{\beta}$ . These two polymorphs differ one from the other for the packing of cellobiose chains. By considering Fig.1.1, where cellobiose units are schematised as light-green ovals, it can be noticed that in the case of  $I_{\beta}$  there is a parallel orientation of the cellobiose units

along the parallel unit cell axis; additionally, its *Bravais* lattice is of single triclinic type. In the case of  $I_\alpha$ , cellobiose units are parallel according to the diagonal and, while the *Bravais* lattice is of two chain-monoclinic unit type.

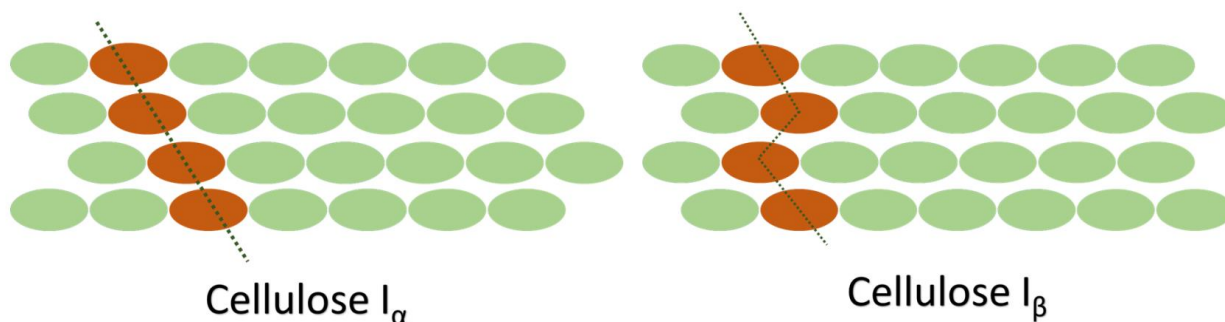


*Figure 1.1.* Schematisation of the packing of the cellobiose units in the most important cellulose allotropes.

The other polymorphs of cellulose, namely II, III<sub>α</sub>, III<sub>β</sub>, IV<sub>α</sub>, and IV<sub>β</sub>, result from the chemical modification of the polymorphs of cellulose I.

With regard to the reactivity of cellulose, the glucopyranosides are characterised by the presence of three free hydroxyl groups, two of them are of secondary type, while one of them is of primary type. The rate of functionalisation reaction of these hydroxylated moieties varies according to their type as well as with the degree of functionalisation. In particular, these hydroxyl groups can be conveniently derivatised resulting in new platform chemicals which find applications as they are (*e.g.* textile industry) or as intermediates for the introduction of other cellulose-preparations (*e.g.* chlorination or azidation). From the industrial and historical point of view, particular relevance has always been given to derivatising procedures like acetylation (cellulose acetate)<sup>6,7</sup>, nitration (cellulose nitrate), and etherification<sup>8,9</sup>. From the lab-scale, azidation, halogenation, and trytylation processes can be seen now as promising strategies for the functionalisation of cellulose via the subsequent use of click-chemistry based reactions.

In recent years, it has been demonstrated that not only the use of derivatisation procedures can be considered as a valuable strategy to valorise cellulose. In particular, this polysaccharide has been considered as a promising starting point for the preparation of nanomaterials, like cellulose nanocrystals and nanofibrils; these nanomaterials are nowadays considered as potential materials for the industry owing to their interesting mechanical, optical, and filmability properties.

### 1.1.2 Hemicelluloses: hetero-polymeric sugars

Hemicelluloses are polysaccharides representing up to the 32.4% of wood. From a chemical point of view, they can be seen as the condensation products of various pyranosidic and furanosidic sugars. Despite of cellulose, these polysaccharides are highly decomposed during pulping operations. In fact, hemicelluloses are more likely to undergo hydrolysis if compared to cellulose. This consideration was at the basis of all the studies made during the Sixties by chemists investigating their composition. In particular, their extraction from wood followed by their hydrolysis was used to obtain the monomeric units constituting them. Then, the quantification of the sugars obtained, resulting in the composition in terms of monosaccharides of hemicelluloses, used to be performed after their methylation, via gas-chromatographical analyses. Because of the natural variability of the sugars that can be condensed in hemicelluloses a plethora of hemicelluloses exists.

Generally, the most abundant hemicelluloses in wood belong to two major groups: glucomannans and xylans.<sup>10</sup> Glucomannans are mainly composed by glucopyranosidic and mannopyranosidic units linked together via  $\beta$ -(1-4) linkages; xylans derive from the condensation of xylanopyranosidic units via the same type of bond existing in glucomannans.

The major hemicelluloses in gymnosperms are glucomannans; these polysaccharides contain glucopyranosyl and mannopyranosyl units linked via  $\beta$ -(1-4) linkages as shown in Fig. 1.2. Random acetylation can be noticed in the C3 and C5 positions.

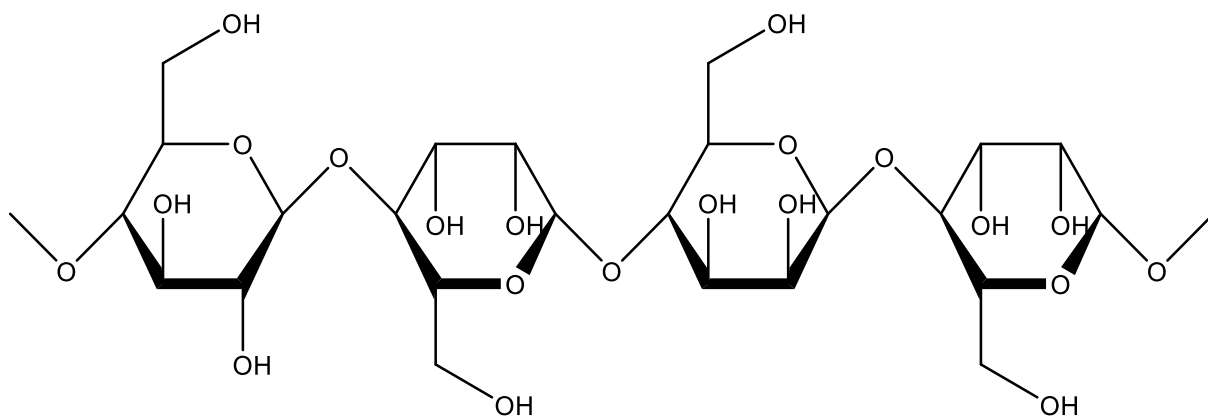


*Figure 1.2.* Typical bonding patterns for a galactoglucomannan; the model contains mannopyranosyl and glucopyranosyl units linked via a  $\beta$ -(1-4) ether linkage.

In some gymnosperm glucomannans, occasional branchings with galactopyranosyl units occur alongside the chain via  $\alpha$ -(1-6) bondings, as shown in Fig. 1.3.

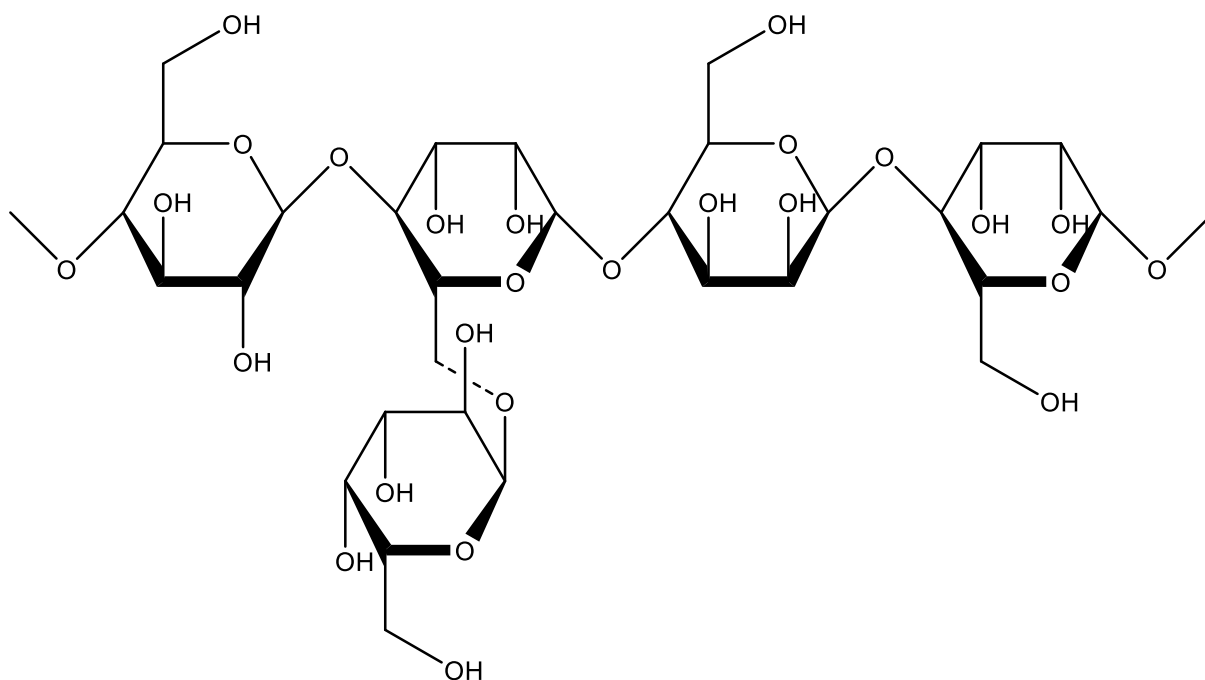


*Figure 1.3.* Galactopyranosyl bond in gymnosperm glucomannans.

Two classes of galactoglucomannans have been distinguished: highly- and low-galactopyranosyl-branched ones. Highly-galactopyranosyl-branched galactoglucomannans are characterised by the ratio of galactopyranosyl:glucopyranosyl:mannopyranosyl approximately 1:1:3/4, while the low-galactopyranosyl-branched ones are characterised by ratio galactopyranosyl:glucopyranosyl:mannopyranosyl of approximately 0.1:1:3/4. Because of the poor branching, galactoglucomannans are poorly soluble in water.

While glucomannans are the most important hemicelluloses in gymnosperms, they are available only in limited amounts in dicotyledon angiosperms. In addition, the difference between dicotyledon angiosperm and gymnosperm glucomannans is represented by the presence of GAL units in gymnosperm ones.

In the case of dicotyledon angiosperms, the most abundant hemicelluloses are xylans, which are characterised by a backbone of xylanopyranosyl units linked via  $\beta$ -(1-4). The example of bonding patterns in an angiosperm xylan is depicted in Fig. 1.4. Acetylation in C2 and C3 positions commonly occurs in angiosperm xylans.

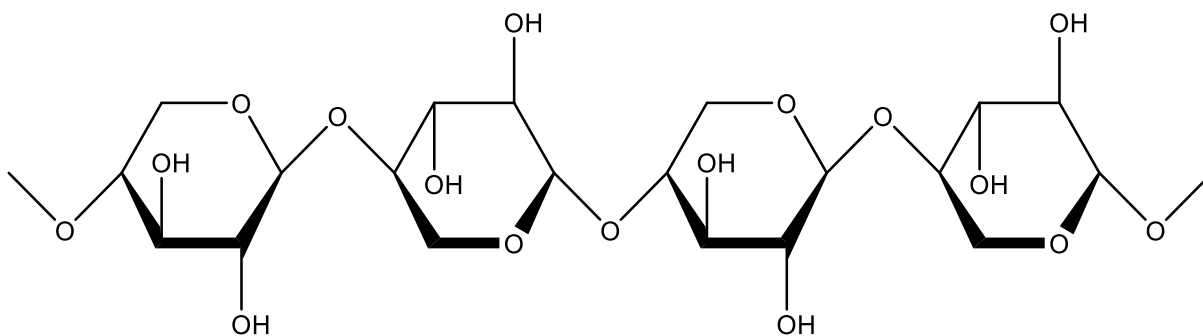


*Figure 1.4.* Typical bonding pattern in a dicotyledon angiosperm xylan. Xylanopyranosyl units are linked via ether  $\beta$ -(1-4) linkages.

Almost every 8 to 20 xylanopyranosyl units, xylanopyranosyl units exhibit branchings with methyl glucuronic acid as depicted in Fig. 1.5.

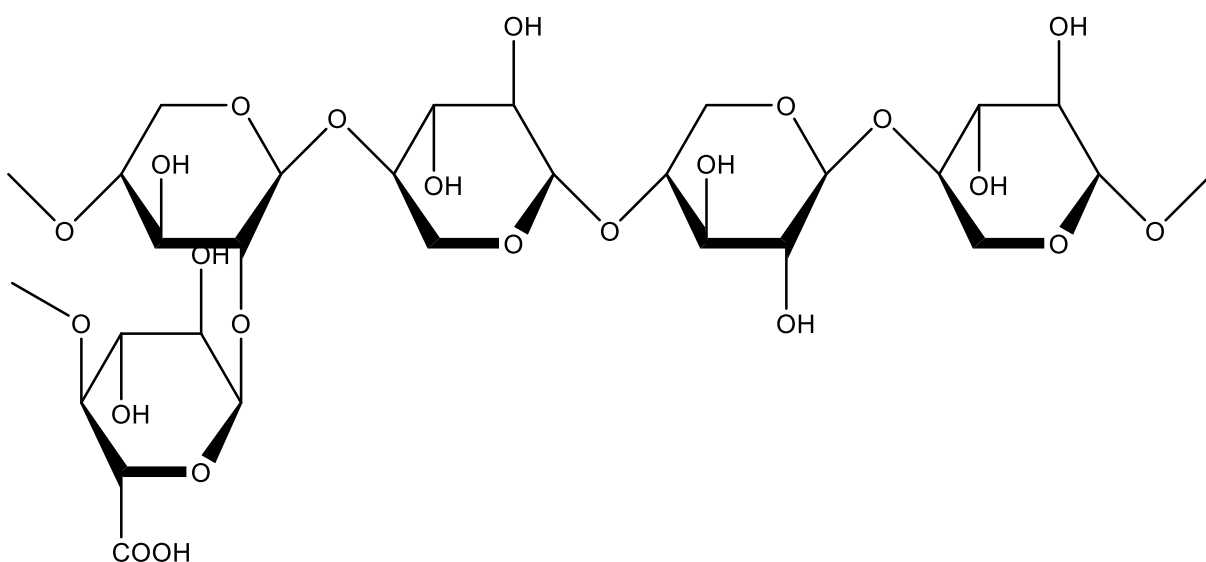


*Figure 1.5.* Methylated glucuronic-acid branching in xylans.

The major difference between gymnosperms' and dicotyledon angiosperms' xylans is represented by the degree of substitution with methyl-glucuronic acid. In fact, gymnosperms' xylans are more branched with methyl-glucuronic acid (substitution every 5 to 6 units); this fact results in a higher acidity if compared to that of dicotyledon angiosperms.

### 1.1.3 Lignin: the most abundant aromatic biopolymer

Lignin is for sure the most interesting biopolymer among those considered in the previous paragraphs. In fact, its structure and reactivity remain debatable topics and researches trying to provide definitive answers to the so many questions on its nature are still on going since almost two century.

From a chemical point of view, lignin can be considered as a polymer deriving from the enzyme-catalysed polymerisation of three alcohols, p-coumaryl (I), coniferyl (II), and synapyl alcohol (III) (Fig.1.6).<sup>11</sup>

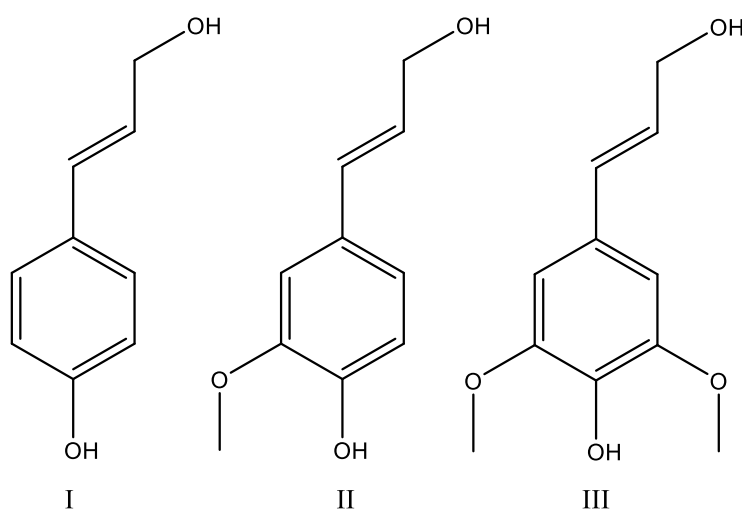


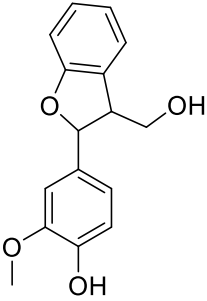
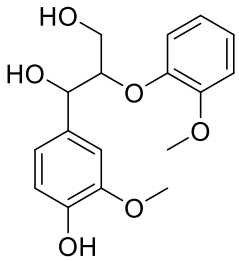
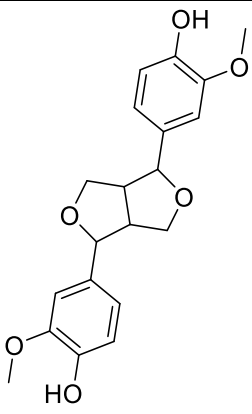
Figure 1.6.. Monolignols: (I) p-coumaryl, (II) coniferyl, and (III) synapyl alcohols.

These three alcohols are generally referred to as *monolignols*. All the three monolignols are not always present in lignins. In fact, it was demonstrated that lignin samples from dicotyledon angiosperms contain both coniferyl and synapyl alcohol, while lignins from gymnosperms are almost only constituted by coniferyl alcohol with traces of synapyl alcohol. Lignins from grasses represent an exception, as they contain all the three monolignols.

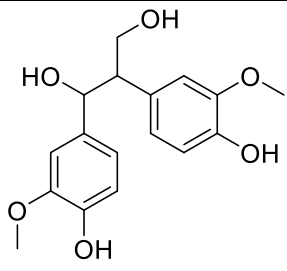
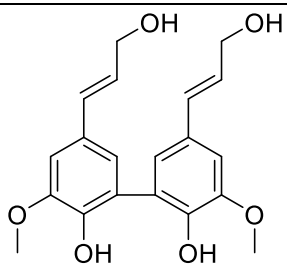
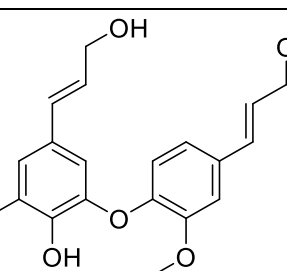
Monolignols cannot be considered only as alcohols. In fact, they are characterised by the presence of four types of functional groups imparting a wider reactivity. These functionalities include (a) the phenolic hydroxyl group, (b) the aromatic ring, (c) the conjugated double bond to the aromatic ring, and (d) the terminal aliphatic hydroxyl group. In addition to those functional groups, the presence of zero, one, or two methoxy groups in *m*- position in the aromatic ring differentiates the three alcohols. The enzyme-catalysed polymerisation of monolignols is a process occurring at the end of the life cycle of cells in plants, and is defined as *end-wise random polymerisation*. This mechanism is based on four steps: (1) the enzyme-catalysed (laccases or peroxidases) conversion of monolignols into

aryloxy radicals, (b) the stabilisation of the aryloxy radical via mesomeric forms distributing the single electron on the aromatic ring and on the aliphatic chain of the monolignol, (c) the radical coupling of aryloxy/phenoxy/quinone methide radicals, and finally (d) the quenching of the high-energy intermediated deriving from the coupling. Due to the existence of various mesomeric forms of the aryloxy radicals, the radical coupling allow the creation of various types of bonding patterns. The most popular one are summarised in Tab.1.2; in the same table the abundancies of the various bonding patterns in different types lignins are also listed.

*Table 1.2* Percentage abundances of the various bonding patterns occurring in lignins from various types of lignocellulosic biomass.

Bonding pattern	Bonding pattern name	Linkage pattern	Dicotyledon angiosperm	Gymnosperm	Grass
	phenylcoumarane	$\beta$ -5'	3-11	9-12	5-11
	guaiacyl-glycerol- $\beta$ -guaiacyl ether	$\beta$ -O-4'	50-65	45-50	69-94
	pinoresinol	$\beta$ - $\beta$ '	3-12	2-6	1-15



	$\beta$ -guaiacyl guaiacyl-glycerol	$\beta$ -1'	1-7	1-10	0-2
	biphenyl	5-5'	1-5	5-25	unknown
	diaryl-ether	4-O-5'	6-7	4-8	unknown

Owing to the different stabilities of the intermediates resulting from the radical coupling, a statistical distribution of the different types of bonding pattern can be noticed. Among them, the most abundant in lignins from various types of lignocellulosic biomasses is represented by the *guaiacyl-glycerol- $\beta$ -guaiacyl ether*. Its formation from coniferyl alcohol can be used to concretise the mechanism end-wise polymerisation previously mentioned. Firstly, the coniferyl alcohol is enzymatically converted into its aryloxy radical, resulting in the coniferyl radical (Fig.1.7).

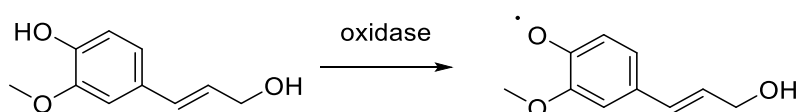


Figure 1.7. Enzyme-catalysed conversion of coniferyl alcohol into an aryloxy radical.

Then, the phenoxy radical is stabilised via the  $\pi$  system (Fig. 1.8).

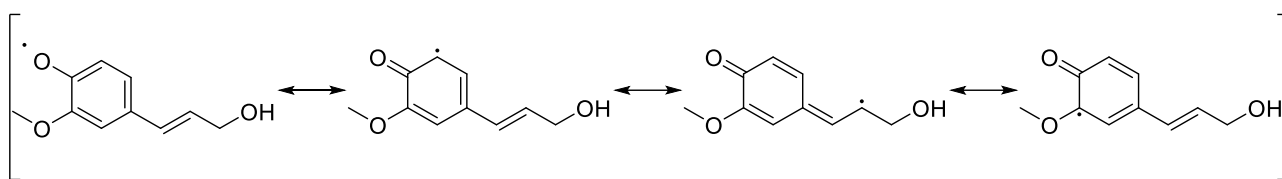


Figure 1.8. Stabilisation of phenoxy-form of coniferyl alcohol via mesomeric forms.

The quinomethide radical undergoes radical coupling with a phenoxy radical (Fig. 1.9).

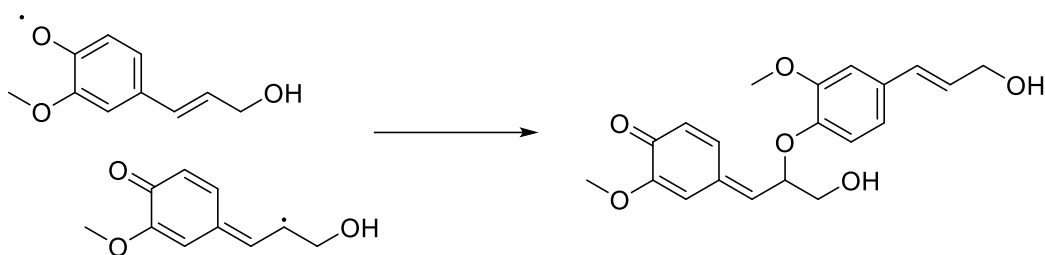


Figure 1.9. Radical coupling of phenoxy- and quinonemethide-forms of coniferyl alcohol.

Finally, the residual quinomethide is quenched by water generating the guaiacyl-glycerol- $\beta$ -guaiacyl-ether (Fig. 1.10).

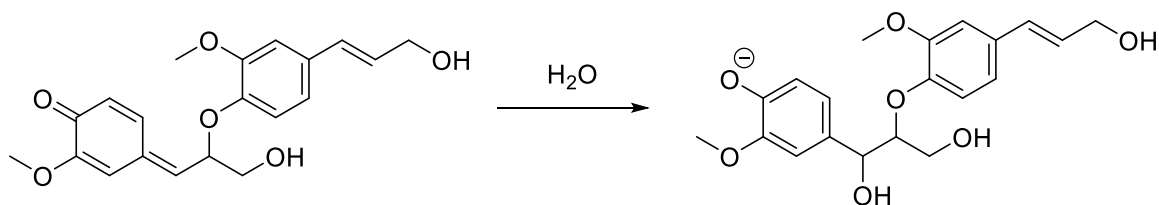


Figure 1.10. Quenching of radical coupling product with water.

Because of the intrinsic nature of the randomic end-wise polymerisation of monolignols, it is not surprising to observe that it is impossible to isolate the same lignin from different plants, even if they the samples are collected from the same specie.

Attempts to depict a general scheme rationalising the reactivity and structural data available on lignin have always been a challenge for lignin chemists. All the efforts that have been made since the beginning of the modern era of lignin chemistry have been based on the lignin of pine as reference point. The reason for this *a priori* choice is attributed to the relatively simpler chemical composition

(and, consequently, structure) of pine lignin if compared to those of dicotyledon angiosperms or grasses (vide infra, [Paragraph 1.3.1](#)).

The first models for pine lignin were provided by *Klason, Brauns, Adler, and Freudenberg*.<sup>12-18</sup> In particular, the structures suggested by *Adler and Freudenberg* were particularly valuable, as they were in good accordance with the experimental data available at the time resulting from the application of wet-chemistry techniques on lignin. Interestingly, even if the schemes of these *Authors* are from the Sixties of 20<sup>th</sup> century, they contain all the bonding patterns reported in Tab.1.2.

The most common bonding patterns in lignin are divided in two classes, namely condensed and non-condensed structures. The existence of these structures in lignin samples was revealed by the usage of wet-chemistry characterisation techniques like nitrobenzene or permanganate oxidations or acidolysis. (vide infra, [Paragraph 1.3](#)). Non-condensed structures include *phenylcoumarane*, *pinoresinol*, and  $\beta$ -*guaiacyl guaiacyl-glycerol* bonding patterns and their genesis resemble the one of *guaiacyl-glycerol- $\beta$ -guaiacyl ether* bonding pattern previously described. The difference in the type of mesomeric forms participating to the radical coupling step and the type of quenching (external or internal). In the case of *phenylcoumarane*, the radical coupling occurs between quinomethide and a C5 radical with an internal quench (Fig. 1.11).

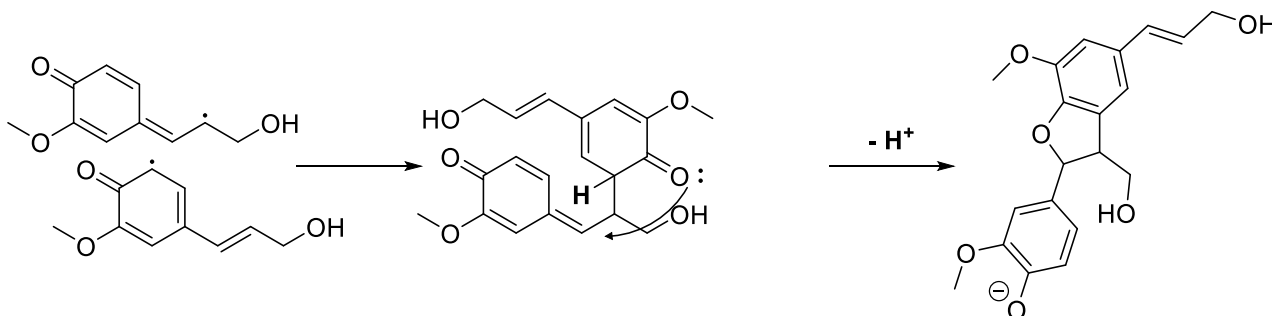


Figure 1.11. Formation of *phenylcoumarane* bonding pattern from coniferyl alcohol radicals.

In the case of *pinoresinol*, the radical coupling involves two quinomethide; the quench is internal, via the hydroxyl group in  $\gamma$ -position (Fig. 1.12).

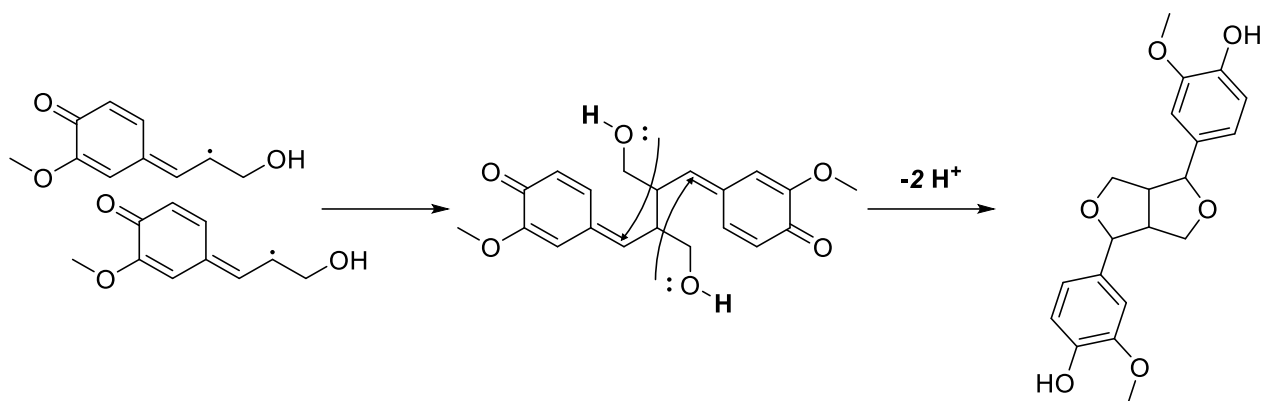


Figure 1.12. Formation of *pinoresinol* bonding pattern from coniferyl alcohol radicals.

$\beta$ -*guaiacyl guaiacyl-glycerol* bonding pattern results from the coupling of a C1 radical with a quinomethide; the quench process is the result of the dealkylation of the structure bearing the radical in C1 (Fig. 1.13).

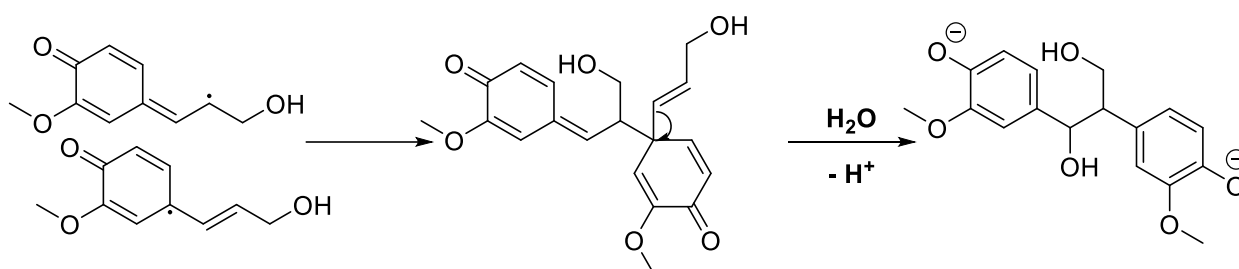


Figure 1.13. Formation of  $\beta$ -*guaiacyl guaiacyl-glycerol* bonding pattern from coniferyl alcohol radicals.

Condensed structures are primarily represented by *diaryl ethers* and *biphenyls*. Similarly to non-condensed structures, condensed bonding patterns derive from the radical coupling followed by the quench. In the case of *diaryl ethers*, the radical coupling involves an aryloxy radical and a C5 radical (Fig. 1.14).

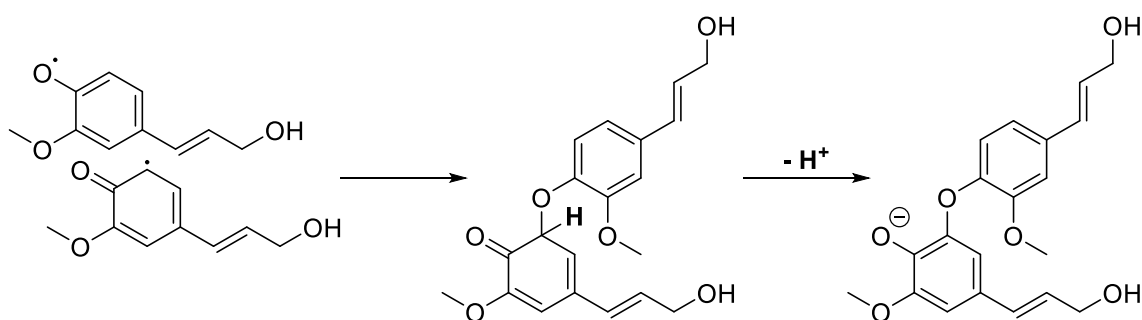


Figure 1.14. Formation of *diaryl ether* bonding pattern from coniferyl alcohol radicals

While in the case of *biphenyls*, two C5 radicals undergoes the coupling step followed by the elimination of a couple of hydrogen atoms restoring the aromaticity of the aromatic rings according to the following mechanism (Fig. 1.15):

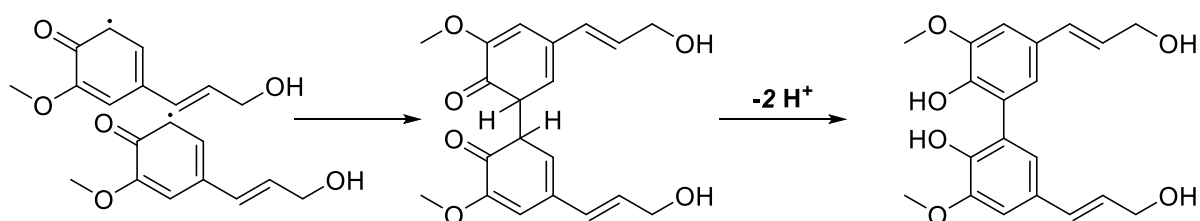
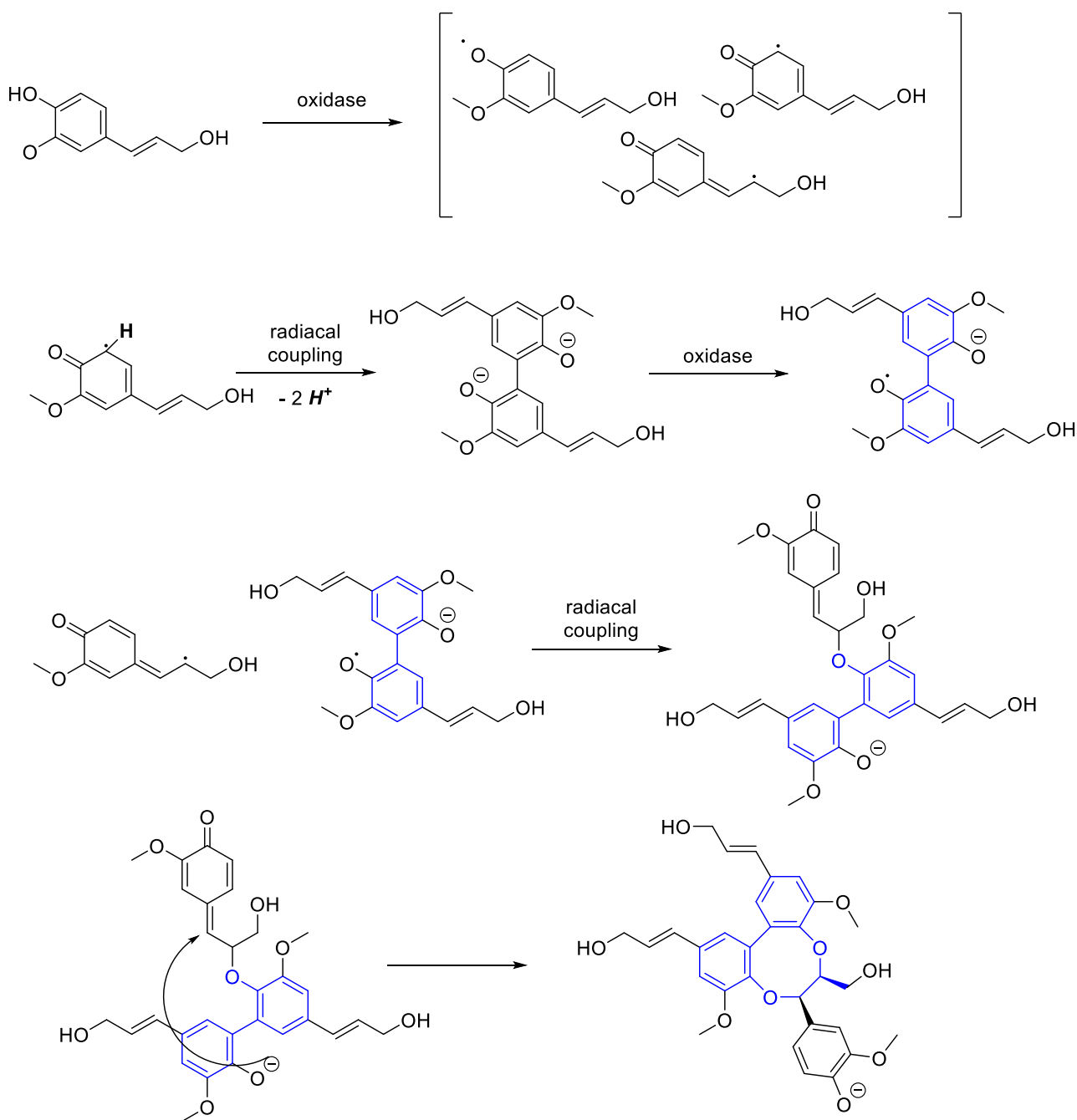


Figure 1.15. Formation of *diaryl ether* bonding pattern from coniferyl alcohol radicals

Traditional methods for studying lignin structure (see [Paragraphs 1.3.1 to 1.3.3](#)) were undermined from the end of the Eighties in favour to instrumental techniques. In particular, the use of spectroscopic techniques, especially nuclear magnetic resonance, has become pivotal in the work of modern lignin chemist. This extremely powerful tool permitted to confirm the existence of all the bonding patterns revealed by *Adler* and *Freudenberg* and also permitted to discover new ones. With that regard, the identification of dibenzodioxocyn (DBDO) pattern by *Brunow* was particularly relevant.<sup>19-21</sup>



*Figure 1.16.* Dibenzodioxocyn biosynthesis from biphenyl units and coniferyl alcohol via peroxidase activation of phenolic substrates.

The presence of DBDO in lignin, whose biosynthetic pathway is summarised in Fig.1.16, has been considered for a long time a proof demonstrating the branched nature of lignin in plants. In the point of view of the supporters of this theory, the presence of the hydroxyl groups in C4 position would play a role in the formation of additional linkages in lignin, creating a network point for three lignin chains. Moreover, more recently, the nature of DBDO as branching point was critically questioned

by *Crestini*.<sup>22</sup> In fact, by coupling bidimensional NMR techniques, <sup>31</sup>P NMR analyses, and derivatisation followed by reductive cleavage data on lignin, she developed a methodology to study the branching and the condensation degree of lignin preparations. The most interesting aspect of her research is represented by the fact that she concluded that biphenyls, as well as diphenyl ethers, are present in lignin only as terminal groups. This observation led to the conclusion that DBDO does not act as a branching site, but just as an additional bonding pattern which laterally adorns the linear chain constituted by the structures mentioned in Tab.1.2. According to her finding, *Crestini* developed a model rationalising her findings and taking in consideration all the available spectroscopic data on lignin. This model is depicted in Fig.1.17 and it is now the most credited structure, as it is fully in accordance with the existing literature.

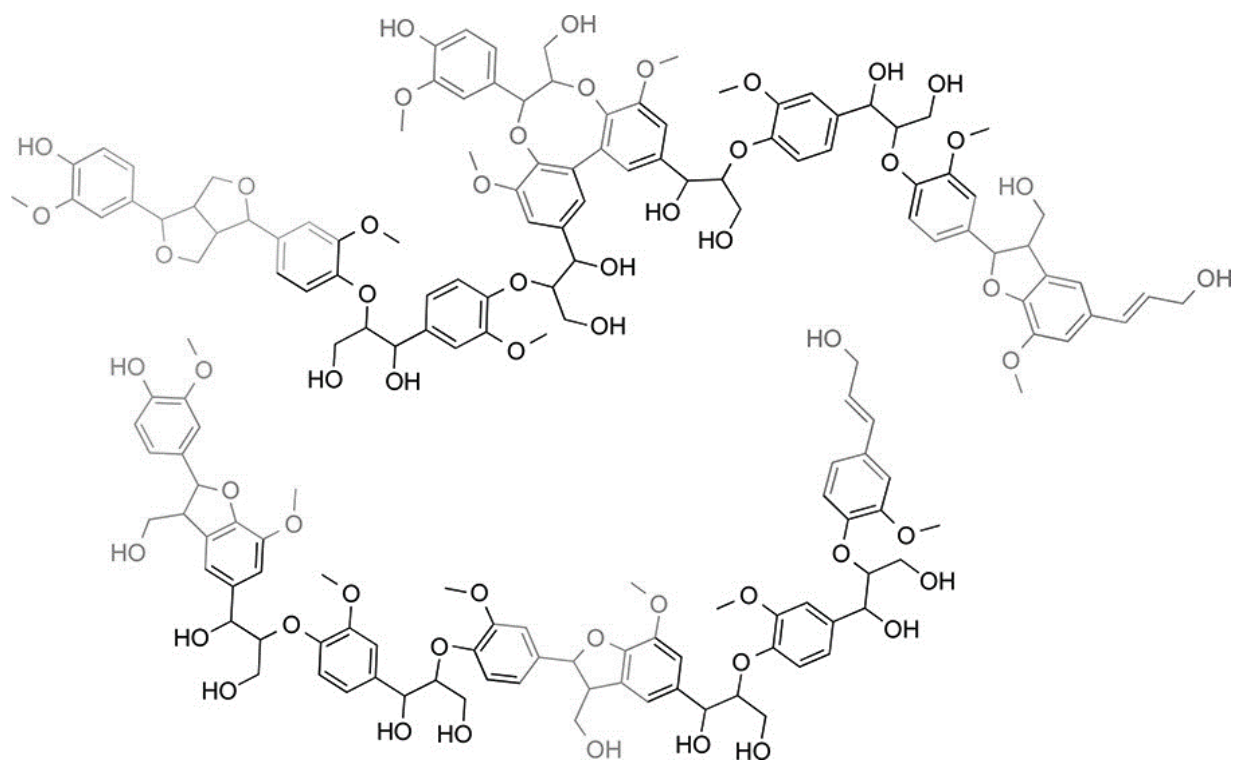


*Figure 1.17.* Structure of milled wood lignin. The lack of branching on the DBDO structure demonstrates the absence of branching justifying the network structure in native lignin.

## ***1.2. Lignin isolation from wood***

Since the first experiments of *Payne* on lignin various strategies have been developed for its isolation from wood. Because of the labile nature of some bonds on lignin the approach used to perform its

isolation can result in a material whose physico-chemical properties drastically differ from those of the polymer in wood. Consequently, in view of structural studies on different lignin, or on the lignin from plants of the same *clade*, the only way to make reliable comparison is based on performing the isolating using the same approach.

In general, in the point of view of the writer, it is possible to classify the existing methods for the lignin isolation methods in four groups:

- carbohydrate hydrolysis-based methods;
- organosolv methods;
- structure preserving methods;
- industrial methods.

The various methods are reported in Tab. 1.3, 1.4, 1.5, and 1.6. In the case of some lignin preparations, the name of the scientist developing the method is used to refer lignin prepared with it. For instance, by isolating lignin from a plant using *p*-dioxane/water mixture on milled wood at room temperature, the resulting product would be indicated as *Björkman spruce lignin*, as the original protocol based on the use of *p*-dioxane/water mixture was developed by *Björkman*.

*Table 1.3* Carbohydrate hydrolysis-based methods for lignin isolation.

<b>Lignin name</b>	<b>Description</b>	<b>Reference</b>
<i>Klason lignin</i> (“acid insoluble lignin”)	Oven dried wood is hydrolysed with 66% sulfuric acid for 48 hours; then, additional acidic hydrolysis to remove the bounded sulfuric acid or the residual is performed with boiling diluted hydrochloric acid.	<sup>23</sup> TAPPI Standard Method T 222 om-02
<i>Willstätter-Zechmeister lignin</i> (“hydrochloric acid lignin”)	Oven dried and solvent-extracted wood is treated with concentrated hydrochloric acid saturated with gaseous hydrogen chloride followed by the dilution of the reaction	<sup>24</sup>



	mixture resulting in the total hydrolysis of carbohydrates.	
<i>Purves lignin</i> (“periodate lignin“)	Oven dried and solvent-extracted wood is treated with sodium periodate in acetic acid buffer resulting in the dissolution of the carbohydrates.	<sup>25</sup>
<i>Freudenberg lignin</i> (“cuprammonium hydroxide lignin” or “cuproxam lignin”)	Oven dried and solvent-extracted wood is pre-hydrolysed with diluted sulfuric acid and then treated with cuprammonium hydroxide (copper (II) complex with ammonia) resulting in the dissolution of cellulose.	<sup>26</sup>

Table 1.4 Organosolv based methods for lignin isolation.

<b>Lignin name</b>	<b>Description</b>	<b>Reference</b>
<i>Dioxane lignin</i>	Oven dried and solvent-extracted wood is refluxed in a diluted hydrochloric acid solution in 9:1 dioxane/water	<sup>16,27</sup>
<i>Alcohol lignin</i>	Oven-dried and solvent-extracted wood is refluxed in a diluted hydrochloric acid solution in ethanol.	
<i>Wise lignin</i> (“ethanolamine lignin”)	Oven-dried and solvent extracted wood is refluxed with ethanolamine.	<sup>28</sup>

Table 1.5 Structure preserving methods for lignin isolation.

<b>Lignin name</b>	<b>Description</b>	<b>Reference</b>
<i>Brauns lignin</i>	Ethanol is percolated on oven dried and solvent-extracted wood.	13,14
<i>Björkman lignin</i> (“milled wood lignin”)	Finely milled wood is solvent-extracted and lignin is isolated via treatment with dioxane/water mixture. The resulting product is purified with dichloro-ethylene.	29,30
<i>Enzymatically liberated lignin</i>	Solvent extracted and oven dried wood is treated with a mixture of enzymes containing cellulases and hemicellulases. Then, lignin is isolated via Brauns or Björkman methods from the degraded sample.	31,32

Table 1.6 Industrial and other specialty methods yielding lignin from biomass.

<b>Lignin name</b>	<b>Description</b>	<b>Reference</b>
<i>Alkali lignin</i>	Grinded wood is treated with 5% (m/V) sodium hydroxide solution at 130-170°C.	Soda processes, for instance Sjostrom textbook <sup>33</sup>
<i>Kraft lignin</i>	Grinded wood is treated with a sodium hydroxide/sulfide mixture at 130-170°C.	Kraft processes, for instance Sjostrom textbook <sup>33</sup>
<i>Lignosulfonates</i>	Grinded wood is treated with sodium, calcium or magnesium sulphite/bisulphite at various pH conditions at 130-170°C	Lignosulfonate processes, for instance Sjostrom textbook <sup>33</sup>
<i>Holmberg lignin</i> (“lignin thioglycolic acids”)	Oven dried and solvent extracted wood is refluxed with	

	thioglycolic acid in 2 F hydrochloric acid for seven hours.	
--	---	--

Carbohydrate hydrolysis-based methods include the preparation of *Klason*, *Willstatter-Zechmeister*, *Purves* and *Freudenberg* lignins.<sup>23–26,34</sup> Due to the strong oxidising conditions at which these treatments occur, not only ether bonds cleavage occurs, but also other chemical reaction modifying lignin structure can occur. All these transformations result in a variation of the structure of lignin driving to preparations which are not suitable for structural studies. Organosolv lignins are isolated by the use of solvents in acidic conditions.<sup>35</sup> Various solvents have been studied; ethanol, dioxane and ethanolamine are just examples of the possible preparations via Organosolv method.<sup>16,28</sup> Differently from carbohydrate hydrolysis-based methods, Organosolv processes allow to isolate lignin with a lower degree of modification on the structure. In addition, these methods are faster if compared to structure-preserving methods, and, generally, requires only a refluxing step of the wood in a specific solvent.<sup>17</sup>

Even if Organosolv processes produce lignin preparations whose structures are close to the one of native lignins, hydrolysis or mild oxidation can occur.<sup>17</sup> To preserve lignin structure as much as possible other methodologies are required, resulting in the isolation of the so called “native lignins”. These preparations are respectively *Brauns*, *Björkman* and the enzymatically liberated lignin.<sup>13,14,29–32,36</sup> *Björkman* method remains the most relevant as it is the one routinely used for structural studies of lignin; lignin preparations obtained with this approach are frequently indicated also as “milled wood lignin”. The protocols to isolate *Brauns*, *Björkman* and the enzymatically liberated lignins rely on the use of neutral solvents on finely milled wood. Unfortunately, differently from carbohydrate-hydrolytic and Organosolv methods, the yields of “native lignins” are low and some carbohydrate impurities can remain in the samples.

Another lignin preparation especially suitable for biological and microbiological studies, is *Holmberg* lignin. This lignin isolated via a functionalising-extracting approach based on the action of thioglycolic acid on wood. The isolated functionalised lignin is not suitable for structural studies.

All the lignin preparations mentioned and summarised in Tab.2.1, 2.2., and 2.3 are isolated with extracting procedures that can only be applied in small batches. Only Organosolv lignins are currently entering in the industrial world because of the modern biorefinery industry. Technical lignins are produced on large scale in the industry, are classified into three types, soda, kraft, and liginosulfonates.

Both soda and kraft lignins result from sulfate process; the reactions dominating this technology are going to be described in detail in [Paragraph 1.4](#). In general, temperature ranging between 130 to 170°C are required for these processes and lignin is dissolved in strongly alkaline conditions. The acidification of alkaline lignin solutions, which is operated by the use of strong inorganic acids (e.g. sulfuric acid), or via carbon-dioxide bubbling (LignoBoost), results in the precipitation of soda or kraft lignin. Owing to the harsh conditions of sulfate pulping, technical lignins are characterised by a strongly modified structure if compared to the one of native lignin; in particular, new functional groups, such as carbonyls, double bonds and mercapto-groups, appear, while others, like *phenylcoumarane*, disappear.

Lignosulfonates are obtained from the action of sulphurous acid and its salt (sulphite and bisulphite) on the aliphatic domain of lignin, converting lignin into sulfonated species (lignosulfonic acid). These species are highly soluble in water, consequently they cannot be isolated via acidification, but only via concentration/evaporation steps for their solutions. Differently from sulfate pulping, where only alkaline pH can be used, in the case of lignosulfonate process a wide range of pH can be used, from acidic to alkaline. Depending on the pH at which the isolation of lignin is performed the nature of sulfonic groups in lignin changes. In fact, in the case of alkaline conditions, the products obtained after evaporation of water are sulfonic acids salts of lignin, the so-called lignosulfonates.

### ***1.3. Methods for structural elucidation of lignin***

In order to understand the chemical structure of lignin preparations, the development of specific techniques for its characterisation is pivotal for the lignin chemist. In fact, owing to either its polymeric nature or its intrinsic complexity, none of the available existing techniques allows, on its own, to properly depict a full image of a lignin sample. Consequently, the lignin chemist has to work with various tools which can provide him with some specific information such as, for instance, its reactivity (e.g. content of sulfonic groups), the distribution/amount of functional groups or binding units, or the molecular weight. Traditionally, characterisation methods are distinguished in two classes: wet-methods and solid-state methods. Wet-methods include all the traditional degradations techniques (e.g. nitrobenzene and cupric oxide oxidations), titrimetric techniques (conductometric and potentiometric analyses), spectroscopic methods in solution (e.g. ultraviolet spectroscopy, nuclear magnetic resonance, and electron paramagnetic spectroscopy), and molecular weight determinations (e.g. cryoscopic methods, ultracentrifugation, and gel permeation chromatography). Solid state methods comprise all the solid-state spectroscopic techniques (e.g. solid state nuclear

magnetic resonance and Fourier transformed infrared spectroscopy), microscopy and thermal analyses. A relatively dated summary of all the most prominent and well established techniques in lignin chemistry was released and edited in 1992 by *Lin and Dence*.<sup>37</sup>

In the following paragraphs, a brief description of some of the most historically prominent techniques used for lignin characterisation is reported, followed by a brief summary on the actual use of NMR for structural elucidations. Then, a paragraph on <sup>31</sup>P NMR is reported; in fact, this technique drastically changed the life of lignin chemist, giving him the chance to get extremely valuable information on lignin structure and reactivity with an extremely fast and reliable procedure.

### 1.3.1 Nitrobenzene oxidation

Among the various characterisation techniques, nitrobenzene oxidation is probably the most important, as it permits to understand the composition in terms of monolignols of a lignin sample.

The action of alkaline nitrobenzene on 1-phenyl-olefins was a known reaction when it was firstly applied on lignin. In fact, by treating isoeugenol with alkaline nitrobenzene, *Bischler* demonstrated the oxidative cleavage of the olefinic bond obtaining vanillin. In the light of that, *Freudenberg* and co-workers in 1939 reported for the first time the application of this reaction on an extractive free-spruce wood, observing the formation of vanillin with high yields (25% w/w on total *Klason* lignin). Not only vanillin was obtained, but also, in smaller amount, the oxidation products of vanillin, like vanillic acid, 5-carboxyvanillin and also some traces of guaiacol.<sup>38–40</sup> These results confirmed that lignin was an aromatic polymer and also supported the existing hypothesis on the fundamental role of coniferyl alcohol as a constituting block of softwoods.

Some years after, in 1944, nitrobenzene oxidation was used by *Creighton* and *Hibber* to perform taxonomic studies on plants. In particular, by analysing via this oxidative technique some dicotyledon angiosperms, like ashwood (*Fraxinus americana*), poplar (*Populus*), and yellow birch (*Betula lutea*), they observed that the major constituents of the products mixture were both vanillin and syringaldehyde.<sup>41,42</sup> This observation permitted to the scientific community to recognise that a distinction between dicotyledon angiosperms and gymnosperms can also be made in “chemical terms” by considering the composition of their lignins and revealed the role of synapyl alcohol in the dicotyledon angiosperms lignin.

In 1967 the presence of *p*-hydroxy-benzaldehyde in the reaction mixture of the degradation products of a lignin was noticed by *Higuchi*.<sup>43</sup> In fact, after extracting lignin from grass by the use of *Björkman* method, its analyses via nitrobenzene oxidation resulted in a more intricate products mixture than that

of dicotyledon angiosperms and gymnosperms, from which it has been possible to identify also p-hydroxy-benzaldehyde in high amounts.

All these experimental data, which are schematised in Fig. 1.18, highlighted the complexity of the lignins in grasses and permitted to create a general chemical criterium for the classification of plants. In general, it is nowadays recognised that dicotyledon angiosperms are plants whose nitrobenzene oxidation results in either vanillin and syringaldehyde; gymnosperms' are those plants yielding, under nitrobenzene oxidation conditions, mostly vanillin; finally, grasses, are those plants whose nitrobenzene oxidation products are constituted by vanillin, syringaldehyde, and p-hydroxybenzaldehyde.

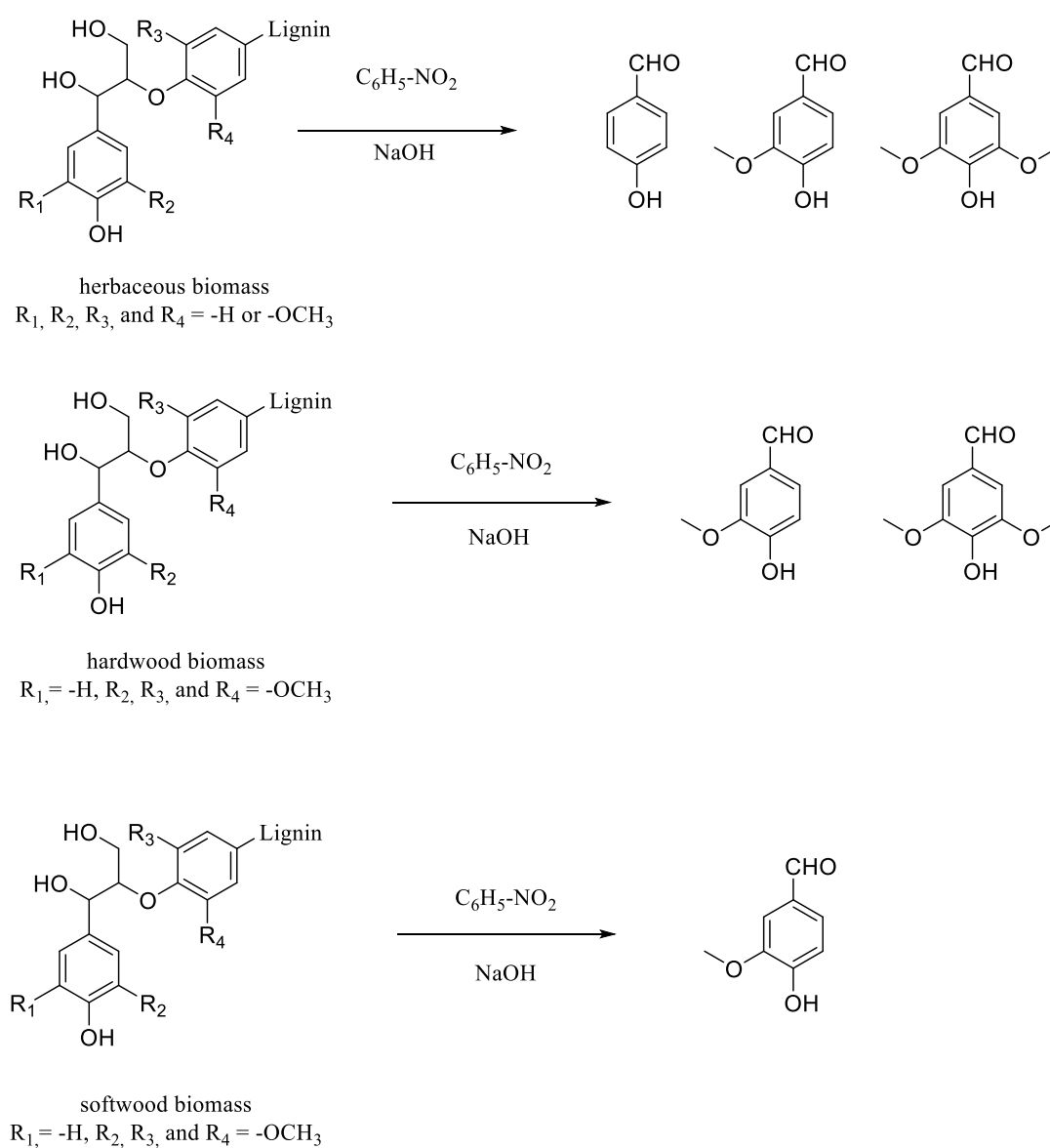


Figure 1.18. Most relevant degradation products from nitrobenzene oxidation of various types of plant.

Nitrobenzene oxidation was used extensively in the last eighty years, in particular when data regarding the quantitative composition of lignin in terms of monolignols were needed. Moreover, it is an extremely elaborate technique. In fact, even if the oxidation is step a quite easy operation (heat in a bomb lignin with a 2 N sodium hydroxide solution and nitrobenzene), the work-up operations based on subsequent extractions, concentration, dilution, products derivatisation and chromatographic analyses can easily introduce some procedural mistakes in non-expert workers. These unintentional errors drive to unprecise results which misrepresent the reality.

### 1.3.2 Permanganate oxidation

From one side, nitrobenzene oxidation degrades lignin into aldehydes, which can be easily correlated to the amount of the various monolignols in a lignin preparation. From the other side, permanganate oxidation gives the chance to detect specific dimeric condensed structures in lignin as well as the substitution patterns of lignin aromatic rings.

Permanganate oxidation is based on the benzylic oxidation of alkylbenzenes, a well-known reaction in organic chemistry involving the use of strong oxidising agents. In general, the target of this reaction is the alkyl chains of phenyl structures, which are cleaved independently from their length resulting in the formation of carboxylic groups.

*Freudenberg* firstly applied the benzylic oxidation to study lignin structure in 1936. The starting point for his work was a potassium hydroxide mildly hydrolysed extractive free-lignin, which was methylated with dimethyl sulphate. Methylation step, resulting in the functionalisation of all the free-hydroxylated moieties in lignin, was necessary to maintain selective the subsequent oxidation to the alkyl groups. Then, the subsequent oxidation was performed using potassium permanganate in neutral conditions; the various oxidation products were finally identify via traditional methods.<sup>44</sup>

In the products mixture, the one confirming the presence of condensed structures in lignin were dehydroveratryl and 4,5'-dicarboxy-2,2',3-trimethoxy-diphenylether (or 4,5'-dicarboxy-2,2',3,6'-tetramethoxy-diphenylether in dicotyledon angiosperms), corresponding respectively to *biphenyl* and *diaryl ether* bond patterns. In addition, derivatives of veratric with carboxyl groups in 5- (isoemphinic acid) or 6- (m-hemphinic acid) positions, as well as 3,4,5-trimethoxy-phthalic acid were found. These products confirmed the presence of additional alkyl bonds in 5 and 6 positions in the case of gymnosperms and dicotyledon angiosperms. A schematic reaction equation is reported in Fig. 1.19.

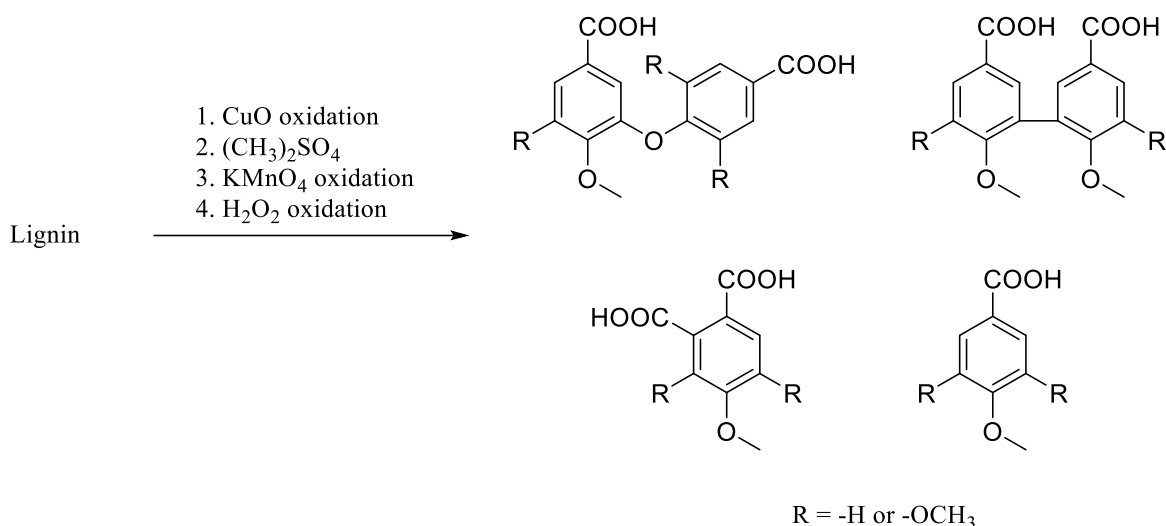


Figure 1.19. Some products from potassium permanganate oxidation of lignin.

Modification on the original method to perform permanganate oxidation were suggested by various *Authors*; in particular *Miksche* implemented the procedure of *Freudenberg*. In fact, *Miksche* and co-worker suggested the caustification after the neutral permanganate oxidation followed by an additive mild oxidation of lignin by the use of 30% hydrogen peroxide. After the adjunctive oxidation step, in order to favour the analyses of the reaction mixture via gas-chromatography, the same authors suggested the derivatisation of the products with diazomethane.<sup>45</sup> All these modifications resulted in a robust methodology which has been used for a long period of time.

This technique, with all the modifications suggested during the years, has been widely used by different generations of lignin chemists. Unfortunately, this analytical method requires a high experienced operator as the steps are many and not that obvious, likewise the case of nitrobenzene oxidation. At the same time, this technique is even more complicated if compared to the other degradative one suggested by *Freudenberg*; in fact, not only the oxidation steps are two instead of one, but there are also two derivatisation steps that have to be taken into account. All these observations, coupled either with the high hazard at which the operator is exposed while using diazomethane and the development of advanced spectroscopic techniques allowing to identify and quantify the various types of condensed structures in lignin (e.g.  $^{13}\text{C}$  NMR or HSQC), displaced this technique approximately at the end of the XX century more and more to niche applications. Permanganate oxidation can nowadays be considered as an abandoned technique..



### 1.3.3 Acidolysis and thioacidolysis

Acidolysis and thioacidolysis are two techniques based on the degradation of lignin structure in dioxane. Chronologically, acidolysis anticipated thioacidolysis; in fact, the last can be considered as an implementation of the first one.

From a practical perspective, acidolysis involves a refluxing step of a lignin sample in a 0.2 M hydrochloric acid solution in dioxane. Products are then isolated and determined after derivatisation via gas-chromatography. The election of dioxane *in lieu* of other oxygen containing solvents, like ethanol, is justified by the higher solubility of lignin in its 9/1 mixtures with water. Similar procedures with ethanol, which are referred to as *ethanolysis*, have been investigated.

Acidolysis is based on two types of cleavages on labile structures resulting respectively in the formation of C6-C3 or C6-C2 low molecular weight compounds.

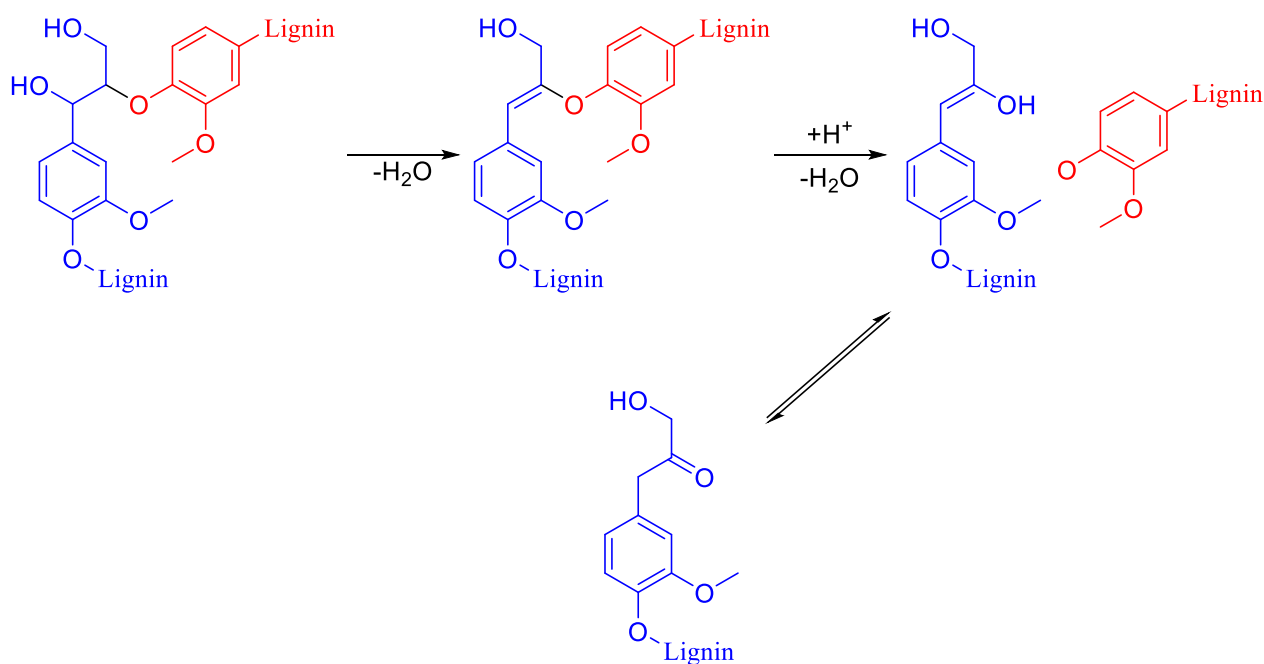


Figure 1.20. Favoured reaction mechanism for the degradation of arylglycerol- $\beta$ -aryl ether via acidolysis.

The first cleavage type relies on two steps, as depicted in Fig. 1.20. (a) The dehydration of  $C_\alpha$ - $C_\beta$  bond with the formation of an olefinic system, and (b) the protonation of the aryloxy oxygen coupled with its nucleophilic substitution with water. The second step allow to the formation of an enol which tautomerise forming the corresponding a 1-aryloxy-3-hydroxy-propan-2-one structure. This ketone undergo  $C_\alpha$  oxidation forming an *Hibbert* ketone.

The second reaction pathway (Fig. 1.21), which occurs less frequently,<sup>46</sup> involves (a) the de-formylation in  $\gamma$ -position coupled with the dehydration of the  $C_\alpha$ - $C_\beta$  bond, and (b) the cleavage to the one reported in the first mechanism via aryloxy oxygen protonation, water nucleophilic substitution and keto-enol tautomerisation of the product. In this case of this second reaction pathway, the C3-aliphatic chain is converted into a C2-chain with a terminal formyl group.

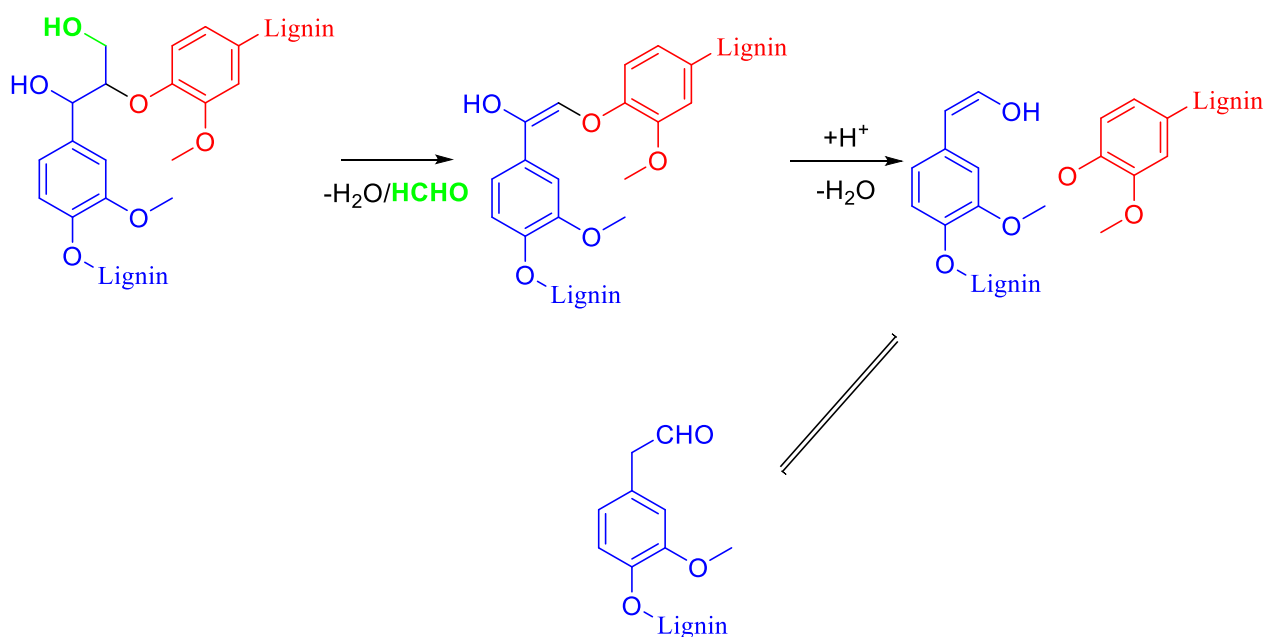


Figure 1.21. Alternative reaction pathway for lignin acidolysis.

Products obtained from the acidolysis of lignin model compounds have been identified and allowed to confirm the presence of certain interunit bonds in lignin. In particular, acidolysis was applied for the first time by *Adler* in 1957; this methodology gave him the chance to demonstrate the presence of *arylglycerol- $\beta$ -ethers*.<sup>15</sup> Other patterns confirmed by the same technique have been  $\beta,5'$ ,  $\beta,\beta'$ , and  $\beta,1'$ .

*Lapierre* and her co-workers, *Monties* and *Rolando*, during the Eighties purposed a newer version of acidolysis taking place in anhydrous dioxane, in presence of boron trifluoride etherate and ethyl-mercaptan.<sup>47-49</sup> This modification permitted to quantify either the amount of the various arylglycerol- $\beta$ -aryl ethers (as mercapto-ethylated products) or the ratio of the monolignol constituting the sample (depending on the nature of the C6 products). The reaction mechanism resulting in the degradation of the lignin sample relies on the action of boron trifluoride etherate, in which boron trifluoride acts as a strong Lewis acid causing its addition to the oxygen in the  $\alpha$ -position with respect to the C6 ring. Then, ethyl-mercaptan, a mild nucleophile, can reach the carbon bonded to the oxygen functionalised

with boron trifluoride; a nucleophilic substitution results in the substitution of the former hydroxyl coupled with the insertion of a thioethoxy group. This reaction drives to the formation of an  $\alpha$ -mercapto-ether bond. The action of boron trifluoride/ethyl-mercaptan system continues also on  $C_\beta$  and  $C_\gamma$  oxygens, cleaving the *arylglycerol- $\beta$ -aryl ether* bond, introducing additional mercapto-ether bonds in the respective positions. This reaction mechanism is depicted in Fig. 1.22.

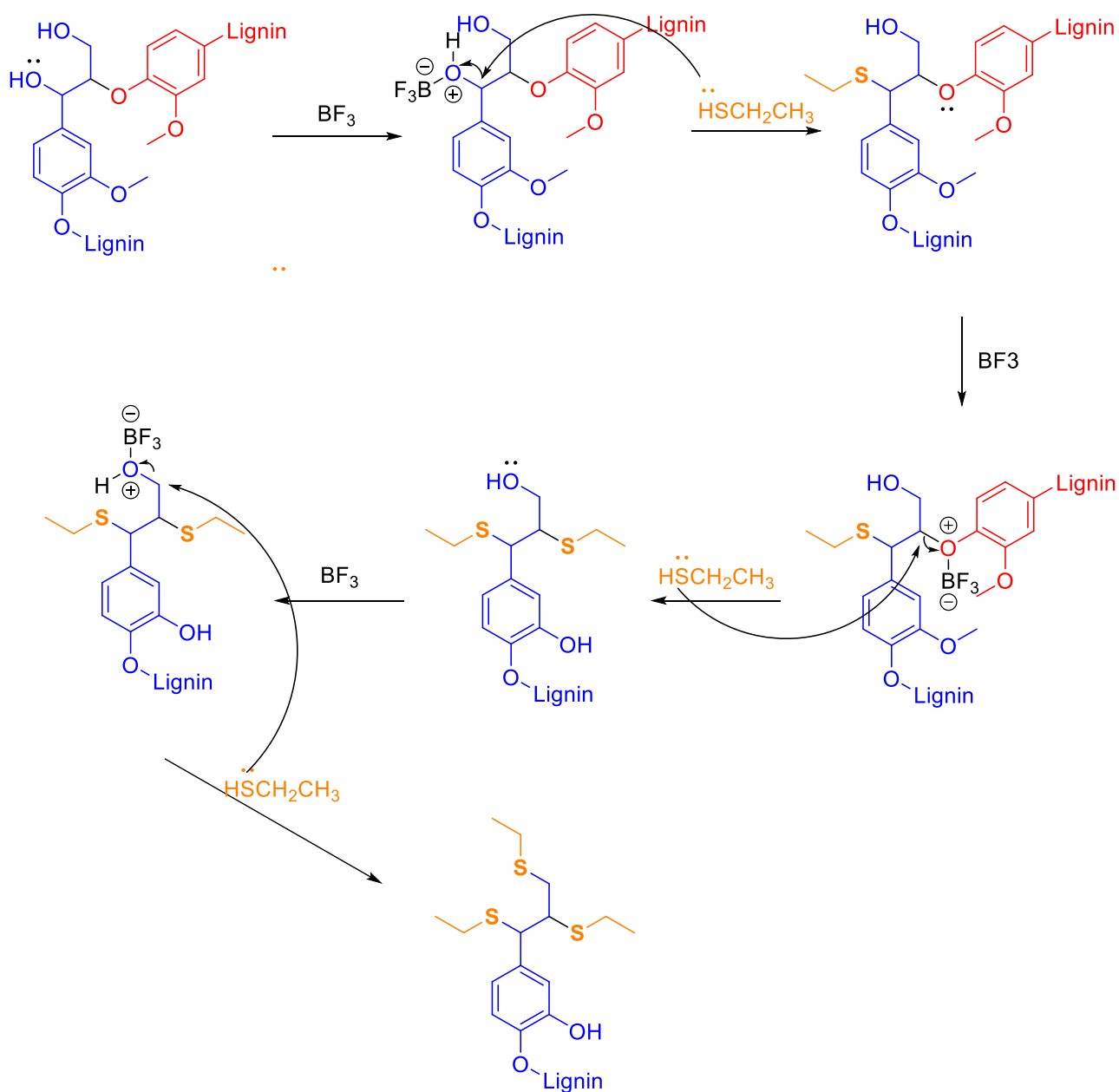


Figure 1.22. Thioacetolysis mechanism on  $\beta$ -O-4' mechanism.

Acidolysis and thioacidolysis have been applied during the last years and, as previously mentioned, the information they provide are particularly relevant for the study of the bonds linking together the monomeric units of lignin in non-condensed structure.

A scheme summarising the information available from all the degrading techniques mentioned in the previous paragraphs is reported in Fig. 1.23.

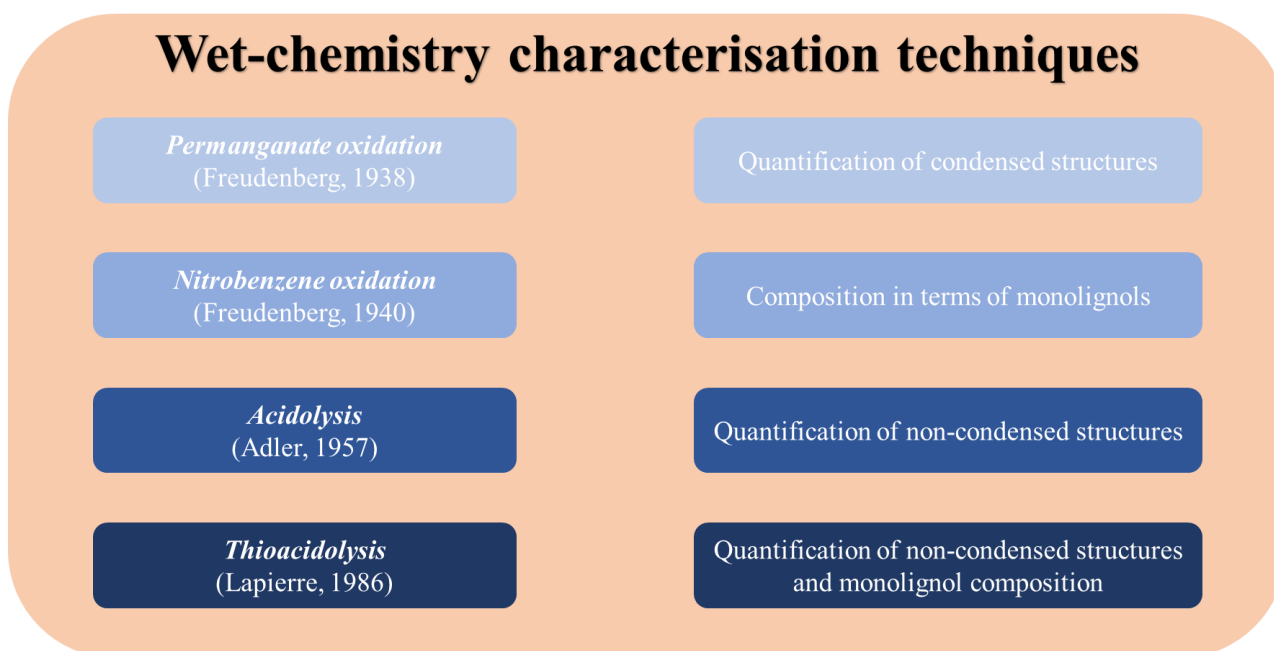


Figure 1.23. Structural information available from the traditional degrading techniques in Lignin Chemistry.

The combination of the information resulting from all these techniques permits to create a good picture of the chemical structure of the analysed lignin; moreover, the use of all of them is a quite tedious and extremely time-consuming operation. In fact, since the Sixties, when spectroscopic techniques have started entering in the laboratories of lignin chemists, the need of fast, reliable and robust methods to perform lignins characterisation has been felt.

### 1.3.4 Spectroscopic techniques in lignin chemistry

Spectroscopy is one of the most important tool the modern chemist can use to characterise lignin. In this optic, different spectroscopic techniques have been applied for the study of lignin preparations. In particular, the ones which have been mostly used are:

- Ultraviolet and visible spectroscopy (UV-vis);
- Fourier-Transformed Infrared spectroscopy (FT-IR);
- Nuclear Magnetic Resonance (NMR).

In a chronological perspective, UV-vis spectroscopy was the first technique applied to study lignin, followed by FT-IR and then NMR. However, because of the limitations of UV-vis and FT-IR methods, nowadays the most promising technique to understand the features of lignin is NMR.

#### **1.3.4.1 Traditional NMR analyses in lignin**

Elemental analysis reveals that the major constituents of lignin are carbon, hydrogen and oxygen, consequently carbon and proton NMR can be satisfactorily used to investigate its structure. Of these two nuclei, proton is the most naturally abundant and sensitive in NMR experiments.

During the Sixties the first studies on lignin via proton NMR were performed; the aim of these analyses was the determination of the chemical shifts of typical protons in lignin via the use of model compounds reproducing lignin bonding patterns. With regards to  $^{13}\text{C}$  NMR analyses of lignin, only during the Seventies this strategy became relevant due to the development of acquisition protocols based on Fourier transformations.

Advantages and disadvantages related to the use of  $^1\text{H}$  and  $^{13}\text{C}$  NMR techniques in lignin analyses can be highlighted. From one side, collecting  $^1\text{H}$  NMR spectra is faster and easier than  $^{13}\text{C}$  NMR ones; additionally, the resolution of  $^1\text{H}$  NMR spectra is better, permitting an easier correlation of the peaks with known structures.<sup>50</sup> Unfortunately, due to the small range of chemical shifts investigable via  $^1\text{H}$  NMR (*commonly 8-10 ppm*), the spectra of lignin preparations are characterised by the presence of overlapped peaks; this fact results in difficulties in performing precise assignments of structures (Fig. 1.23).

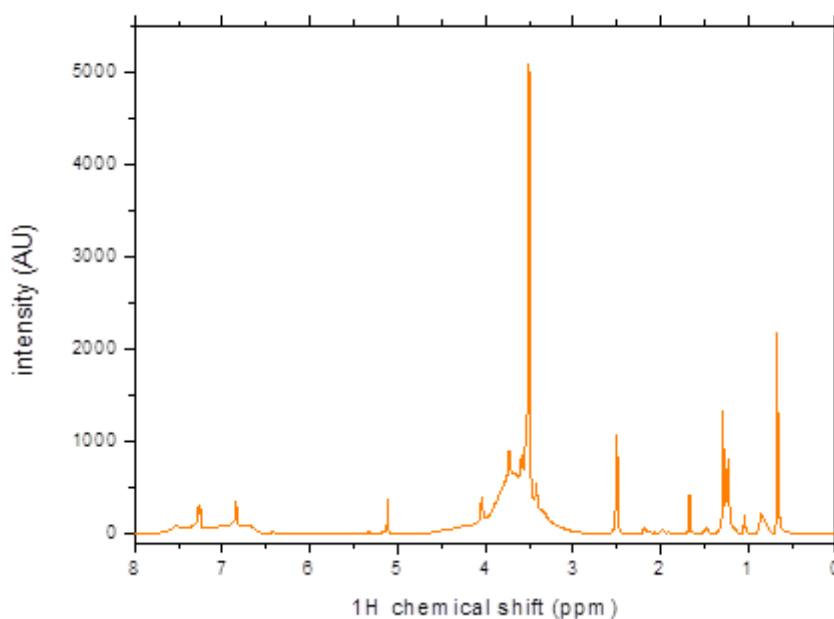


*Figure 1.23.*  $^1\text{H}$  NMR spectrum of softwood kraft lignin in hexa-deuterated dimethylsulfoxide. The overlapping of the signals is evident in all the chemical shifts region. Spectrum acquired with a *Bruker* 400 MHz NMR spectrometer.

From the other side,  $^{13}\text{C}$  NMR profit of a wider range of chemical shifts; this fact permits to easily identify the various inter-unit patterns in lignin preparations (Fig. 1.24). In addition, due the broad dispersity of signals for lignin preparations in  $^{13}\text{C}$  NMR, the quantitative analyses can be performed by the use of an internal standard (e.g. 1,3,5-trioxane) using specific pulse-programmes (e.g. inverse gated decoupling).<sup>51,52</sup> Unfortunately, the long acquisition time required to obtain spectra of good quality coupled and the need of spectrometer working at high field (at least, more than 500 MHz) represent the serious limitations for this spectroscopic technique.

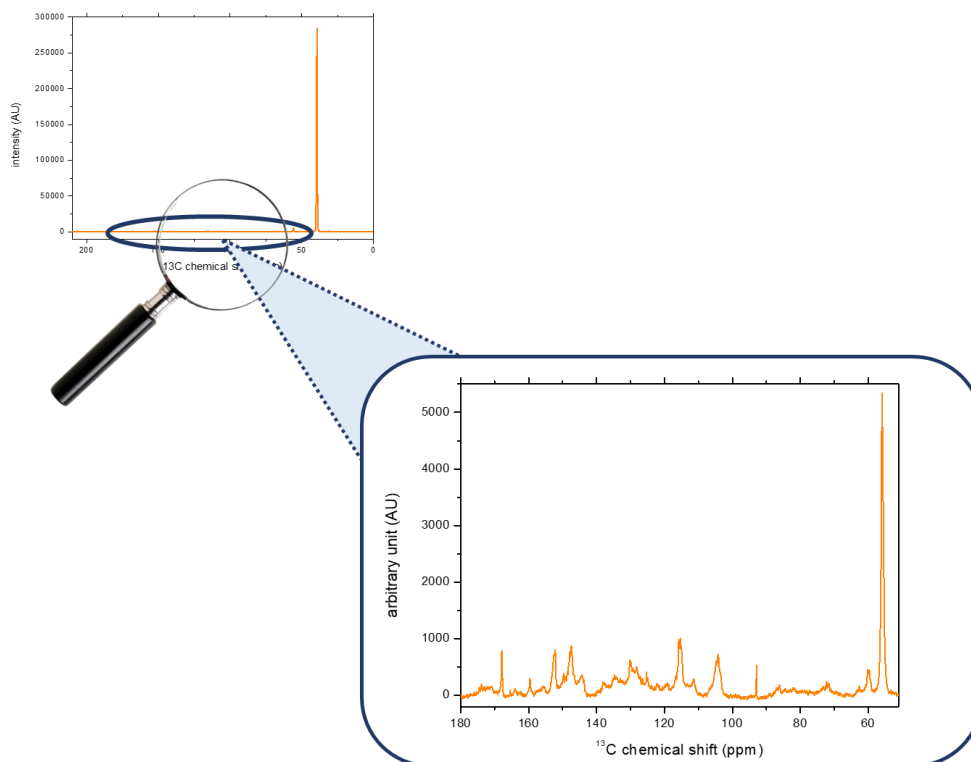


*Figure 1.24.*  $^{13}\text{C}$  NMR spectrum of softwood kraft lignin in hexa-deuterated dimethylsulfoxide in presence of chromium (III) acetylacetonate as relaxation agent. The magnification of the region of chemical shifts comprised between 50 and 180 ppm highlights the diagnostic part of the spectrum, where characteristic signals can be clearly noticed (*e.g.* guaiacyl peak at 110 ppm). Spectrum acquired with a *Bruker* 400 MHz NMR spectrometer.

The assignments of NMR signals in  $^1\text{H}$  and  $^{13}\text{C}$  NMR analyses of lignin preparations are reported in Fig. 1.25 and 1.26.

$\delta^a$	Assignment
1.26	Hydrocarbon contaminant
2.01	Aliphatic acetate
2.28	Aromatic acetate
2.62	Benzylic protons in $\beta$ - $\beta$ structures of secoisolariciresinol type, benzylic protons in 3-aryl-1-propanol units
3.81	Protons in methoxyl groups
4.27	$H_\gamma$ in several structures
4.39	$H_\gamma$ in, primarily, $\beta$ -O-4 structures (erythro forms) and $\beta$ -5 structures
4.65	$H_\beta$ in $\beta$ -O-4 structures (methylene protons in cinnamyl alcohol units)
~4.80 <sup>b</sup>	Inflection possibly due to $H_\alpha$ in pinoresinol units and $H_\beta$ in noncyclic benzyl aryl ethers (threo forms).
5.49	$H_\alpha$ in $\beta$ -5 structures ( $H_\alpha$ in noncyclic benzyl aryl ethers, $H_\beta$ in 2-aryloxypropiofenones).
6.06	$H_\alpha$ in $\beta$ -O-4 structures ( $H_\alpha$ in $\beta$ -1 structures, $H_\beta$ in cinnamyl alcohol units)
6.93	Aromatic protons (certain vinyl protons)
7.29	Chloroform (solvent)
7.41	Aromatic protons in benzaldehyde units and vinyl protons on the carbon atoms adjacent to aromatic rings in cinnamaldehyde units
7.53	Aromatic protons in benzaldehyde units
9.64	Formyl protons in cinnamaldehyde units
9.84	Formyl protons in benzaldehyde units

<sup>a</sup> Values refer to the highest point of the peak.

<sup>b</sup> Inflection includes contributions from unidentified signals (Ede et al. 1990).

Figure 1.25. Chemical shift assignation for acetylated spruce lignin. (table from Lundquist K., "Proton (<sup>1</sup>H) NMR Spectroscopy" in Lin S., Dence C. (eds., "Methods in Lignin Chemistry", Springer-Verlag, Berlin 1992).

Structure or functional group	Frequency range, ppm
Aromatic C total	102–162
Aromatic-CH	102–127
Aliphatic-COR	58–95
Methoxyl	54.5–56.5
C-3/C-5 in $\beta$ -O-4 S e	150.8–153.3
C <sub>γ</sub> H <sub>2</sub> OH <sup>a</sup>	58.4–64
C-2/C-6 <sup>b</sup> in S	102.3–107.5
C <sub>β</sub> in $\beta$ - $\beta$ and $\beta$ -5	53.4–54
Acetyl carboxyl carbons	
Primary hydroxyl groups	170.4–171.6
Secondary hydroxyl groups	169.5–170.4
Phenolic groups	168.5–169.5

<sup>a</sup> Except C- $\gamma$  in  $\beta$ - $\beta$  units found at 71.2 ppm.

<sup>b</sup> Except C-2/C-6 in p-hydroxyphenyl units.

Figure 1.26. Chemical shift assignation for acetylated spruce lignin. (table from Robert D., "Carbon-13 Nuclear Magnetic Resonance Spectrometry" in Lin S., Dence C. (eds., "Methods in Lignin Chemistry", Springer-Verlag, Berlin 1992).

Another critical point to consider while planning NMR analyses of lignins is represented by the election of the optimal solvent to use. In the past, <sup>1</sup>H and <sup>13</sup>C NMR spectra used to be recorded using deuterated chloroform (CDCl<sub>3</sub>) as solvent. Due to the polar nature of lignins, their solubilisation in



that solvent is almost impossible; moreover, the functionalisation of their hydroxylated moieties via acetylation permits to circumvent this limit and to obtain lignins solutions in  $\text{CDCl}_3$ . In order to acetylate lignins a tedious and time-consuming procedure has to be meticulously applied; this derivatisation involves the dissolution of the sample in pyridine, followed by the functionalisation of the hydroxylated moieties via the use of acetic anhydride. The resulting acetylated preparations are highly soluble in  $\text{CDCl}_3$  (more than 200 mg per 600  $\mu\text{L}$  of  $\text{CDCl}_3$ ) making possible to obtain highly concentrated solutions suitable for both  $^1\text{H}$  and  $^{13}\text{C}$  NMR analyses.

Recently, the need to use acetylated lignins was permanently circumvented by the use of hexadeuterated dimethyl sulfoxide ( $\text{DMSO-d}^6$ ). In fact, it was known since the beginning of modern Lignin Chemistry that dimethyl sulfoxide was being a good solvent for lignin preparations, moreover its deuterated form was not easily available until the late Nineties of the last Century. This reality changed thanks to the development of new labelling procedures, who drastically reduced the cost of  $\text{DMSO-d}^6$ . The limit of  $\text{DMSO-d}^6$  if compared to the traditional acetylated lignin/ $\text{CDCl}_3$  system is represented by the lower solubilising power; in fact, it is quite difficult to solubilise more than 80 mg of lignin preparation in 600  $\mu\text{L}$  of  $\text{d}^6$ -DMSO without coupling the dissolution with sonication and heating of the mixture. More recently, *Ralph* suggested the use of a 1:1 mixture of  $\text{DMSO-d}^6$  and pyridine- $\text{d}^5$  as solvent to collect NMR spectra of lignin preparations and finely ball-milled wood samples.<sup>53</sup> The major advantage of this system is represented by the comparable solubility of the samples with the traditional approach based on the use of acetylated preparations. *Ralph* system is particularly useful while performing bidimensional NMR while, in the case of mono-dimensional  $^1\text{H}$ , the overlap of DMSO and pyridine signals with those of the sample, seriously affect the quality of the final spectra.

#### 1.3.4.2 2D NMR analyses

Bidimensional NMR (2D NMR) spectra represent an implementation of traditional mono-dimensional analyses permitting the correlation of two nuclei that are processed at the same time. 2D NMR is particularly relevant for the identification of structures in lignin preparations which cannot be easily identified via traditional  $^1\text{H}$  and  $^{13}\text{C}$  analyses. *Ralph* was one of the pioneer of the application of 2D NMR on lignin, and his works spread throughout more than three decades since the Eighties; a full survey of his work until 2010 recently appeared in “*Lignin and Lignans*”, edited by *Heitner, Dimmel, and Schmidt*.<sup>54</sup>

Various 2D NMR experiments have been applied for studying lignin structure; in general they can be classified in three classes: (a) homonuclear correlation of vicinal nuclei, (b) homonuclear correlation of close-in-space nuclei, and (c) heteronuclear correlation of vicinal nuclei.

The homonuclear correlation of vicinal nuclei has been applied on both  $^1\text{H}$  and  $^{13}\text{C}$ . From the  $^1\text{H}$  side, COSY and TOCSY programs are commonly used. These two experiment differs for the mixing times; in fact, TOCSY typically mixing times are between 80-120 ms, while ones COSY lie between 10-30 ms. By varying mixing time, it is possible to correlate vicinal protons (COSY) or proton systems characterised by same spin systems (even if they are not close in space, TOCSY). In particular, TOCSY demonstrated its relevance for the identification of various type of bonding patterns in lignins.<sup>55-58</sup> For the  $^{13}\text{C}$  side, the applicability of homonuclear correlation is almost impossible on natural lignin because of the extremely low isotopic abundance of  $^{13}\text{C}$ . Moreover, INADEQUATE experiments have been applied on isotopically enriched lignin preparations in order to study the inter-unit bonds.<sup>59,60</sup>

The homonuclear correlation of close-in-space nuclei have been tested for  $^1\text{H}$ ; moreover, owing to the short range of action of this technique (protons with a maximum distance of 5 Å) and the lack of regularity in lignins, the only interaction revealed via NOESY were those between methoxyl protons and C2-protons in guaiacyl units and C2/C6-protons in syringyl units.<sup>55</sup>

Finally, the heteronuclear correlation of  $^1\text{H}$  and  $^{13}\text{C}$  is probably the most useful way to fully elucidate the carbon-skeleton of lignin samples. In fact, it provides in a fast way a matrix where signals coming from two different nuclei are correlated; in this way it is possible to demonstrate the connectivity of protons with the respective carbon. An extremely valuable example of the utility of HSQC is represented by the identification of the DBDO structure in relatively recent times by *Brunow*.<sup>19-21</sup> An example of an HSQC spectrum of a lignin preparation is reported in Fig. 1.27, where the aliphatic and the aromatic signals are highlighted.

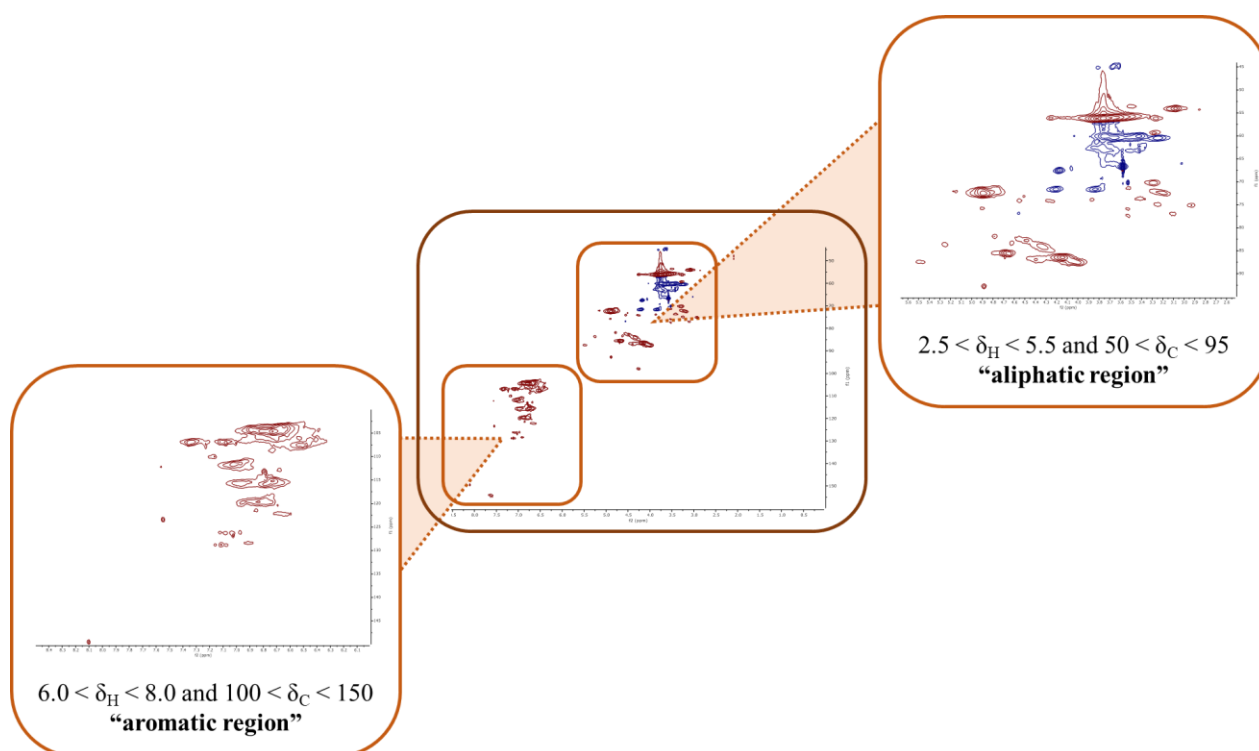


*Figure 1.27.* HSQC NMR spectrum of a softwood kraft lignin. On the  $x$ -axes of the matrix the  $^1\text{H}$  spectrum of the samples is reported, while the  $^{13}\text{C}$  is reported on the  $y$ -axes. In general, HSQC spectra can be divided into two areas of interest, the *aliphatic* and the *aromatic region*. In the aliphatic region ( $2.5 < \delta_{\text{H}} < 5.5$  and  $50 < \delta_{\text{C}} < 95$ ) signals corresponding to the propanoic side chains of lignins can be identified as well as methoxy groups, while the aromatic one ( $6.0 < \delta_{\text{H}} < 8.0$  and  $100 < \delta_{\text{C}} < 150$ ) correlating peaks related to the phenyl domains are provided.

Spectrum acquired with a *Bruker* 400 MHz NMR spectrometer.

These are just some examples of 2D NMR programmes. HMBC, HSQC-TOCSY and ROESY are some of the other existing acquisition methods for investigating polyphenols.

The current frontiers on which the spectroscopic studies of lignin preparations are represented by the switch from the second dimension to the third or the fourth one. In fact, these enhancements were recently applied for the structural studies of nitrogen-containing biomolecules, like proteins or enzyme, however their potentialities in isotopically labelled lignin have recently started to be considered in Lignin Chemistry.

### 1.3.4.3 $^{31}\text{P}$ NMR: the key for the fast and reliable analyses of reactive groups in lignin

The previously described NMR techniques permit the elucidation of the nature of the skeletal structure of lignin preparations. Moreover, poor information can be obtained on the nature and content

of the various hydroxylated moieties. These groups play a pivotal role in the reactivity of lignins and, since the beginning of the 20<sup>th</sup> Century, various approaches have been developed to characterise and quantify them. Unfortunately, all these techniques provide limited information.

In this scenario, <sup>31</sup>P NMR has been successfully applied for the characterisation of hydroxyl groups in lignins. This methodology of analyses was developed by *Argyropoulos* between the end of the Eighties and the early Nineties; several modifications were then suggested by the same *Author* during the upcoming years in view of its implementation.<sup>61–65</sup> In 2019 a standard version of the method, updated with the notable studies of *Crestini* on the application of the same for the characterisation of tannins, was published on *Nature Protocols*.<sup>66</sup> More recently, the writer of this thesis had the pleasure and the honour to revise the method, as co-author of *Argyropoulos* and *Crestini*, to offer a simplified methodology in order to train newbies in Lignin Chemistry. This paper is published with additional video contents, supporting the operations and the calculations necessary to reach the final results, on the *Journal of Visual Experiments*.<sup>67</sup>

This methodology is based on the labelling of the hydroxylated moieties of lignin preparations with a phosphorous-containing reagent, 1-chloro-4,4',5,5'-tetramethyl-1,3,2-dioxaphospholane (TMDP). The functionalisation reaction involves the nucleophilic attack of hydroxyl groups via the labile phosphorous-chlorine bond, resulting in the formation of new phosphorous-oxygen bond with the liberation of hydrochloric acid. This mechanism is schematised in Fig. 1.28.

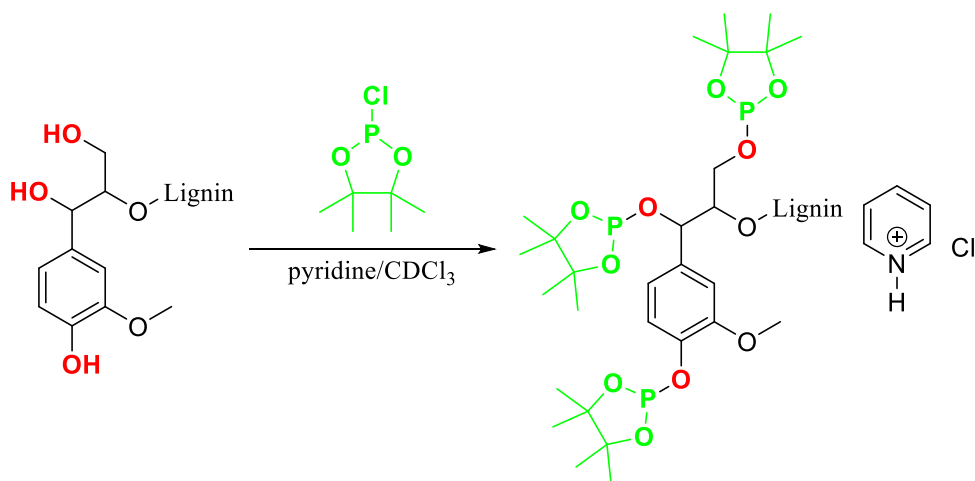
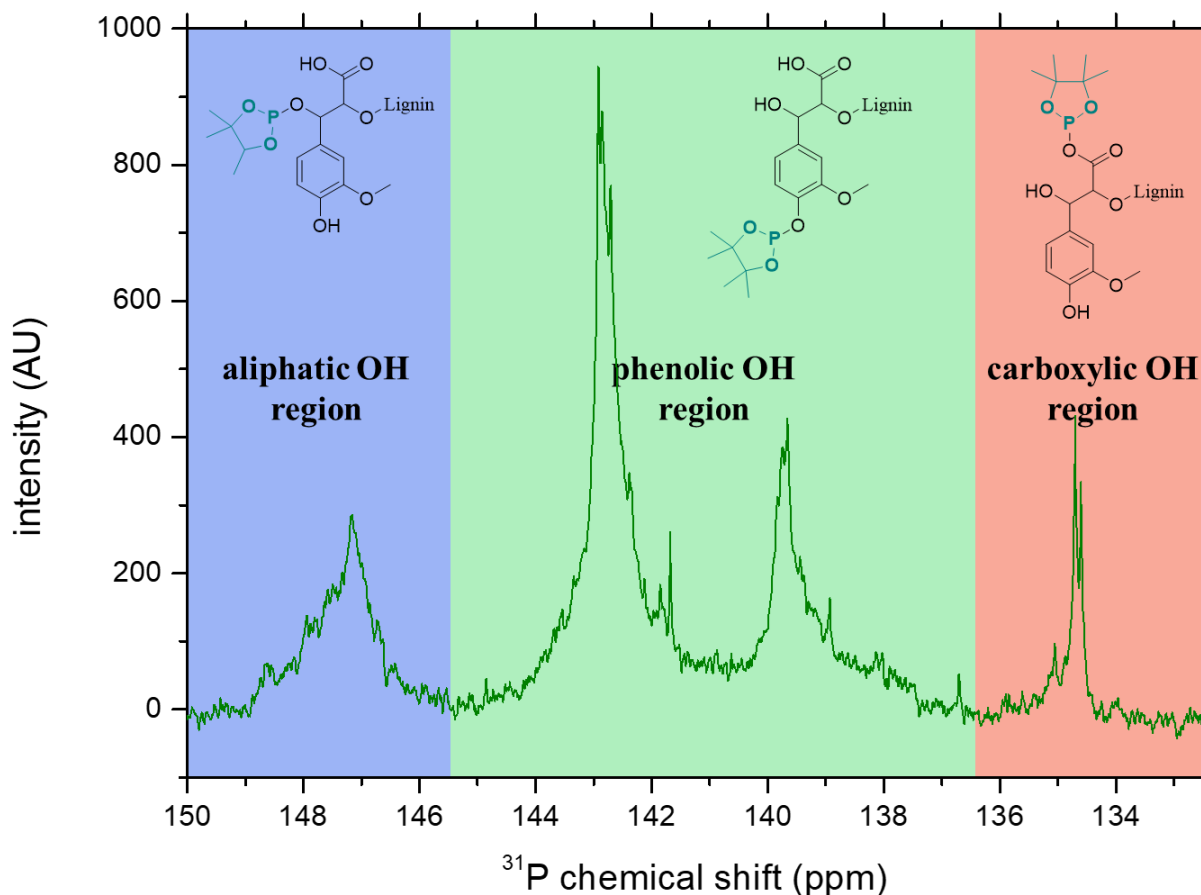


Figure 1.28. Derivatisation of lignin b-O-4' model compound with TMDP.

The reaction is performed in pyridine/CDCl<sub>3</sub>; pyridine acts both as solvent for the lignin sample as well as neutralising agent for the formed hydrochloric acid. CDCl<sub>3</sub> is used instead of normal chloroform so it can act as signal to lock the sample during the <sup>31</sup>P NMR analyses.

The use of TMDP as marking agent is not accidental. In fact, the derivatised hydroxylated groups with TMDP provide NMR signals characterised by specific chemical shifts, permitting their differentiation upon their nature (aliphatic, phenolic, and carboxylic). A schematisation for the various region of the  $^{31}\text{P}$  NMR spectrum of a derivatised lignin preparation is provided in Figure 1.29.



*Figure 1.29.*  $^{31}\text{P}$  NMR spectrum of a hardwood kraft lignin. The intervals of the spectrum corresponding to the various hydroxylated moieties are highlighted. In particular, aliphatic hydroxyl groups lie between 145 to 150 ppm, phenolic hydroxyl groups between 144 and 136.5, and carboxylic groups range between 136 and 134 ppm. Spectrum acquired with a *Bruker* 300 MHz NMR spectrometer.

TMDP permits not only to discriminate the hydroxyl groups in aliphatic, phenolic, and carboxylic, but it also allows to differentiate phenolic hydroxyl groups depending on their nature (e.g., guaiacyl, syringyl, p-hydroxy-phenyl, ...). With that regard, it is interesting to notice that another labelling agent was initially considered for the derivatisation of lignins, 1-chloro-4,5-dimethyl-1,3,2-

dioxaphospholane. Moreover, this reagent failed in providing reliable signals in distinguishing the various types of phenolic hydroxyl groups, so it was abandoned.

$^{31}\text{P}$  NMR is commonly used as a quantitative methodology to characterise lignins hydroxyl groups. In order to do that, the analysis is performed in presence of an internal standard (IS), such as cholesterol, which is phosphorylated at the same time of the sample. The peak area of IS then referred to the one of the lignin phosphorylated moieties and, by a simple mathematical calculation, the determination of the content of the various functional groups can be performed.

Another interesting aspect of  $^{31}\text{P}$  NMR analyses of lignin deals with the fact that the composition of the various types of phenolic hydroxyl groups coincides with the data obtained via nitrobenzene oxidation for the estimation of the S/G ratio (syringyl units/guaiacyl units); the advantage, in this case, is that the  $^{31}\text{P}$  NMR analyses is in a faster and easier than the nitrobenzene oxidation.

#### ***1.4. Kraft lignin: a focus on the chemistry of the most important technical lignin***

When referring to kraft lignin, the product resulting from the precipitation of black liquors from the wastes deriving from the separation of lignin from cellulose via the kraft process is referred. In the following paragraphs a brief overview on the reactions occurring during kraft pulping on lignin in lignocellulosic biomass, as well as the description of the major features of kraft lignin are provided.

##### **1.4.1 Reactions occurring during pulping**

For a long time the reactions occurring during kraft pulping were not properly understood;<sup>23</sup> moreover, the work of various researchers, in particular *Gierer*, helped understanding the chemistry of delignification. All these researches were elegantly and masterfully summarised in a couple of review papers appeared on *Wood Science and Technology* respectively in 1985 and 1986.<sup>68,69</sup> In these two papers not only sulfate pulp is reviewed, but also sulfite pulp is described in depth. More recently, *Gratz* and *Chen* reviewed again the topic considering also a process which seemed to be extremely promising at the end of the 20<sup>th</sup> Century, anthraquinone process.<sup>70</sup>

The lignin structures are affected by kraft process are:

- internal  $\beta$ -aryl glycerol ethers with free hydroxyl group in C $\alpha$ ;
- terminal  $\beta$ -aryl glycerol ethers with non-etherified hydroxyl groups in C $\alpha$ ;
- $\beta$ -guaiacyl-glycerol-1-guaiacyl bonds ( $\beta$ -1');
- $\alpha$ -ether bonds (phenylcoumarane and pinoresinol);

- methoxyl groups.

In the case of internal  $\beta$ -aryl glycerol ethers with free hydroxyl group in  $C\alpha$ , the hydroxyl group in  $C\alpha$  is firstly neutralised by alkaline conditions forming an alkyl-alcoholate; the benzylic alcoholate attacks, via nucleophilic substitution,  $C\beta$  forming an epoxide liberating a lignin residue. An additional hydroxyl ion from the reaction medium can finally act on the epoxide causing its opening reaction forming a vicinal diol. (Fig.1.30) This reaction pathway is slower than that occurring on substrate with free phenolic hydroxyl groups.

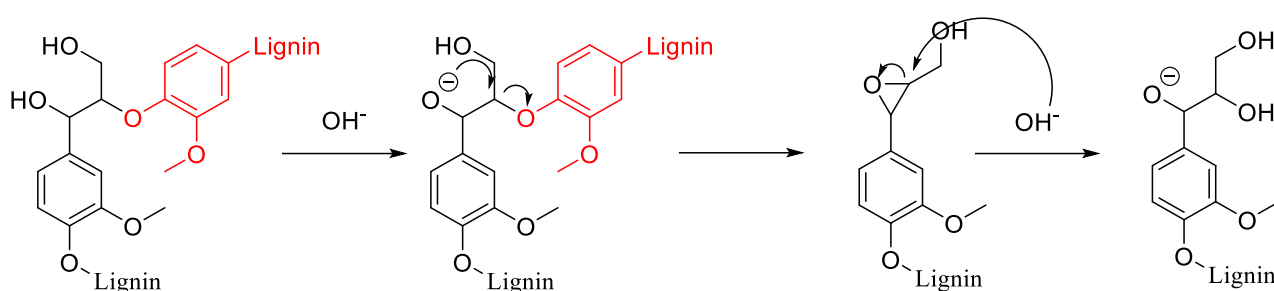


Figure 1.30. Degradation of guaiacyl-glycerol- $\beta$ -guaiacyl ether-like lignin structure in alkaline conditions.

In the case of  $\beta$ -aryl glycerol ethers with free hydroxyl groups in  $C\alpha$  and  $C4$  the reaction mechanism is slightly different. Initially, the neutralisation occurs on the phenolic hydroxyl group resulting in the formation of an aryloxy anion which promptly rearranges in the form of a quinone methide structure. The nucleophilic addition of a sulfhydryl anion, available in the pulping mixture, on quinone methide results in the restoration of the aromaticity of the system; then, the intermediate undergoes a nucleophilic substitution on  $C\beta$  forming a thiirane-like structure. Thiirane rearranges forming a quinone methide structure bearing a thiolate function on  $C\beta$ . Because of the drastic reaction conditions, sulphur is removed from lignin structure as elemental sulphur with the conversion of quinone methide structure to the corresponding arylenol. The arylenol, as well as the thiirane, are not stable forms. In fact:

- *arylenol structures* are converted into apocynin, via deformylation, or into vanillin via  $C\alpha$ - $C\beta$  cleavage;
- *thiirane structures* are transformed via the thio-ether bond opening resulting in the formation of 1-guaiacyl-2-mercapto-propan-3-ol; alternatively, the same substrate can undergo the elimination of sulfur as sulfide anion followed by the hydroxylation of both carbon atom in  $C\alpha$ - $C\beta$  allowing to obtain 1-guaiacyl-glycerol.

These mechanisms are summarised in Fig.1.31.

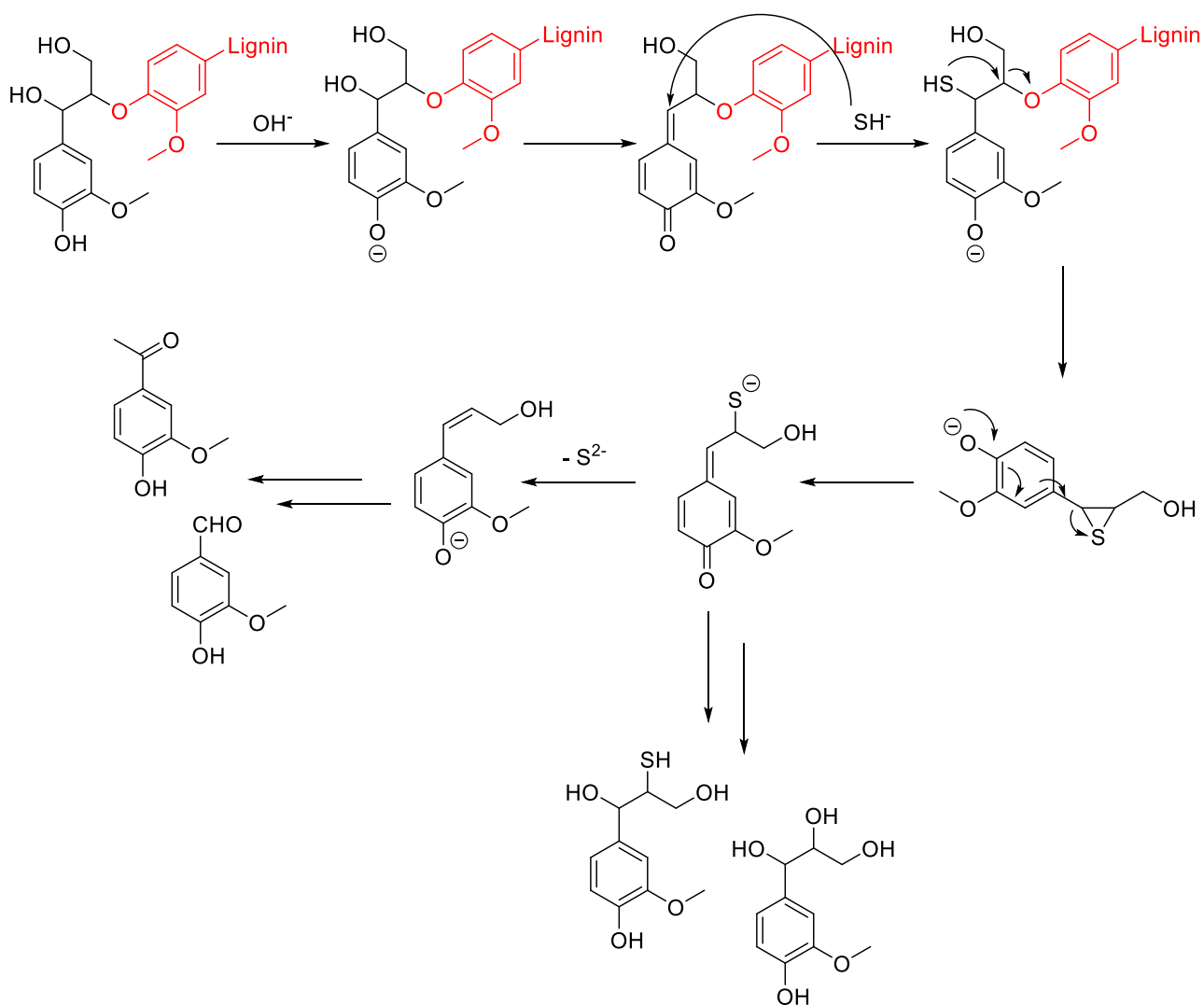


Figure 1.31. Degradation of guaiacyl-glycerol- $\beta$ -guaiacyl ether via nucleophilic attack of sulfhydryl anion.

$\beta$ -1' bonds undergoes a similar depolymerisation path, forming stilbenoid systems (Fig. 1.32). In particular, during the kraft cooking the tandem nucleophilic attack of hydrogenosulphide/hydroxyl ions produces a quinomethide structure. The elimination of the terminal carbon unit ( $\text{C}_\gamma$ ) of this species, as a formyl group, paves the way for the restoration of the aromaticity of the ring resulting in the formation of the stilbenoid bonding pattern.



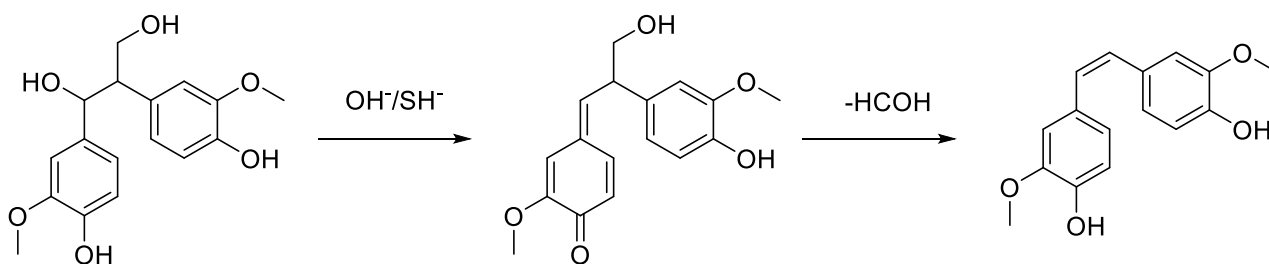


Figure 1.32. Degradation mechanism of 1,2-diguaiacyl-glycerol ( $\beta$ -1').

Pinoresinol and phenylcoumarane ether structures are not degraded under kraft pulping conditions. Instead, they rearrange generating stilbenes. For instance, in the case of terminal *phenylcoumarane* (Fig. 1.33), after the ionisation of the terminal phenol, the aryloxy anion rearranges to a quinone methide structure in presence of sulfhydryl anion. Finally, the deformylation in  $\text{C}\beta$  followed by the restoration of the aromaticity of the ring results in the formation of a stilbenoid structure.

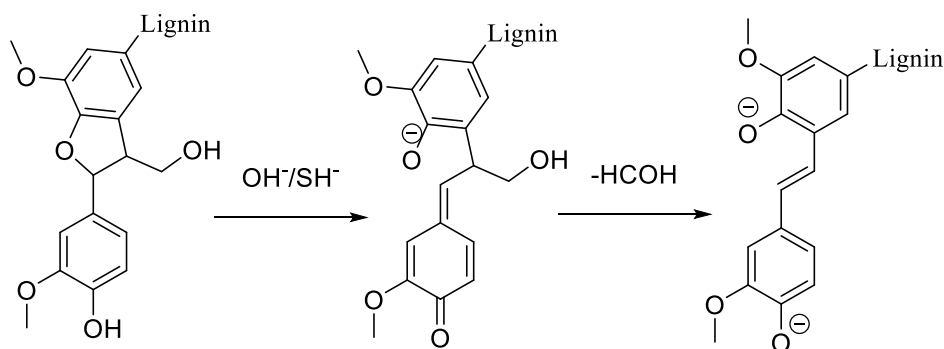


Figure 1.33. Reactivity of *phenylcoumarane* pattern under kraft pulping conditions.

For a long time it was believed that also lignin *condensation reactions* would have occurred during kraft pulping. This hypothesis was elegantly summarised by *Gierer* in 1970, who carefully rationalised the mechanisms for the formation of  $\alpha$ -5',  $\alpha$ -1', and *diaryl methane* bondings.<sup>71</sup> Moreover, as of now these theories are confuted by part of scientific community owing to the lack of spectroscopic proofs confirming the existence of condensed bonding-pattern in kraft lignins.

Finally, the nucleophilic attack of sulfhydryl anion on lignin methoxy groups results in their dealkylation with the formation of new hydroxy groups in C3 and C5 positions. In the case of the attack of terminal phenolics, catechol groups are formed. The by-product of the demethylation reaction is mercapto-methane, the sulphonylated equivalent of methanol. In kraft pulping conditions, mercapto-methane acts in the same way as sulfhydryl anion; in fact, it demethylates lignin becoming converted into dimethyl-mercapto-ether, the sulphonylated analogue of dimethyl ether. Finally, due

to the harsh reaction conditions at which Kraft delignification is performed, dimethyl-mercapto-ether is oxidised into dimethyl-disulphide, an extremely odoriferous compound.

### 1.4.2 On the structure of Kraft lignin

For a long time, the only model to describe its structure was the one developed by *Marton* in 1968, and further reported in *Sarkanen – Ludwig* treatise on lignins.<sup>72</sup> This structure is reported in Fig.1.34 and, in the point of view of *Marton*, it would have sufficed to depict pine kraft lignin.

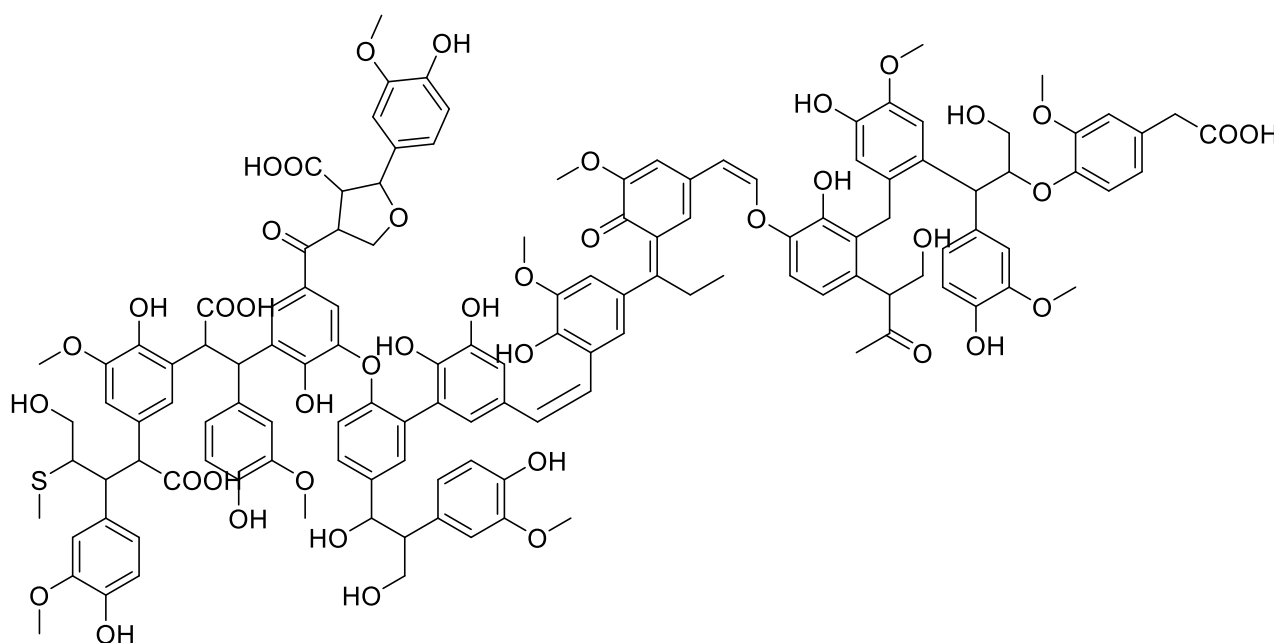


Figure 1.34. Pine kraft lignin structure according to *Marton*.

Not only the lack of pinoresinols units ( $\beta$ - $\beta'$ ) can be noticed in *Marton*'s model, but also the formation of rings condensation with formaldehyde (deriving from the demethylation of methoxyl groups) as well as the oxidation of terminal alcohols (C $\gamma$ ) in carboxyl group, the formation of carbonyls, stilbene units (1,2-diaryl-vinyl systems), and the presence of sulfhydryl groups are evident.

In perspective, *Marton*'s effort is extremely valuable, as rigorously rationalised all the data available at the time on kraft pulping reactions occurring on lignin structure. In addition, this models permitted to justify the dark colour of kraft lignin as it couples unsaturated systems in such a way to have chromophore centres.<sup>73</sup>

This model has been used for almost fifty years; then, *Crestini* was able to review the results of *Marton* in such a way to offer a completely different view of softwood kraft lignin.<sup>74</sup> The approach

followed by *Crestini* for the characterisation of softwood kraft lignin was based on the coupling of standard spectroscopic techniques, such as quantitative  $^{13}\text{C}$  NMR, with  $^{31}\text{P}$  NMR and semiquantitative HSQC NMR spectroscopy, and a fractionation processes followed by the optimised gel permeation chromatography (GPC) system she developed in 2016.<sup>75</sup>

GPC analyses permitted to discover the existence of two fractions in kraft lignin, a high molecular weight one and a low molecular weight one. These two fractions differ each from the other not only for the molecular weight and various bonding pattern occurring in their structures, as demonstrated by the use of semiquantitative HSQC, but also for the content of the various hydroxylated moieties. With that respect, *Crestini* concluded that the low molecular weight fraction of kraft lignin is characterised by a highly condensed structure, resembling those of tannin-like polyphenolic materials; the high molecular weight fractions is more similar native lignin, differing for the high dealkylation degree of the side chains (demethylation).

In order to understand the genesis of these two fractions, the gel-degradation theory can be considered. In fact, lignin degradation mechanisms under kraft conditions resembles to the opposite of standard polymerisation mechanisms, where monomeric molecules initially interact each other resulting in the formation of oligomers. On their turn, oligomers polymerise again generating polymeric chains. This mechanism is not infinite; in fact, when the interacting oligomers reach a certain level of complexity, the polymerisation mixture turns into a gel (the moment is indicated as “*gelation point*”), practically stopping the reaction. Similarly, the degradation of lignin can be considered as a process starting with the elimination of low-molecular weight compounds from wood. Then, as the pulping proceeds, the complexity of the lignin parts removed by the action of  $\text{OH}^-/\text{SH}^-$  increases, removing initially monomeric compounds, then oligomers. The degradation process should theoretically continue up to the *de-gelation point*, where the lignin chains are completely removed from wood; unfortunately, this event never occurs during pulping.

In conclusion, from one side, the high molecular weight fraction can be seen as the result of the extensive depolymerisation of lignin, which is also justified by the extend of the degradation of its chains. From the other side, the acetone soluble can be considered as the product of the re-condensation process involving low molecular weight compounds deriving from lignin.

The softwood Kraft lignin model developed is depicted in Fig.1.35.

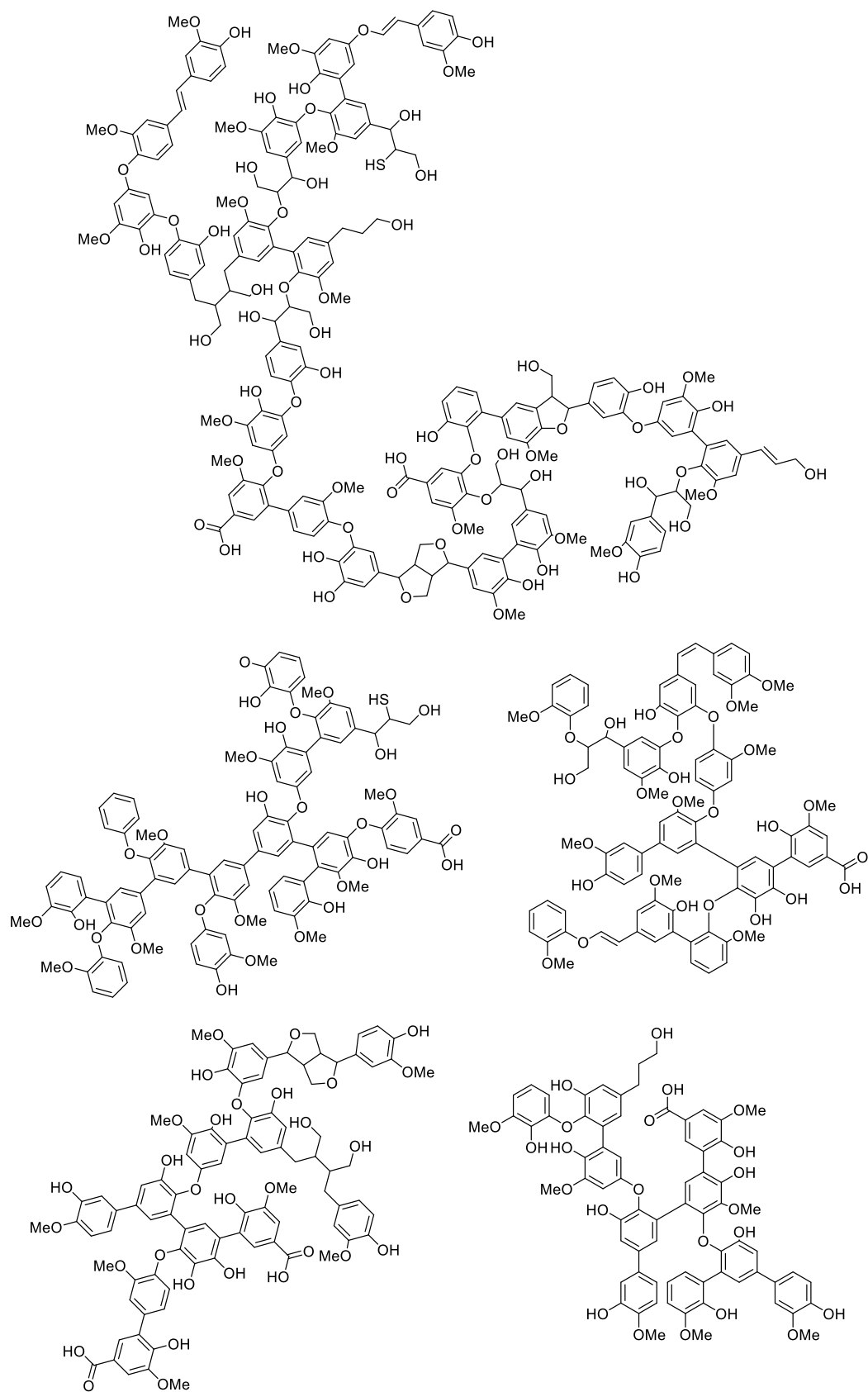


Figure 1.35. Softwood Kraft lignin structure according to *Crestini*.

### ***1.5. On the actual promising pathways for the valorisation of lignin***

The annual production of kraft lignin is unneglectable; in fact, a recent study demonstrated that for every tonne of pulped birch or pine, an amount between 330 to 490 kilogrammes of lignin can be obtained.<sup>76</sup> With that in mind, by considering that the annual production of pulp in 2020 reached 116 millions of tonnes, it is not surprising to notice that the annual production of lignin ranges between 50 to 70 millions of tonnes.

In the case of pulping industry, lignin does not represent a real waste. In fact, by burning lignin, energy can be produced and used for routine operations of the chemical facilities. Moreover, this use is extremely limiting, as it does not consider the aromatic polymeric structure of lignin. In view of that, in order to fully profit of its chemical nature, as well as its abundance and relatively low cost (100-300\$ per tonne, depending on the purity degree), different valorisation pathways have been suggested in the last decades. *Nadányi* recently summarised the major applications for technical lignins.<sup>77</sup> In particular, the following are of particular relevance:

- *Lignin biocomposites*. The coupling of lignin with natural-fibrous materials results in an enhancement of the physical and thermal properties of these materials. In particular, these products have shown potential applicability in car industry, especially as acoustical and thermal insulators.<sup>78</sup>
- *Production of bio-oil*. The application of thermochemical processes to lignin allow the production of mixtures rich in high-value phenolics, like guaiacol, syringol, vanillin, *p*-vinyl-guaiacol, and other aromatic alcohols. These compounds constitute the so called “bio-oil”, whose potential is now at the centre of various investigations in order to exploit its potential as bio-fuels which can substitute oil-deriving ones.<sup>79</sup>
- *Production of benzene, toluene, and xylene*. Benzene, toluene, and xylenes constitute one of the most valuable fraction of oil, the so-called *BTX-fraction*. In fact, these products play a pivotal role in modern organic industry, as they are the platform chemicals for several bulk chemicals (e.g. production of acetone, phenol, terephthalic acid, ...) which are fundamental for other productions (e.g. resins, synthetic fibres, ...).<sup>80</sup> The application of catalytic hydrogenolytic treatments on lignin substrates demonstrated their efficiency in the isolation of BTX; as of now, the development of selective catalytic process for the selective isolation of one of the aromatic compounds is the challenge.<sup>81</sup>
- *Production of low-molecular weight alcohols for polyurethanes industry*. Owing to the polyol nature of lignin, its potential reactivity with di-isocyanates (especially toluol-di-isocyanate) has been recently investigated in order to produce a new class of bio-polyurethanes.<sup>82</sup> With

that regard, not only unmodified lignin, but also polyols deriving from the depolymerisation of lignin have been used.<sup>83</sup>

- *Production of resins.* Phenolated resins are among the most important marketed resins. The possibility to use lignin in phenolic-resins in order to substitute oil-based phenols is a current research topic, showing promising results, especially in terms of water-barrier-effect.<sup>83</sup>
- *Lignin-based nanomaterials.* Promising lignin-based nanomaterials which are expected to have potential applications are carbon nanofibers and nanoparticles. The substitution of unsustainable polyacrylonitrile-deriving carbon nanofibers can be conveniently achieved by the use of lignin. With that regard, the spinning of lignin solutions via the use of advanced techniques (e.g. electrospinning<sup>84,85</sup>) followed by the carbonisation/thermostabilisation steps seems a promising approach.

Of all of these applications, in order to maximise the potentialities deriving from the polymeric nature of lignin as well as its aromaticity and capability to self-aggregate, particular relevance has recently been given by the lignin community to lignin-based nanoparticles (LNPs). As it is going to be discussed in the following paragraph, their preparation is relatively simple, if compared to the other approaches to valorise lignin, and their applicability in the production of fine chemicals is extremely appealing.

### ***1.6. Lignin nanoparticles: small size high-value applications***

Even if the existence of particles from technical lignins was known since the Sixties of the Last Century (e.g. *Goring et al.* identified and analysed sodium lignosulfonate particles via electron microscopy in 1964<sup>86</sup>), LNPs were firstly critically considered by *Frangville* only in 2012.<sup>87</sup> Since that moment, an exponential growth in the interest for these nanomaterials have been reported not only for their higher sustainability if compared to traditional nanoparticles, but also for the wide variety of high-value applications LNPs have demonstrated in both biomedical and material science areas. From one side, biomedical applications as antibacterial,<sup>88-90</sup> antioxidant,<sup>91,92</sup> drug- and carry-delivery systems<sup>93-95</sup> have been demonstrated. From the other, their potential use in preparation of advance nanocomposites<sup>96</sup> or UV-absorbents<sup>82,97</sup> absorbents have also been demonstrated.

With respect to the strategies to prepare LNPs, different approaches have been suggested during the last ten years. Review papers on the existing scientific literature have already been published. Of particular interests the works of *Zhao*, *Beisl*, and *Iravani* are among the most quoted.<sup>98-100</sup>

In general, the preparation of LNPs can be achieved by various strategies which can be divided in two major classes, *precipitation* and *non-precipitation* techniques.

On the one hand, precipitation techniques represent a wide group of approaches involving the isolation of LNPs by acting on the composition of the solvent system in which lignin has been previously dissolved. Acid-catalysed precipitation, flash precipitation, dialysis, solvent-exchange, and supercritical antisolvent processes are the most important strategies. Acid precipitation is based on the preparation of alkaline solutions of lignin followed by the drastic pH-change via the addition of strong inorganic acids (e.g. nitric acid).<sup>87</sup> The disadvantage of the acid precipitation is represented by the long time required to acidify the lignin solution, resulting in aggregation phenomena of the already formed LNPs. In order to overcome this issue, flash precipitation was developed; in this case the acidification of the lignin solution is not gradual but drastic and instantaneous, followed by the dilution of the solution to stop the aggregation process.<sup>101</sup> Dialysis processes profit of the use of dialytic membranes for the removal an organic solvent from a lignin solution in an organic solvent/water solution resulting in the isolation of LNPs.<sup>92</sup> Solvent exchange methods are the methods nowadays most commonly used relying on the dissolution of lignin in an organic solvent followed by a dilution step with water. The drastic exchange in the environment surrounding solvated lignin molecules permits the aggregation of LNPs. Various solvents have been considered in view of that, like acetone, ethanol, and tetrahydrofuran (THF), moreover the one which seemed to be the more promising has been identified in THF or ethanol-water mixtures (70:30).<sup>94,102,103</sup> Finally, supercritical antisolvent processes are based on the interaction of supercritical carbon dioxide with lignin solutions, causing the precipitation of LNPs.<sup>104</sup>

On the other hand, non-precipitation techniques profit of chemical and physical phenomena favouring the aggregation of LNPs. This class of methods include homogenisation, emulsification, and sonochemical synthesis approaches. Homogenisation-based methodologies involve the shearing of lignin preparations by the use of mechanical or pressure effects on lignin preparations.<sup>105</sup> Emulsification processes are based on the preparation of lignin dispersion by the use of an emulsifier; the resulting emulsions are then treated with a reticulating agent (e.g. epichlorohydrin) which is finally cross-linked resulting in the isolation of LNPs.<sup>106</sup> Finally, sonochemical synthesis of LNPs relies on the activation of lignin molecules via the use of a radiation driving to the formation of radicals. Then, these radicals undergo re-polymerisation forming new aggregation networks corresponding to LNPs.<sup>107</sup>

In general, the size of LNPs size obtained with the various strategies ranges from 10 to 1200 nm. The shape of them is not only spherical; in fact, also irregular, hollow spherical or, cuboidal particles were noticed.<sup>87,104,105,108–110</sup>

In order to modulate the properties of LNPs, especially their size and hydrophobicity, which are respectively correlated to their biocompatibility and possible applicability for the preparation of composite materials, the control on the structure of the lignins used for their preparation plays a pivotal role. In fact, the modulation of the content of specific functional groups seems a reasonably convenient strategy for tailoring of LNPs properties. With that regard, particular relevant seems to be the content of hydroxyl groups, as this parameter is already known for being involved in the LNPs aggregation phenomena.<sup>111</sup>

### ***1.7. Tailoring the structure of lignin preparations via the use of laccases. An evergreen in Lignin Chemistry***

In view of tailoring the chemical and physical properties of lignins prior to nanosizing, two types of approaches can be considered, stoichiometric and catalytic methodologies. From one side, stoichiometric approaches commonly results in a targeted functionalisation of certain domains. An example of that is provided by the previously mentioned acetylation treatments (see [Paragraph 1.3.4.1](#)), which selectively esterify lignin hydroxylated moieties resulting in an implementation of the hydrophobicity of the treated sample. Moreover, on the large scale, these processes are critical as the evaluation of the cost of the derivatising agent as well as the need to carefully control the efficacy of the derivatisation are unneglectable. From the other side, the use of catalytic strategies to achieve modification operations, like oxidation or depolymerisation reactions, are sustainable on the large scale, especially when an efficient and robust catalyst is used (especially if it can be conveniently recycled). Moreover, not all catalytic processes are selective to a specific transformation or to a functional group. Additionally, in some other cases, the conditions required for the efficient use of catalysts are particularly harsh, especially in oxidation and reduction treatments, resulting also in the competitive thermal degradation of lignin. An alternative to the standard catalytic system is represented by the use of milder biotechnological approaches. In particular, by profiting of the gentle conditions at which microorganisms operate, as well as their high selectivity for certain types of substrate, they can conveniently transformation the lignocellulosic biomass. Moreover, the degrading mechanisms operated by microorganisms relies on the capability of these organisms to secrete certain types of enzymes, which can efficiently modify lignocellulosics. Different enzymes are nowadays



known in the area of wood biodegradations, moreover the focus of the upcoming paragraphs would be on laccases. In fact these enzymes are a promising ally in the modification of lignin and in the following paragraphs, after a short introduction on the role of microorganisms on the biodegradation of lignin, a description of their catalytic features, as well as their decaying action on lignin is provided.

### **1.7.1 Which are the lignin degrading microorganisms and what do they have in common?**

The microorganism-induced biodegradation of woody tissues is a phenomenon causing the decomposition of lignocellulosic biomass and its organization as carbon dioxide. With regards to the specific degradation of lignin, until the Sixties it was believed that the only type of microorganisms able to carry out its degradation was a specific type of fungi, the so called “white-rot fungi” (WRF). Moreover, later researches demonstrated the ability of “brown-rot fungi” (BRF) and bacteria to degrade lignin also.

WRF were generally described by *Käärrik* as a class of fungi causing the extensive degradation of both the polysaccharidic and lignin domains in wood.<sup>112</sup> *Polyporus versicolor*, *Polyporus berkeleyi*, and *Trametes versicolor* are just some example of which demonstrated extensive degradation activity against lignin domains in wood.<sup>113–115</sup> A preferential degrading activity against lignin was not demonstrated for all the WRF; in fact, only some of them seem to selectively decompose lignin without modifying the polysaccharidic domains, like *Polyporus versicolor*. The reason for these results can be found on early studies by *Ishikawa* who demonstrated that WRF producing high amount of enzymes catalysing the degradation of phenolic systems (the so called *phenoloxidases*) degrade lignin more extensively than those that do not.<sup>116,117</sup> The general effect of WRF on lignin preparation was extensively studied. Even if the decrease in the content of methoxy groups coupled with an incrementation in the content of carbonyl groups was demonstrated, no significant variation in the molecular weight of lignin preparation was observed.<sup>31,116–118</sup>

Differently from WRF, BRF are characterised by a high selectivity for the degradation of the polysaccharidic part of wood; in fact, the residues of BRF-degraded lignocellulosic biomass is mostly represented by lignin. Even if BRF can fully degrade cellulose and hemicelluloses, their action also result on a partial degradation of lignin part of wood, as observed by *Kirk*. In particular, by analysing a milled wood lignin isolated from spruce treated with *Poria monticola*, he was noticed a drastic decrease in the content of methoxy groups, on either guaiacyl or syringyl moieties.<sup>119</sup> Subsequent studies by the same *Author* on the same substrate using a different BRF, *Lenzites trabea*,

demonstrated also the increase in content of phenolic hydroxyl groups, deriving from the fungi-induced direct hydroxylation, as well as the augmentation of carbonyl and carboxyl groups, similarly to what was previously observed for WRF-decayed lignins.<sup>32</sup>

Finally, bacterial degradation of lignin was for a long time a debatable topic; in fact, when *Ander* and *Eriksson* critically reviewed the existing literature older than 1978, they concluded that some of the proofs testifying the bacterial-degrading activity for lignin substrates were misleading.<sup>120</sup> Among the various bacteria with confirmed lignin-degrading activity, *Pseudomonas* seem the more promising for the degradation of different types of lignin preparations (milled-wood, acidolysis, and Kraft).<sup>121-123</sup> Unfortunately, little details are available on the changes actually occurring on lignin structure after the bacterial treatment, as the majority of the studies is focussed especially on the effective degradation to carbon dioxide.

As mentioned above, WRF, BRF and bacteria capable to degrade lignin substrates are able to synthesize proteins catalysing the decay of lignin. These proteins pertain to a class of enzymes which is generally referred to as *phenoloxidases*. Phenoloxidases are divided in two sub-categories, *peroxidases* and *laccases*. Both of them cause the oxidation of lignin via the transfer of electrons from the phenolic substrate to an electron acceptor. The major difference between lignin-degrading peroxidase (manganese peroxidases) and laccases is represented by the type of metal centres involved in the redox process and the electrons acceptor used. In fact, if manganese peroxidases profit of Mn(II)/Mn(III) centres and hydrogen peroxide to catalyse the oxidation, laccase are based on the Cu(I)/Cu(II) redox couple and oxygen as electrons acceptor.

Laccases and peroxidases have been critically considered for the valorisation of lignin. Moreover, in view of scaling up their use in the industry, peroxidases seem to be more critic if compared to laccases. In fact, the major limitations derive from the use of hydrogen peroxide as electron acceptor. From one side, hydrogen peroxide is more expensive than oxygen. From the other side, hydrogen peroxide is a strong oxidising agent. This fact would result in a higher corrosion of the industrial apparatus used, meaning higher costs. Consequently the use of laccases seems to be more favourable.

Three aspects should be considered while working with laccases:

- the structure of the catalytic site;
- the mechanism of action on phenolic substrates;
- the mechanism of action of mediators in order to extend the oxidising power of laccases not only to phenolic substrates, but also to non-phenolic hydroxyl groups.

All these topics are going to be discussed in the following paragraphs.

## 1.7.2 On the structure of laccase

Laccases are extracellular glycoproteins characterised by molecular weight ranging from 60 to 80 kDa, of which almost the 20% is represented by a carbohydrate-part.<sup>124,125</sup> As it has been previously mentioned, the origin of the catalytic activity of laccases resides on the presence of copper atoms. In fact, for each laccase molecule, four copper atoms can generally be found. These atoms are not chemically equivalent. In fact, they differ each from the other because of their chemical-physical features. The first researcher demonstrating this fact was *Nakamura*, who noticed that the absorption spectrum of copper in laccase was characterised by the presence of two maxima (280 and 615  $\mu\text{m}$ ).<sup>126</sup> This observation paved the way for further spectroscopic analyses, especially electron paramagnetic resonance analyses, permitting to discern the existence of three different types of copper atoms per molecule of laccase.<sup>127,128</sup> In fact, copper centres are nowadays classified as type 1, type 2, and type 3 centre. The type 1 centre is constituted by one copper atom and it is called “blue copper”. The type 2 centre is represented by a single copper atom. The type 3 centre is constituted a binuclear antiferromagnetic copper complex. A schematisation of laccase structure is provided in Fig.1.36.

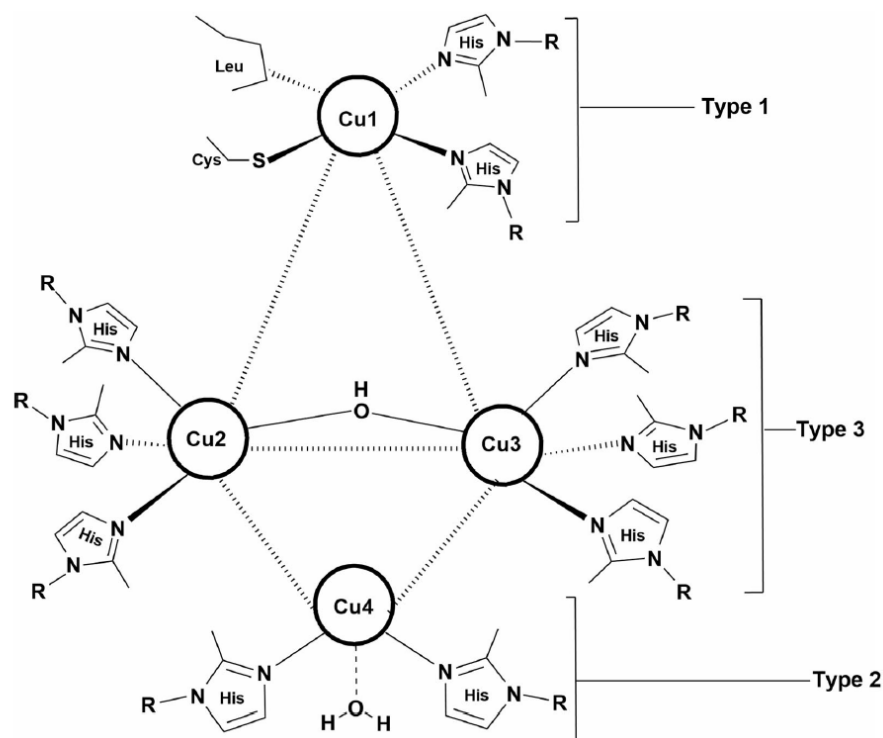


Figure 1.36. Graphic schematisation for the structure of a laccase. The presence of three copper centres characterised by different structural features is highlighted.<sup>125</sup>

As it was highlighted by *Thurston*, the analyses of the copper content in fungal laccases can sometimes provide results suggesting that only three atoms per laccase molecule are available.<sup>129</sup> Moreover, as it was demonstrated by *Reinhammar*, type 2 copper centre is particularly labile, and extensive purification steps via electrophoresis can favour the release of that centre, resulting in misleading characterisation results.

Of the three copper centres, only type 1 is directly involved in the oxidation of substrates. In fact, the “blue copper” acts in the electrons subtraction from the substrate oxidised. Then, the removed electrons are transferred to the type 3 and type 2 centres, which are finally used for the reduction of oxygen, the final electron acceptor, which is converted into water. The complete redox cycle for an oxygen molecule requires the removal of four electrons from the substrate.

The ability of a laccase to decay a phenolic substrate is dependent on the difference in redox potentials between the type 1-copper centre of laccase and the one of the substrate that has to be transformed.<sup>130</sup> Depending on their origin (WRF, BRF or bacterial), natural laccases have redox potentials ranging from 120 to 800 mV. Therefore, as the redox potential of phenolic systems lie between 500 to 1000 mV, it becomes clear why the electron abstraction laccase-catalysed is possible. Moreover, differently from phenolics, other hydroxylated moieties, like aliphatic alcohols, are characterised by higher redox potentials (>1000 mV); in view of that, their laccase-catalysed oxidation is not possible if no other compounds (see [Paragraph 1.7.4](#)) are used.

### **1.7.3 On the action of laccase on phenolic substrates**

The basis to elucidate the action of laccase on lignin are represented by the activation mechanism that these enzyme causes on phenolics and the identification of the target substrates. With that regard, the pioneering studies of *Becconsall*, *Benfield*, and *Fahraeus* should be mentioned. *Becconsall* discovered that certain types of enzyme can activate phenolic substrates via the formation of aryloxy-radicals.<sup>131</sup> *Benfield* confirmed the findings of *Becconsall* for laccases, demonstrating also the oxidising power of laccases from *Polyporus Versicolor* and *Rhus Vernicifera* on *p*-catechol and syringol, highlighting that depending on the origin of the laccase the optimum pH for their action varies.<sup>132</sup> Finally, *Fahraeus* observed the selectivity of laccases for phenolic substrates, like catechols, hydroquinones, guaiacol and its derivatives, resorcinol, and phloroglucinol.<sup>133</sup>

With these premises in mind, the of the action of laccases on lignin started at the end of the Sixties. The approach which has been followed for decades has been based on the treatment of model compounds mimicking limited part of lignin structure with the enzyme. These compounds were

mostly composed of two aromatic rings linked together especially with  $\beta$ -O-4' and  $\beta$ -1' linkage patterns. The analysis of the degradation products has been used to generalise the so obtained results on both native and technical lignins.

Among the first studies on laccase-catalysed oxidation of lignin particularly important is the works of *Kirk*. In fact, *Kirk* was the first who carefully investigated the action of fungal extracts on syringyl- $\beta$ -guaiacylglycerol ether and the counterpart containing a carbonyl on  $C_\alpha$ . In the first case, he demonstrated that the action of fungal enzymes resulted on the activation of syringyl- $\beta$ -guaiacylglycerol model resulting in two types of reactions: (a) the formation of 4-O-1' ethers, and (b) the  $C_\alpha$  oxidation of the model. In particular, in both cases the formation of the aryloxy radicals on the C4 of the syringyl moiety is the first step. Then, the re-arrangement of the structure in a quinone-like system follows with the subsequent attack on C1 radical by another aryloxy radical, generating guaiacoxy-acetaldehyde and (4-syringoxy)-syringylglycol- $\beta$ -guaiacyl ether. Alternatively, the protonation of the ether oxygen, the rearrangement of the quinone into a form containing a double-bond on the C3-position with the methoxy group, and the re-aromatisation of the ring results on the product of benzylic hydroxyl group oxidation (formation of a carbonyl on the  $C_\alpha$ ). In the second case, with the carbonyl-containing compound on  $C_\alpha$  position, he observed the formation of the same type of product described in the first case, corresponding to the 4-O-1' ether (and guaiacoxy acetic acid).<sup>134</sup> Even if the researches of *Kirk* were pivotal in order to lay the foundations for a rigorous study of the action of laccases against phenolic substrates, the use of fungal extracts represents a critic point. In fact, the extracts used were a mixture of enzymes deriving from the mycelia of mushrooms containing, in perspective, not only laccases. In view of that, more precise studies were needed. An answer to this need was provided by a couple of papers by *Kawai* of 1988 and 1993; these studies provided insightful information on the laccase-catalysed decay of respectively  $\beta$ -1' and  $\beta$ -O-4' lignin units, the most abundant bonding patterns in both angiosperm and gymnosperms lignins.<sup>135,136</sup> In these studies the use of  $\beta$ -1' and  $\beta$ -O-4' model compounds permitted to generalise the action of laccase onto three types of reaction mechanisms:

- ***alkyl-aryl cleavage***, causing the cleavage of the bond linking C1 with  $C_\alpha$ . The products of this reaction are a phenol containing a hydroxyl group on C1, and an aldehyde corresponding to the former C3-chain with the formyl group on former  $C_\alpha$ .
- ***$C_\alpha$ - $C_\beta$  cleavage***, causing the cleavage of the bond linking  $C_\alpha$ - $C_\beta$  on the aliphatic C3-chain without damaging the aromatic rings. On former  $C_\alpha$  a formyl group appears, while on  $C_\beta$  an hydroxyl groups results.
- ***$C_\alpha$ -oxidation***, causing the oxidation of the benzyl hydroxyl group into a ketonic carbonyl.

The products resulting from these decay mechanisms for a guaiacyl-glycerol- $\beta$ -guaiacyl model are summarised in Fig. 1.37.

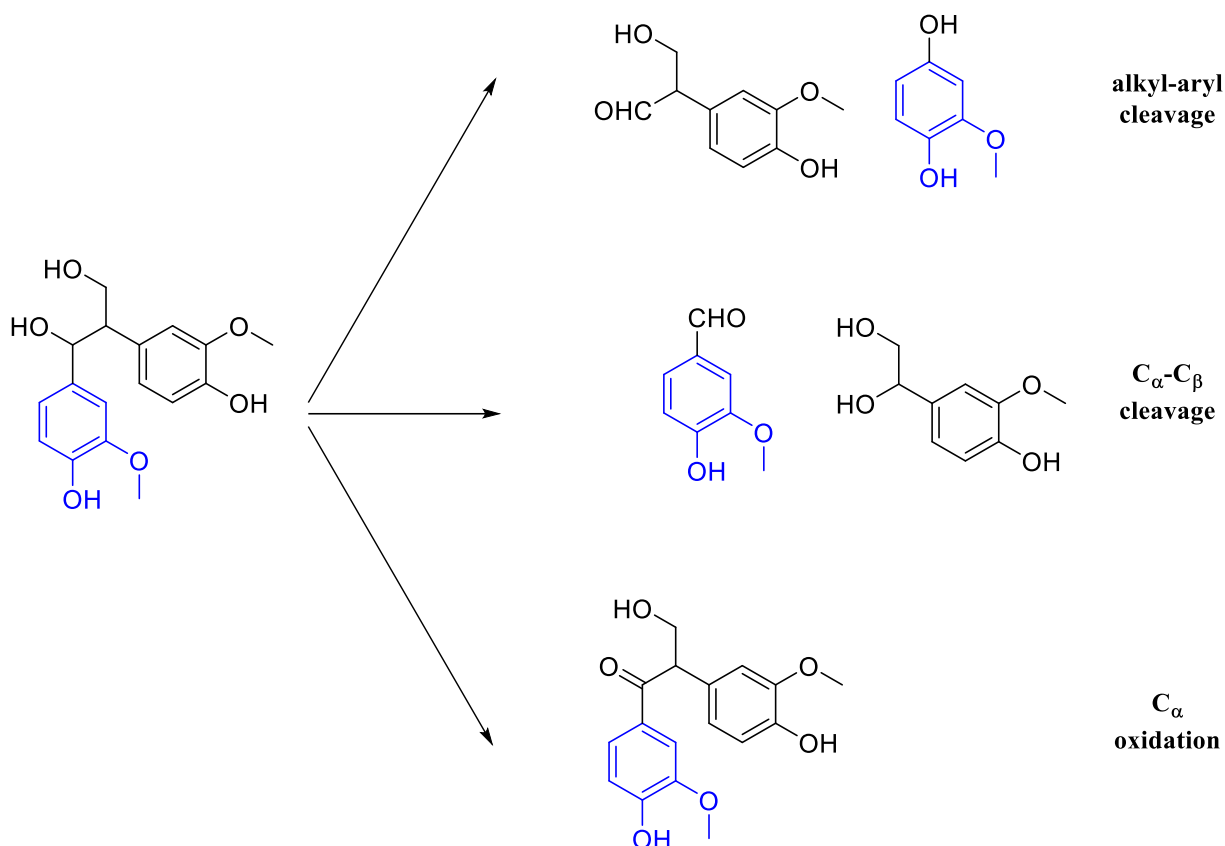


Figure 1.37. Degradation products from laccase-oxidation of guaiacyl-glycerol-2-guaiacyl model compound according to *Kawai*.

These pathways are still a powerful rationalisation permitting to understand the formation of low-molecular weight compounds during the decay of lignin when it is treated with laccases. Unfortunately, the efficacy of the models used by *Kawai* to describe the transformation occurring on technical lignins is limited. In fact, technical lignins contain lower amount of  $\beta$ -O-4' bonding patterns than native lignin, due to the reactions occurring during pulping. In addition, new structures can be found in Kraft lignins which are not available on native lignins. These species are biphenyls (5-5'), and stilbenes.<sup>137-139</sup> In order to elucidate the effect of laccases on technical lignins, *Crestini* made a meticulous screening on the action of laccase against lignin model compounds for these structures.<sup>140</sup> The results of her research can be summarised as it follows:

- diaryl-methanes ( $\alpha$ -5') are partially demethylated, with a partial oxidation of methyl groups with partial hydroxylation of formation of formyl groups;

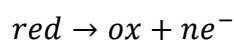
- biphenyls (5-5') undergo either demethylation or oxidation of linked methyl groups with the formation of formyl groups;
- stilbenes are mostly stable to laccase-catalysed oxidation.

All the data deriving from the researches on model compounds supported the existing studies suggesting that laccases play a relevant role in the reactions occurring during ligninolysis.<sup>141,142</sup> Moreover, it should also be noticed that laccases are also involved in the synthesis of lignin from the monolignols; in fact, they serve as radical generators promoting then the polymerisation.<sup>143</sup> In view of that, the action of these enzymes on lignin should be seen from two different perspectives. From one side, the depolymerisation can occur resulting in the formation of low-molecular weight compounds. From the other side, the radical formed by the action of laccase on lignin can also result in an additional polymerisation, resulting in the increase of the molecular weight of lignin. However, the depolymerisation of lignins was demonstrated only by poor evidences; in fact it was observed only for synthetic lignins (DHP) rich in free phenolic groups, which are way different from real samples.<sup>144,145</sup> This fact convinced that the only reasonable pathway for laccase-mediated lignin oxidation is represented by the polymerisation.

In perspective, even if the overall reaction pathway for the oxidation of lignin with laccases is generally elucidated, there is still confusion on the effects of these enzymes on lignin. In particular, it remains unclear the extent of the modifications that can occur on the substrates, as well as the possibility to tailor the effect of the enzyme or to control the release of certain low molecular weight compounds from lignins.

#### **1.7.4 Laccase redox-mediators: overcoming the energetic barrier to oxidise non-phenolic substrates**

As already mentioned, in order to accomplish the oxidation of a compound, the reduction potential of the oxidising system has to be way more higher than that of the substrate to transform. In the case of laccases, as previously mentioned, their standard reduction potential ( $E^0$ ) lies between 120 and 800 mV; moreover, these  $E^0$  are lower than those of the most abundant aliphatic structures of lignin, *guaiacyl-glycerol- $\beta$ -guaiacyl ether* and *2,3-diguaiacyl-propan-1-ol* units (>1000 mV). Consequently, the oxidation of aliphatic moieties in lignin via laccase is technically unfeasible. Moreover, by considering the generic redox system:



it is well known that the reduction potential varies according to the *Nernst* equation:

$$E = E^0 + \frac{R \cdot T}{n \cdot F} \cdot \ln \frac{[ox]}{[red]}$$

where  $E^0$  is the standard redox potential of the system,  $R$  is the gas-constant ( $8.314 \text{ J}\cdot\text{mol}^{-1}\cdot\text{K}^{-1}$ ),  $T$  is the temperature at which the potential has to be estimated,  $n$  is the number of electrons exchanged in the redox system,  $F$  is the *Faraday* constant ( $96485 \text{ C}$ ),  $[ox]$  is the molar concentration of the oxidised form in the system, and  $[red]$  is the one of the reduced form at the same time.

In view of that, it seemed reasonable the possibility to tailor the reduction potential of laccases in order to expand their catalytic activity also against non-phenolic substrates. As the modulation of the concentration of the species was not a feasible operation (according to *Nernst* equation), studies on the use of redox mediators favouring laccase activity appeared at the beginning of the Nineties.

Mediators are electron transferers; their action is based on their activation, on the type 1 copper centre in laccase, resulting in the generation of a radical species. Then, these laccase-activated radical species can diffuse into the non-phenolic moieties of the substrate. The interaction of the activated mediator molecules with suitable substrate (*e.g.* an hydroxyl group) cause the depletion of electrons of the last, converting again the mediator in its un-active form (no-radicals) that can once-again be activated by laccase. Practically, the laccase/mediator system can be seen as a bi-cyclic transformation, where oxygen and lignin substrates act as reagents. A pictorial description of this phenomenon is depicted in Fig.1.38.

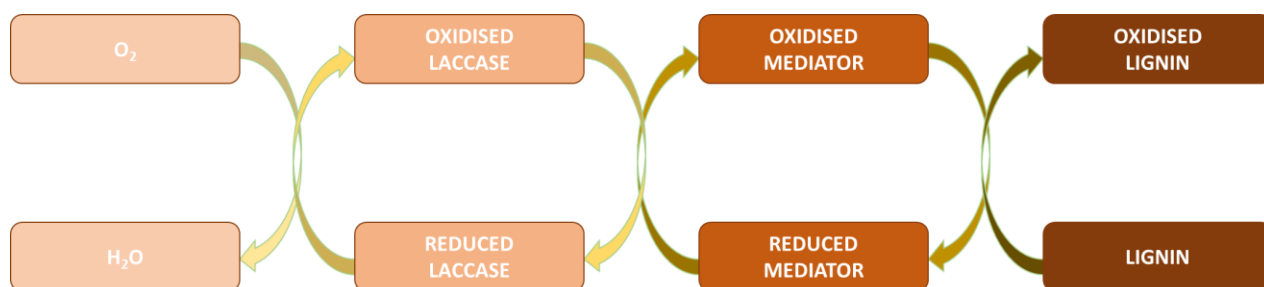


*Figure 1.38.* Synergistic action of laccase and mediators in the conversion of lignin into its oxidised form in presence of oxygen as electron acceptor.

The application of mediators to favour the enzymatic decay laccase-catalysed of lignins was introduced for the first time by *Bourbonnais* and *Paice* in 1990.<sup>146</sup> In fact, they investigated the action of laccase on lignin models ( $\beta$ -O-4', veratrole alcohol, and  $\beta$ ,1') in the presence and in the absence of 2,2'-azino-bis (3-ethylbenzothiazoline-6-sulfonic acid) (ABTS) as redox mediator. In particular, they were able to demonstrate that the presence of ABTS, which at the time was known to be activated by laccase in the form of a radical species, permitted the oxidation of non-phenolic substrates in all



the model compounds. In particular, both  $\beta$ -O-4' and veratryl alcohol resulted in the oxidation of the benzylic hydroxyl group, resulting in both cases in the formation of carbonyl compounds; in the case of  $\beta$ -1' model, the cleavage of the C $_{\alpha}$ -C $_{\beta}$  bond was also observed. These results paved the way for all the further investigations carried out in the upcoming decades.

The characteristics that a compound should possess to be considered as a redox-mediator were summarised by *Rochefort* while discussing the use of redox mediators for the enzymatic bleaching of pulps.<sup>147</sup> In particular, a mediator should

- be a substrate for laccase;
- be stable in both its oxidation states (radical and un-radical), otherwise its migrations through the non-phenolic systems is limited;
- have a fast electron exchange rate with the enzyme;
- be characterised by a higher formal potential than the one of the substrate it has to oxidise.

In the case that all of these requirements are fulfilled, the mediator can be conveniently employed for the oxidation of non-phenolic substrates. In general, radical mediators can be classified in two classes, depending on their origin. In fact there are *natural* and *synthetic mediators*. From one side, natural mediators are represented by a wide group of phenolic compounds (vanillin, monolignols, guaiacol, etc...) which can be easily found in wood as extractives or exudates (especially in heartwood) or as metabolites deriving from the action of laccase on lignin.<sup>148</sup> Therefore, it is almost impossible to exclude their presence while studying laccase-catalysed decay of lignins. From the other side, synthetic mediators are compounds which are not-wood related; four are the most important mediators for the laccase-system, ABTS, 1-hydroxybenzotriazole (HBT), 2,2,6,6-tetramethylpiperidin-1-yloxy (TEMPO), and syringaldazine. Of them, the most commonly used in are ABTS and HBT.

In an attempt to rationalise the action of mediators on the laccase-system, three theories have been developed. The first hypothesis on their mechanism of action was reported by the same *Bourbonnais* and *Paice*, who claimed that ABTS was able to subtract an electron from the substrate to oxidise.<sup>149,150</sup> This theory was then confuted by the work of *Potthast*, who later studied the oxidation of benzylic alcohols via laccase; in her opinion, the redox mediator should have played a not-well-defined action on laccase causing the enhancement of its redox-potential.<sup>151</sup> The last theory rationalising the action of mediators was purposed by *Fabbrini*.<sup>152,153</sup> In fact, *Fabbrini* theorised that the action of mediator would not have be based on the electron abstraction on the non-phenolic substrate, but on an hydrogen-atom abstraction on the same position. Then, the resulting radical, would have then undergone the various transformations resulting in the oxidation of the substrate. Of these three

reaction mechanisms, the nowadays most credited one is *Fabbrini* hypothesis. This theory was then investigated in depth by *Crestini*, resulting in general kinetic and thermodynamic considerations on the chemistry of the action of mediators on non-phenolic substrates.<sup>154</sup>

In order to fully understand the oxidation of lignin in presence of a mediator, *Crestini* coupled experimental studies on laccase catalysed apocynol (1-(4-hydroxy-3-methoxy-phenyl)-ethanol) oxidation in 5 mM HBT, with computational studies on electron densities for the same reaction. In this way, she demonstrated that radical mediators drastically change the kinetic of the oxidation of substrates. In particular, she observed that the *Gibbs* energy content for the benzylic radical, which is generated via the hydrogen atom abstraction on the benzylic carbon, and the aryloxy radical, which is formed by the standard action of laccase on phenols, is the same. Consequently, from a thermodynamical point of view, both structure should be formed in presence of the radical mediator at the same time. Nevertheless, computational studies demonstrated that the radical mediator kinetically favour the formation of the benzylic radical. Once this radical is formed, then it can undergo in different degradation pathways, like the disproportionation, the radical coupling, or the oxygen addition resulting in the degradation of the substrate. This research by *Crestini*, based on a strong experimental background, permitted to provide an answer on the doubtful effect of mediators on non-phenolic substrates; these observations paved the way for further studies on the real effect of laccases on lignin structures.

## 2. Aim of the research

The present thesis work investigates the application of laccases for the modification of technical lignins in view of their use for the preparation of advanced and properties-enhanced technological nanomaterials. In particular, the conceptual nodes of the present research activity can be considered as revolving around three major questions:

- How do laccases **modify the structure** of technical lignins?
- Can the fractionation operation coupled with the laccase-mediated oxidation be used to **tailor the properties** of lignin nanoparticles?
- Is it possible to **prepare composite** materials with enzymatic deposited lignin nanoparticles in order to modify the properties of nanofibrillated cellulose?

The answers to these questions are provided in the following sections. In particular:

- Chapter 3 discusses the action of laccases on two types of technical lignins and their acetone insoluble and soluble fractions. In particular, gymnosperm Kraft lignin and wheat-straw Organosolv lignin were submitted to laccase oxidation. Their structures were studied before and after the enzymatic treatment via  $^{31}\text{P}$  NMR and GPC analyses. In addition, in order to better understand the overall effect of laccase on these lignins, the GC-MS analyses of the low molecular weight products formed during the laccase-mediated oxidation mixture were performed.
- Chapter 4 investigates the possibility of tailoring the properties of technical lignin nanoparticles via the pre-treatment of an angiosperm kraft lignin with a tandem strategy based on its fractionation and laccase-mediated oxidation. In particular, considerations related to the nanoparticles size as well to their hydrophobicity are discussed.
- Chapter 5 explores the possible use of laccase in order to favour the deposition of kraft lignin nanoparticles on lignin-rich cellulose nanofibrils resulting in the preparation of lignin-rich composites. The mechanical and thermal properties of the resulting composite materials were then compared to those of a counterpart of composites prepared with no enzyme. The contextualisation of the results with existing literature on similar cellulose-lignin composites is also discussed.

### 3. How do laccases modify the structure of technical lignins?

*In this Chapter the oxidising activity of laccase on two technical lignins (kraft and Organosolv) is investigated by studying the effects on either pristine or acetone insoluble and soluble fractions. The polymerisation mechanisms occurring on the substrates as well as the depolymerisation of terminal phenolated moieties are carefully evaluated by the use of  $^{31}\text{P}$  NMR, GPC, and GC-MS analyses of the low molecular weight products deriving from their enzymatic degradation. Mechanistic aspects of the oxidation as well as the rationalisation of the formation of the low-molecular weight products is discussed according to the existing literature. Additionally, the evaluation of the pH range in which the enzyme used for the research exhibits phenol-degrading properties as well as the optimisation of the spectrophotometric test for the determination of its catalytic activity are discussed.*

#### 3.1. Introduction

In view of preparing high-value materials from technical lignins, the need to tailor their properties plays a fundamental role. As previously discussed in *Chapter 1*, the use of enzymes working under mild conditions represents a sustainable alternative to traditional heterogeneous catalytic systems to achieve these modifications. Commonly used enzymes finding applications in this sector are phenol-oxidases, whose catalytic action is especially exerted on phenolic moieties of lignins. As these enzymes are oxidases, their catalytic action is based on redox processes involving electrons transfer from the substrate to an electron acceptor (e.g. hydrogen peroxide or oxygen). Among the various phenol-oxidases, laccases represent a valuable group of enzymes owing to their wide availability in nature as well as the low-cost of the electron acceptor needed (oxygen).

General studies attempting to rationalise the effect of laccases on lignins are nowadays available.<sup>135,136,140,155</sup> Moreover, these results are limited, as they are based on the study of the reactivity of monomeric or dimeric lignin models. Even if the advantages of this type of approach have been recently reviewed,<sup>156</sup> their validity remains quite questionable, as the synergistic effects deriving from the contemporary oxidation of different bonding patterns has never been considered before for technical lignins. Consequently, the need to provide a wider view of the overall effect of laccases on the total structure of lignin is still felt.

Technical lignins structures are way more different from those of native lignins, and various issues are related with their use. The major difficulty to consider while evaluating the modifications on technical lignins is represented by their heterogeneous nature, which results from the uncontrolled

reactions occurring during pulping (kraft lignins) or biorefinery operations (Organosolv lignins). In view of that, for the sake of a complete and reliable analyses of effects of laccases on technical lignins, the study of the modifications occurring on their structures should be extended to their fractions, representing more homogeneous starting points.

With these premises in mind, in this Chapter the structure-modifying activity of a laccase was evaluated on two technical lignin (kraft and Organosolve) and their acetone insoluble and soluble fractions. In this research a transgenic laccase was used; the greater advantage of the enzyme employed was represented by its high catalytic activity in a wide range of pH values, involving both acidic and alkaline conditions. By profiting of this characteristic, the enzymatic treatment of technical lignins was performed under alkaline conditions, where all the samples were highly soluble. The enzymatically modified lignins as well as the low molecular weight monomeric compounds deriving from the action of laccase on them were characterised via various techniques ( $^{31}\text{P}$  NMR, GPC, and GC-MS). The so obtained results permitted to depict the overall effect of laccase on kraft and Organosolv lignin.

## **3.2. Results and discussion**

### **3.2.1 Fractionation of technical lignins**

The inhomogeneous nature of polymeric chains of technical lignins is at the base of the heterogeneity of these materials. In fact, different distributions in terms of functional groups, especially hydroxylated moieties, as well as different molecular weights, characterise these polymers. In view of that, as it was recently partially demonstrated by *Vignali*, in order to properly evaluate the action of an enzymatic treatment on technical lignins, the study of biocatalyst reactivity on the various fractions constituting the lignin preparation is needed.<sup>157</sup>

With that respect, two technical lignins were investigated, a softwood kraft lignin (SKL) and a wheat straw Organosolv lignin (WSL). The isolation of acetone fractions was achieved by profiting of their different solubilities in the solvent, according to the first steps of the extensive fractionation protocol developed by *Cui*.<sup>158</sup> The composition in terms of acetone insoluble and soluble fractions of the two lignins is depicted in Fig. 3. 1.

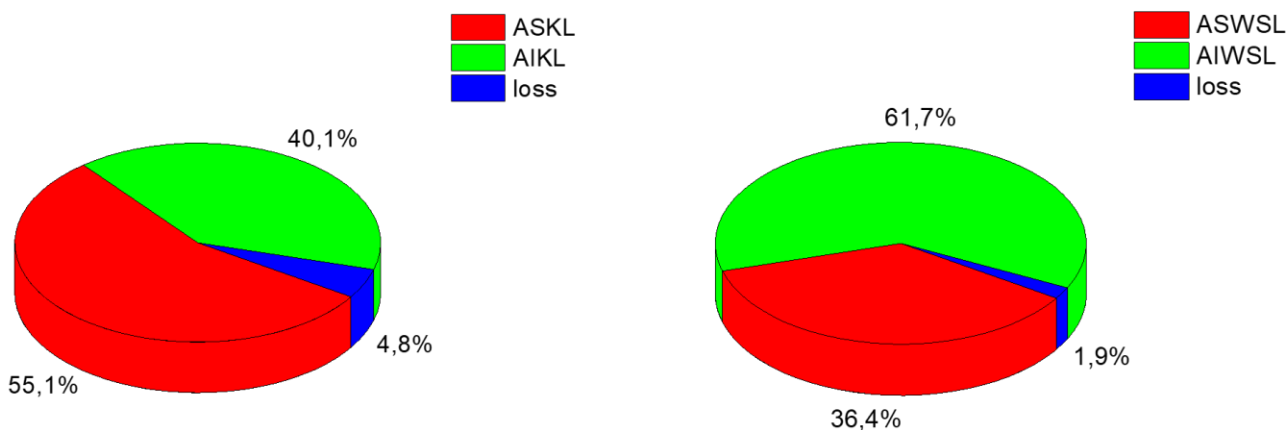


Figure 3.1. Composition of SKL and WSL in terms of acetone insoluble (AIKL and AIWSL) and acetone soluble fractions (ASKL and ASWSL).

SKL fractionation resulted in the acetone insoluble (AIKL) and acetone soluble (ASKL) fractions. SKL and its fractions were characterised via GPC and  $^{31}\text{P}$  NMR. GPC permitted to determine the molecular weight of the fractions and the respective polydispersity indexes (PDI), while  $^{31}\text{P}$  NMR provided with the quantification of the various type of reactive hydroxy groups in the samples. GPC chromatograms for SKL and its fractions are reported in Figure 3.2.

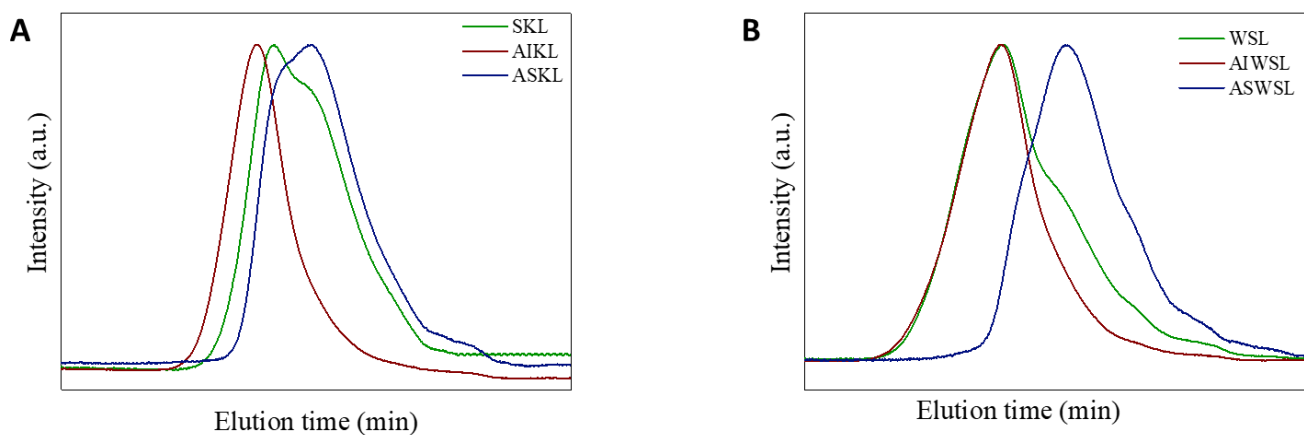


Figure 3.2. Comparison of the GPC for SKL (A) and WSL (B) and the corresponding acetone fractions. Acetone insoluble fractions are characterised by higher molecular weights than those of the acetone soluble counterpart.

The profile of SKL GPC (Figure 3.2 A) demonstrated that ASKL had a lower molecular weight with respect to AIKL, and that both fractions display lower polydispersity index if compared to the SKL. Numerical data for GPC analyses of SKL are listed in Tab 3.1.

Table 3.1.  $M_n$  and PDI for SKL and its fractions.

	$M_n$	PDI
SKL	1200	4.3
AIKL	5300	4.2
ASKL	1000	2.4

The variation in PDI from SKL to its fractions, especially ASKL, was considered as a demonstration of the efficacy of the fractionation treatment; in fact, the reduction of PDI highlighted an homogenising-effect in the lengths of the polymer constituting the SKL.

A comparison of the content of the various hydroxylated moieties in SKL and its fractions, as revealed by  $^{31}\text{P}$  NMR analysis is depicted in Fig. 3.2.

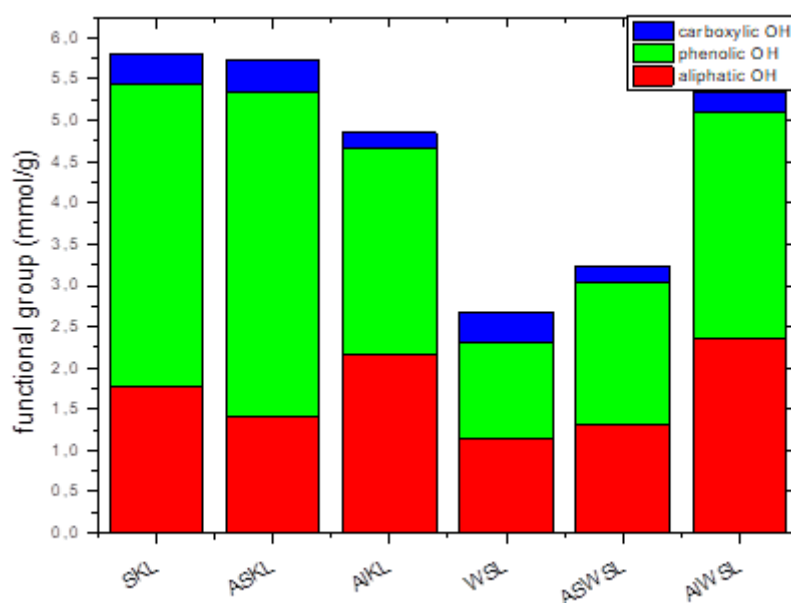


Figure 3.3. Functional group analyses for SKL and WSL and their acetone insoluble (AIKL and AIWSL) and acetone soluble fractions (ASKL and ASWSL). SKL is the sample displaying the higher content in phenolic OH for the SKL series, while AIWSL is the one with the higher content in phenolic OH in the WSL series.

With respect to SKL samples,  $^{31}\text{P}$  NMR analysis revealed that AIKL had the higher content of aliphatic hydroxyl groups if compared to the SKL and ASKL. These hydroxyl groups can be seen as the result of the Kraft pulping on  $\beta\text{-O-}4'$  driving also to the cleavages of ether alkyl-aryl bonds. The

content of carboxylic groups, either aliphatic (e.g. cinnamic acids) or aromatic (benzoic acids), did not vary from SKL to ASKL. On the contrary, with respect to the content of carboxylic groups, it was noticed that AIKL exhibited the lower content among the various SKL preparations. Finally, phenolic hydroxyl groups content in ASKL was higher than those in SKL and AIKL. These data derive from the fact that ASKL chains are shorter than those of AIKL and SKL; consequently, the content of terminal phenolic groups is higher. These characterisation data were in accordance with the previous researches performed by *Crestini* on softwood kraft lignin.<sup>74</sup>

WSL was processed in the same manner as SKL. Even in this case, two fractions have been obtained, the acetone soluble fraction (ASWSL) and the acetone insoluble (AIWSL) one. The composition in terms of fractions is reported in Figure 3.1. In particular, it was observed that WSL had a higher content in acetone insoluble fraction than SKL. WSL and its fractions were then characterised in accordance with the approaches followed for SKL. The chromatograms of the samples are reported in Figure 3.3 B. WSL and AIWSL shared the same maximum, moreover the gaussian of WSL peak was wider. In addition to that, the clear presence of a peak shoulder, which was correlated to the presence of the acetone soluble fraction, differentiate the chromatograms of WSL and AIWSL. ASWSL curve was shifted to the right, corresponding to a lower molecular weight than those of the other samples. These observations were in agreement with the numerical data obtained reported in Tab.3.2.

*Table 3.2.*  $M_n$  and PDI for WSL and its fractions.

	$M_n$	PDI
WSL	2800	14
AIWSL	5400	13
ASWSL	700	2.0

Differences in PDI were evident comparing WSL to ASWSL, confirming the fractionating effect of acetone. Similarly to the case of SKL, <sup>31</sup>P NMR analysis permitted to demonstrate the differences between the starting materials and the fractions with respect to the amount of terminal hydroxyl groups in the samples. These data are graphically depicted in Figure 3.3. From one side, it was observed an incrementation in terms of aliphatic hydroxyl groups going from WSL to AIWSL. Similarly, the phenolic hydroxy groups content followed the same trend. On the other side, no



relevant variation in terms of the amount of carboxylic hydroxy groups in fractions were revealed; in particular, only in the case of WSL a slightly higher than its fractions was detected.

As acetone insoluble and soluble fractions represent the constituent of both SKL and WSL, it should be expected that the sum of the content of the same type of functional group in both fractions resulted in the amount of the same functionality in the unfractionated material. Moreover, as it can be noticed considering the numerical data reported in Tab. 3.10 and 3.11, this fact is not true for the analysed samples. In order to rationalise this occurrence, it was postulated that the insoluble fractions of both lignins, AIKL and AIWSL, would be characterised by a limited solubility in the pyridine/CDCl<sub>3</sub> mixture used to collect the <sup>31</sup>P NMR spectra after derivatisation. In fact, the complete labelling of the hydroxylated moieties would not be complete if the samples are not in solution, resulting in the observed differences while making the calculations to compare the data with the starting material. Anyhow, the amount of undissolved lignins should be limited, as the visual analyses of the lignin/solvents mixture systems did not reveal any undissolved materials in all cases.

In conclusion, by profiting of the same type of fractionation, it was possible to isolate from two different technical lignins two types of fractions, characterised by the same solubility properties, but with different molecular weight and structural features. Afterwards, these samples were tested in the same reaction conditions against the action of a laccase.

### **3.2.2 Identification of the optimum pH for ABTS test**

Prior to the study of the action of laccases on technical SKL and WSL and their fractions, the evaluation of the catalytic activity of the enzyme was asserted. With that regard, owing to ABTS sensitivity to the laccase-oxidation, this dye was used to estimate the laccase activity.<sup>159–161</sup> In fact, in presence of the enzyme, ABTS is oxidised generating a dark-green coloured compound; by following its formation via UV-vis, it is possible to determine the catalytic activity of laccase.

The oxidation mechanism of ABTS, which is represented by a two-electron transfer, is schematised in Fig. 3.4.<sup>162</sup>

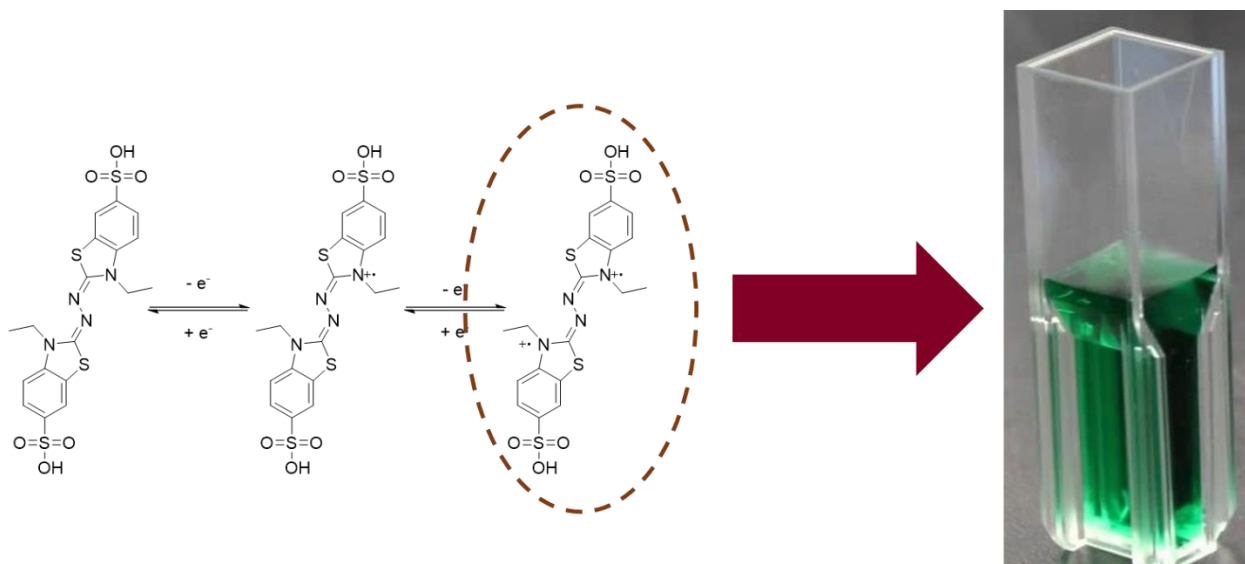


Figure 3.4. Oxidation mechanism of ABTS. Two electrons are abstracted from the thioazoline generating a thioazolinium diradical structure.

Depending on the origin of laccase, the pH at which the catalytic activity determination should be performed varies. With that respect, various pH values ranging from 2 to 10 are reported in literature. Consequently, in order to properly estimate the optimal pH conditions at which determine the enzymatic activity of the laccase used in the following researches, a screening of different buffer solutions was performed. The buffers used for the research are listed in Tab.3.3..

Table 3.3. pH buffer used for the test of the enzymatic activity of laccase with the ABTS.

pH	buffer type	Reference to the protocol
2	glycine hydrochloride	Internal laboratory reference
4	sodium acetate	<i>Sun et al.</i> <sup>163</sup>
5	sodium acetate	<i>Johannes et al.</i> <sup>164</sup>
6	sodium citrate	<i>Childs et al.</i> <sup>165</sup>
7	sodium	
10	hydrogenophosphate/dihydrogenophosphate sodium glycinate	<i>Metgen</i> suggested standard

Experimental details on the protocol to perform the ABTS are reported in the Experimental part of this section.

The profile for the absorbance variation during one minute (recorded at 420 nm) of ABTS solutions during laccase-oxidation in different buffer systems is reported in Fig.3.5.

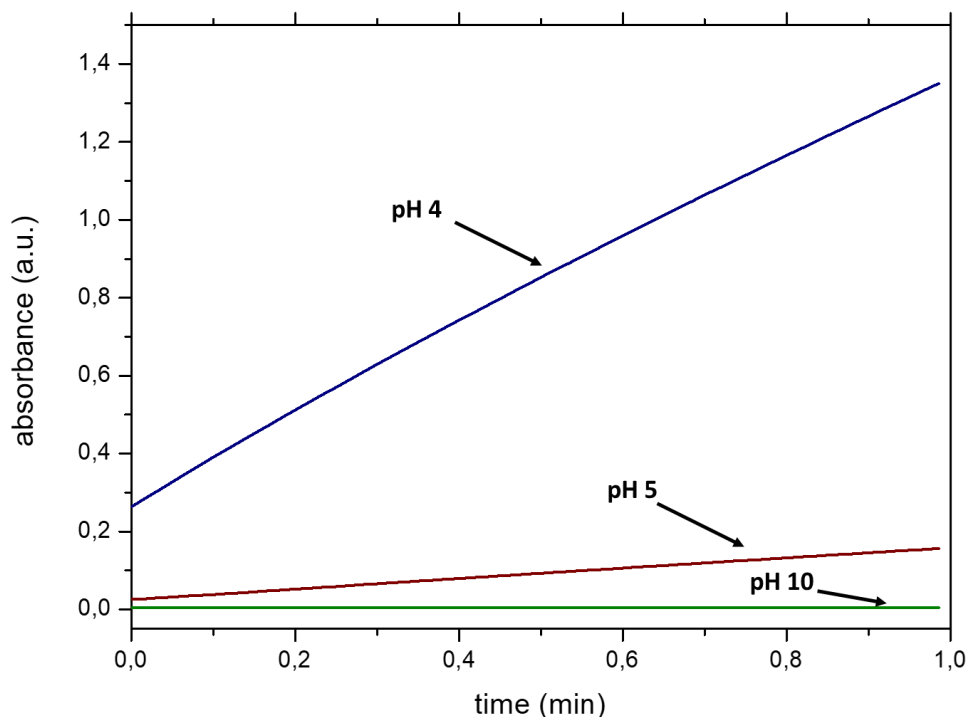


Figure 3.5. Variation of the absorbance vs. time for laccase-catalysed laccase oxidation of ABTS during one minute at different pH values.

From the variation of the absorbance of the solution during one-minute incubation, the activity was determined according to the following formula:

$$laccase\ activity(U/mL) = \frac{\Delta_{absorbance} \cdot 1000\ \mu L}{\varepsilon \cdot 10\ \mu L}$$

where  $\Delta_{absorbance}$  corresponds to the variation of the solution absorbance during one minute ( $\text{min}^{-1}$ ), 1000  $\mu\text{L}$  is the final volume of the solution used to test the enzyme (buffer + ABTS solution + diluted laccase solution),  $\varepsilon$  is the extinction coefficient (assumed as 21.4  $\mu\text{mol}\cdot\text{cm}^{-2}$ ), and 10  $\mu\text{L}$  is the volume of enzyme solution used for the test.

Tests were repeated three times per each buffer and the calculated enzymatic activity from the experimental data are reported in Table 3.4 and depicted in Fig. 3.6.

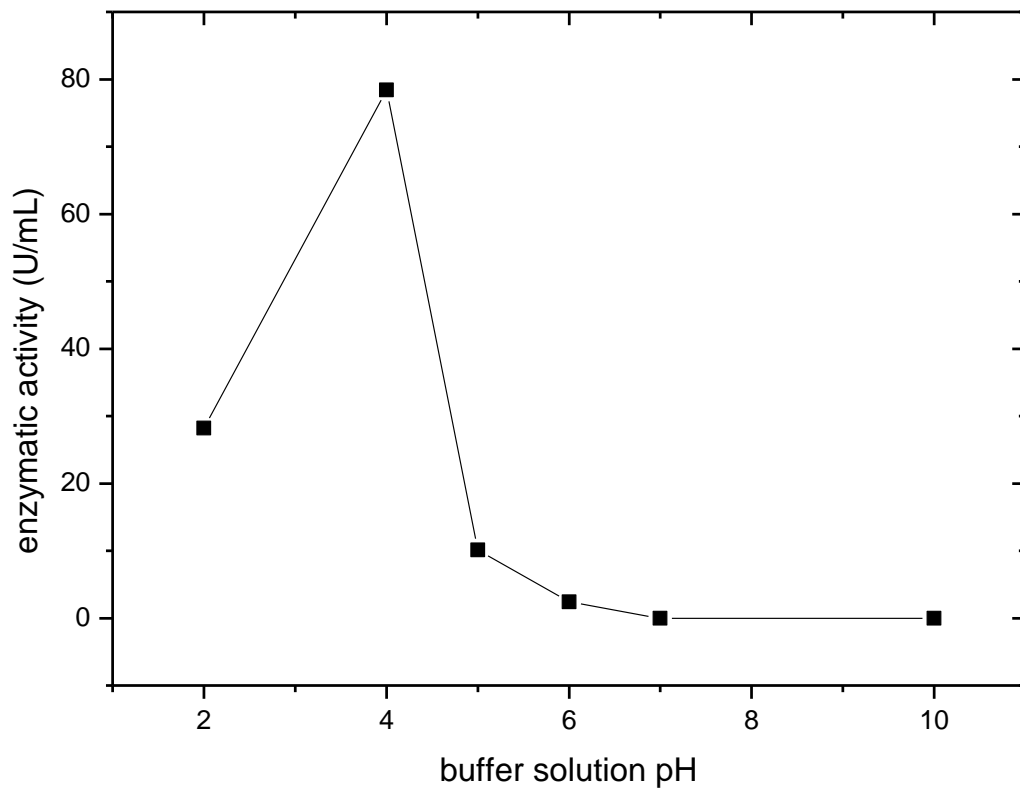


*Figure 3.6.* Laccase solution activity measured via spectrophotometric test at different pH values. The maximum activity was determined working at pH 4 in sodium acetate buffer solution.

Table 3.4. Laccase activity measured via spectrophotometric ABTS test at different pH values.

entry	pH	Activity (U/mL)
<b>I</b>	2	28.1
<b>II</b>	2	29.2
<b>III</b>	2	27.3
<b>average</b>	2	28.2
<b>IV</b>	4	79.0
<b>V</b>	4	77.7
<b>VI</b>	4	78.6
<b>average</b>	4	78.4
<b>VII</b>	5	10.3
<b>VIII</b>	5	9.5
<b>IX</b>	5	10.6
<b>average</b>	5	10.1
<b>X</b>	6	2.2
<b>XI</b>	6	3.1
<b>XII</b>	6	1.9
<b>average</b>	6	2.4
<b>XIII</b>	7	0
<b>XIV</b>	7	0
<b>XV</b>	7	0
<b>average</b>	7	0
<b>XVI</b>	10	0
<b>XVII</b>	10	0
<b>XVIII</b>	10	0
<b>average</b>	10	0

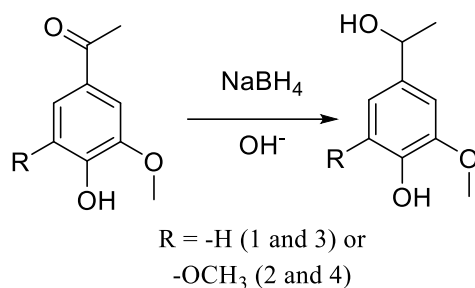
The experimental data demonstrated that ABTS permitted the determination of the activity of the enzyme only in acidic conditions. The maximum catalytic activity was observed in a pH-4 buffered solution.

Even if this test is useful for general purposes, it does not suffice to demonstrate an effective oxidising activity of laccase against lignin-related substrates. Consequently, to check if the laccase can be

conveniently used for the modification of lignin preparations, and to see if the enzymatic activity on lignin substrates is pH-dependent, the enzyme action was tested on a couple of lignin model compounds (apocynol and 4-(1-hydroxyethyl)-2,6-dimethoxyphenol). These species were chosen to model the enzyme activity on substrates containing either aliphatic or aromatic hydroxylated moieties.

### 3.2.3 Evaluation of the role of pH on the conversion of lignin model compounds

Apocynol (3) and 4-(1-hydroxyethyl)-2,6-dimethoxyphenol (4) were synthesised via sodium borohydride reduction of the corresponding carbonylated-compounds according to the following reaction:



The reduction was followed via dinitrophenyl-hydrazine test; the reduction products were isolated from the reaction mixture via solvent extraction. The purity of the products was asserted via FT-IR, demonstrating the disappearance of the carbonyl band ( $1652$  and  $1631\text{ cm}^{-1}$  respectively for 3 and 4) and  $^1\text{H NMR}$ .

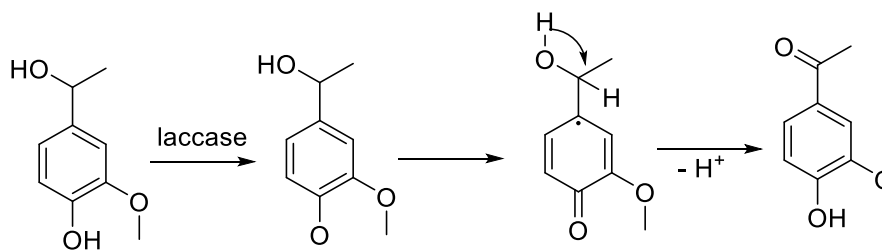
Laccase-catalysed oxidation of 3 and 4 was performed in buffered solutions at different pH values; buffers used were the same reported in Tab.3.4. Due to the poor solubility of the models at certain pH values, it was decided to pre-dissolve them in a small amount of dioxane, as previously reported by *Crestini*.<sup>140</sup> The amount of the enzyme involved in the incubations was standardised to a concentration of  $0.5\text{ U/mL}$  according to the enzyme activity estimated at pH 4 ( $10\text{ U}$  for  $0.23\text{ mmol}$  of model compound). With respect to the incubation time, 16 hours were elected in order to give the samples the possibility to fully react with the enzyme considering also the possibility of a partial degradation of the enzyme.

In order to estimate the conversion of the enzymatic oxidation, the reaction mixture were extracted with ethyl acetate and then analysed via gas-chromatography (GC) . Prior to the extraction, the reaction mixtures were quenched in boiling water for solutions for 10 minutes, resulting in the deactivation of the enzyme. A spot analysis of a reaction mixture from both the oxidation of both 3 and 4 via GC-MS was performed in the same conditions of the GC determinations. The analyses of



characteristic of the used enzyme differentiated it from natural ones, which commonly work in acidic conditions.

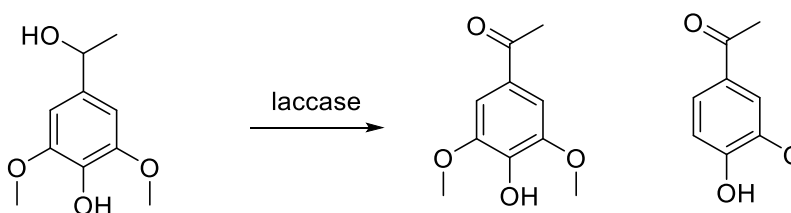
With regard to the genesis of the products, it was supposed that 5 was formed after via the rearrangement of the aryloxy radical of 3 into its quinomethide structure. The abstraction of the hydrogen atom at the benzylic position re-established the aromaticity of the ring, justifying the formation of the carbonyl group.



6 is the demethylation product of 3. Laccase-catalysed demethylation of phenolic substrate is a side-reaction accompanying the oxidation of phenolic hydroxyl group.<sup>166</sup> This reaction pathways is particularly relevant for the possible industrial applications of laccases.<sup>167</sup>

7, a compound which is not directly correlated to lignin structure, was observed only at certain pH value, in low quantities. Even if at the beginning it was believed that 7 would have derived from the thermal decomposition of 3 or 5 in the injection chamber of the gas-chromatograph, this possibility was then excluded as the injection of ethyl acetate solution of 3 and 5 did not show the formation of the peak corresponding to 7. The origin of this product still remains an open question.

The oxidation of 4 resulted in two products, according to the following equation:



The data related to the laccase-catalysed oxidation of 4 are listed in Tab.3.6; the conversion as well as the composition of the products mixture were estimated accordingly to formulae previously applied to 3.



Table 3.6. Laccase-catalysed oxidation of 4 at different pH values.

entry	pH	Conversion (%)	% <sub>8</sub>	% <sub>9</sub>
I	2	72	92	8
II	4	63	95	5
III	5	77	94	6
IV	6	70	87	13
V	7	68	93	7
VI	10	81	92	8

The results obtained for 4 demonstrated the catalytic activity of laccase against syringyl-containing lignin-units, extending the data previously collected for guaiacyl units. In particular, 8 was considered as the C $\alpha$  oxidation product of 4, while 9 was seen as the result of 4 demethylation and oxidation. The conversion data were slightly lower than those obtained for 3; this fact was related to the higher steric hindrance of 4 than 3, deriving from the presence of an additional methoxy-group.

Interestingly, the formation of the product of double demethoxylation was not revealed; the mechanism resulting in that reaction, in the view of the writer, would have been based on the initial oxidation of the benzylic position, followed by the additional oxidation via demethylation of the ring. Clearly, the reaction seems to stop before the third oxidation step.

Finally, *p*-vinyl-syringol, the syringyl-equivalent of *p*-vinyl-guaiacol (7), was not found in the reaction mixture, indicating thus that the dehydration reaction does not take place, or is much slower when 4 is the substrate.

The clear and almost quantitative conversion of lignin model compounds by laccase treatment under alkaline pH values clearly demonstrates that the ABTS test for laccase activity is not sufficiently reliable while considering different pH values.

### 3.2.4 Set up of the enzymatic reactions: general assumptions, calculations, and considerations

The so revealed catalytic activity of the enzyme in alkaline conditions is particularly favourable, as it permits to work in homogeneous conditions with technical lignins. This occurrence derives from the fact that the pK<sub>a</sub> of terminal phenolated moieties in lignin ranges from 7.4 to 11.4; consequently, under alkaline conditions, it is more likely to expect their existence under the phenolate forms instead

of the protonated ones.<sup>168</sup> Negatively charged lignin chains are water soluble, consequently they can be in the same phase of the enzyme, favouring its action.

This possibility to study the laccase action in homogeneous conditions is particularly relevant, as one of the main limitations to the use of natural laccases is represented by the need to work in acidic conditions in order to preserve their activity. A consequence of the use of acidic pH is the heterogeneity of the incubation mixtures, where the enzyme activity is limited only to the surficial area of the lignin treated in dispersion.

Prior to the design of the experimental procedure to perform the enzymatic incubation of technical lignins, their solubility was determined in 50 mM sodium glycinate buffer at pH 10. This buffer would be used afterwards as a medium for the enzymatic reactions. Solubility tests led to conclude that either SKLs (SKL, ASKL, and AIKL) or WSLs (WSL, ASWSL, and AIWSL) were completely soluble in the sodium glycinate buffer when a 2 mg/mL concentration was used. Higher concentration could be reached; moreover, in order to work with diluted systems favouring an homogeneous action of the enzyme on the bulk of lignin, it was preferred to avoid the use of higher concentrations.

Once the concentration of the lignin for the experiments was established, the focus shifted to the design of the experimental procedure. More specifically, the amount of enzyme to be used during the incubations was carefully determined according to three (drastic) assumptions and simplifications:

- the enzymatic activity of laccase remains constant during all the incubation;
- the enzyme does not denaturate during the lignin oxidation;
- the enzymatic activity is not inhibited by the lignin oxidation products.

The micromoles of phenolic OH groups for a specific amount of a lignin preparation can be calculated according to the following formula, which relates the amount of lignin  $x_{lignin}$ , and the content of phenolic hydroxyl groups per gramme ( $OH_{phenolic\ content}$ , mmol/g):

$$\mu mole_{hydroxyl\ phenolic} = x_{lignin}(g) \cdot OH_{phenolic\ content}(mmol/g) \cdot 1000$$

The amount of phenolic hydroxyl groups per gramme for a lignin can be conveniently determined via <sup>31</sup>P NMR.

If the so calculated micromoles of phenolic hydroxyl groups *should* be oxidised in  $h$  hours, the micromoles converted per minute can be calculated with the following formula:

$$oxidised\ \mu mole_{hydroxyl\ phenolic}/min = \frac{x_{lignin}(g) \cdot OH_{phenolic\ content}(mmol/g) \cdot 1000}{h(hours) \cdot 60(min/hour)}$$

The enzyme activity of an enzyme solution refers to the amount of enzymatic units per millilitre of enzyme solution; this means that every millilitre can convert in one minute an amount of micromole of substrate corresponding to its activity (e.g. 1 mL of a 8 U/mL enzyme solution converts 8

micromoles of substrate in one minute). Consequently, it is possible to estimate the volume of laccase that can theoretically convert all the phenolic hydroxyl groups of certain amount of lignin in  $h$  hours via the following proportion:

$$1 \text{ mL} : \text{enzyme activity (U/mL)} = x_{mL,laccase} : \frac{x_{lignin}(g) \cdot OH_{phenolic\ content}(mmol/g) \cdot 1000}{h(hours) \cdot 60(min/hour)}$$

which means:

$$x_{mL,laccase} = \frac{x_{lignin}(g) \cdot OH_{phenolic\ content}(mmol/g) \cdot 1000}{\text{enzyme activity (U/mL)} \cdot h(hours) \cdot 60(min/hour)}$$

This calculation for the amount of enzyme, henceforth referred to as “*stoichiometric amount*” of enzyme, was applied for all the oxidation experiments. In fact, lignin laccase-mediated oxidations were performed by the use of the stoichiometric enzymatic loads with respect to the lignin phenolic units (e1) or by a 100 fold enzymatic excess (e100). Additionally, for the acetone soluble fractions of both lignins, also the e10 experiment was performed, in which a 10 fold enzymatic excess was used. For all the oxidations, the reaction time was set to a relatively long time (16 hours), in order to identify only the final oxidation products and to get rid of transient intermediates which can re-polymerise, as previously demonstrated.<sup>157</sup>

Finally, as the alkaline conditions can favour the decomposition of certain lignin sub-structures (*e.g.* vanillin release), for every oxidation experiment a blank experiment with no enzyme was run at the same conditions in order to normalise the results related to the low molecular weight products. For the estimation of the low molecular weight products, the extraction of the reaction mixture with ethyl acetate was considered for all the samples.

### 3.2.5 Characterisation of low molecular weight lignin oxidation products

The characterisation of the ethyl acetate extracted products from the reaction mixtures for SKL and its fractions revealed the presence of guaiacyl units derivatives. The compositions in terms of percentage of the various low molecular weight products from the enzymatic incubations of SKL are reported in Fig. 3.7. Tab. 3.7 report the yields of the various metabolites per gramme of oxidized lignin. The data were normalised according to those deriving from blank experiments ran with no enzyme.

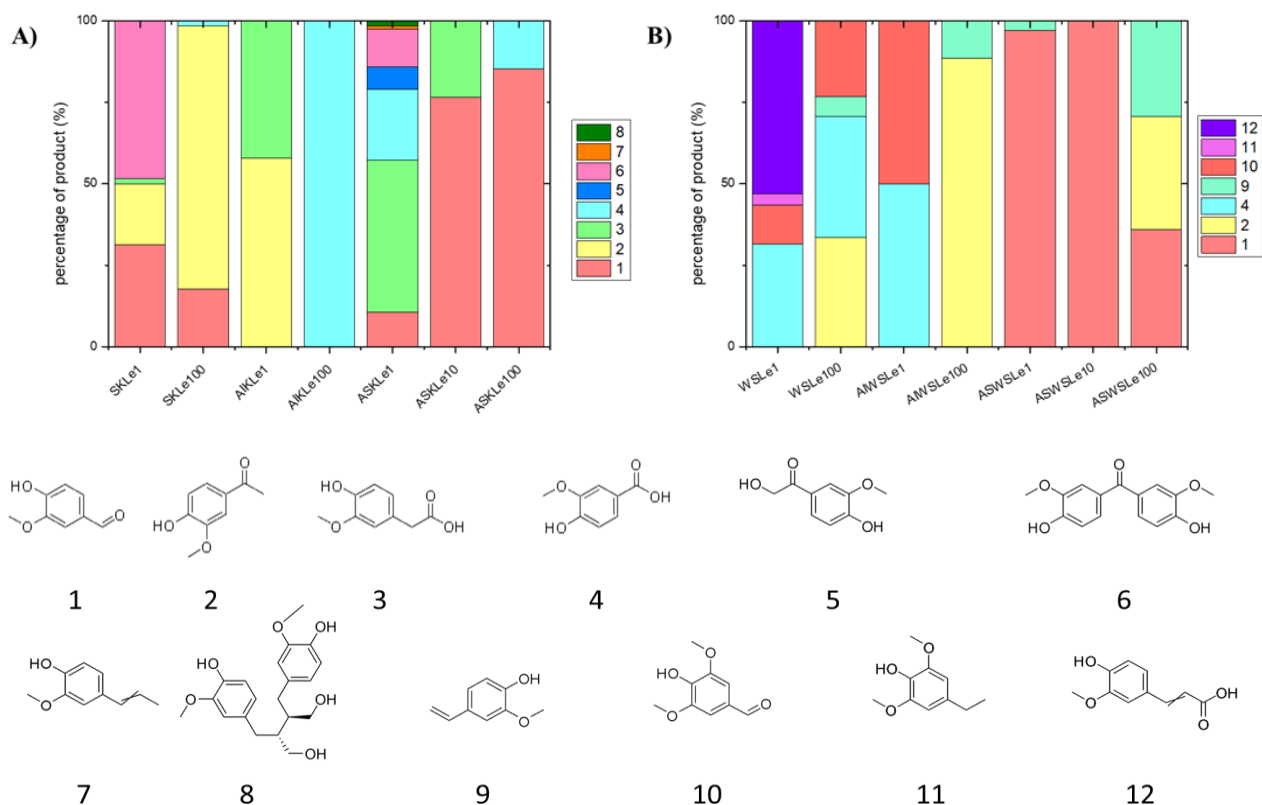


Figure 3.7. Comparison of the compositions of low molecular weight compounds identified and quantified in the reaction mixtures from SKL (A) and WSL (B) and their fractions.

Table 3.7. Yields in low molecular weight compounds isolated from SKL and its fractions after the enzymatic incubation. The structures corresponding to the compounds are reported in Fig.3.7.

Compound	SKLe1	SKLe100	AIKLe1	AIKLe100	ASKLe1	ASKLe10	ASKLe100
1	0.20	3.04			0.63	3.60	5.60
2	0.12	13.9	0.22				
3	0.01		0.16		2.76	1.10	
4		0.25		0.06	1.28		0.96
5					0.4		
6	0.31				0.69		
7					0.06		
8					0.09		
<b>total products (mg/g)</b>	<b>0.92</b>	<b>17.19</b>	<b>0.38</b>	<b>0.06</b>	<b>5.91</b>	<b>4.7</b>	<b>6.56</b>

Table 3.8. Yields in low molecular weight compounds isolated from WSL and its fractions after the enzymatic incubation. The structures corresponding to the compounds are reported in Fig.3.7.

Compound	WSLe1	WSLe100	AIWSLe1	AIWSLe100	ASWSLe1	ASWSLe10	ASWSLe100
1					5.35	0.74	0.71
2		0.39		0.31			0.69
4	0.63	0.43	0.02				
9		0.07		0.04	0.16		0.58
10	0.24	0.27	0.02				
11	0.07						
12	1.06						
<b>total products (mg/g)</b>	<b>2</b>	<b>1.16</b>	<b>0.04</b>	<b>0.35</b>	<b>5.51</b>	<b>0.74</b>	<b>1.98</b>

For all SKL preparations an increase in the products selectivity was noticed when the amount of the enzyme was increased. For instance, by considering SKL, it was observed that a e100 fold of enzyme, resulted in only four products, vanillin (1), apocynin (2), homovanillic acid and vanillic acid (4). Among them, apocynin is the most abundant (>70%). On the contrary, by the use of the e1 stoichiometric enzyme, a more complex mixture of products was observed; beside to vanillin, vanillic acid, homvanillic acid and apocynin, also di-*p*-guaiacoxy-ketone (6) and cis-1-guaiacyl-prop-1-ene (7) were present. By comparing the samples treated with the stoichiometric amount of enzyme (SKLe1, AIKLe1, and ASKLe1) the more intricate products mixture is represented by the oxidation of ASKL. This observation was rationalised owing to the polyphenolic-like structure of ASKL, which exhibits more reactive phenolic sites, as supported by <sup>31</sup>P NMR data.

The compounds obtained from the oxidation of SKL and its fractions by the use of one hundred fold the amount of enzyme are three: vanillin, vanillic acid, and apocynin. The high selectivity for vanillin related products was ascribed to the ease of cleavage of the C<sub>α</sub> - C<sub>β</sub> bond in lignin structures.

The extremely high selectivity for vanillic acid observed in the case of AIKLe100 was rationalised considering three factors. Firstly, the yield of vanillic acid (0.06 mg of vanillic acid per gramme of treated lignin), secondly, the limited amount of phenolic OH in the substrate, and thirdly, the high amount of enzyme available in the system. In particular, as further discussed, the formation of vanillin is the most reasonable product from the oxidation of the samples via a C<sub>α</sub> - C<sub>β</sub> cleavage. Moreover,

because of the high concentration of laccase in the system, it was believed that the so formed vanillin was subsequently converted into vanillic acid via a laccase-mediated oxidation. A similar conclusion was abduced for the formation of vanillic acid in both SKLe100 and ASKLe100. From one side, in the case of ASKLe100 the amount of vanillin obtained from the oxidation is the highest among the other samples (5.6 mg of vanillin per gramme of treated lignin); at the same time, the amount of phenolic hydroxyl in the treated substrate was the highest. Consequently, it was assumed that laccase catalytic action of laccases starts on hydroxyl phenolic groups and continues to the point where the vanillin concentration reaches discrete values becoming a competitive substrate for laccase. However, because of the high content of phenolic hydroxyl groups, the oxidation pathway for them remained the more prominent. From the other side, in the case of SKLe100 apocynin is the major low molecular weight product, while the vanillin content was limited. By following the same logic applied for ASKLe100, the formation of vanillic acid was justified; therefore its low content was related to the low amount of vanillin available for further oxidation.

The rationalisation of the formation of the mentioned products was based on the three types of reaction pathways, alkyl – aryl cleavage ( $C_1-C_\alpha$ ),  $C_\alpha - C_\beta$  cleavage, and  $C_\alpha$ -oxidation.<sup>135</sup> By considering vanillin, its formation can derive from the degradation of  $\beta$ -1 interunit bond (Fig.3.8). The choice of relating the formation of the product with  $\beta$ -1' interunit bonds instead of  $\beta$ -O-4' (Fig. 3.9) derives from the limited occurrence of the latest structures in kraft lignin,.

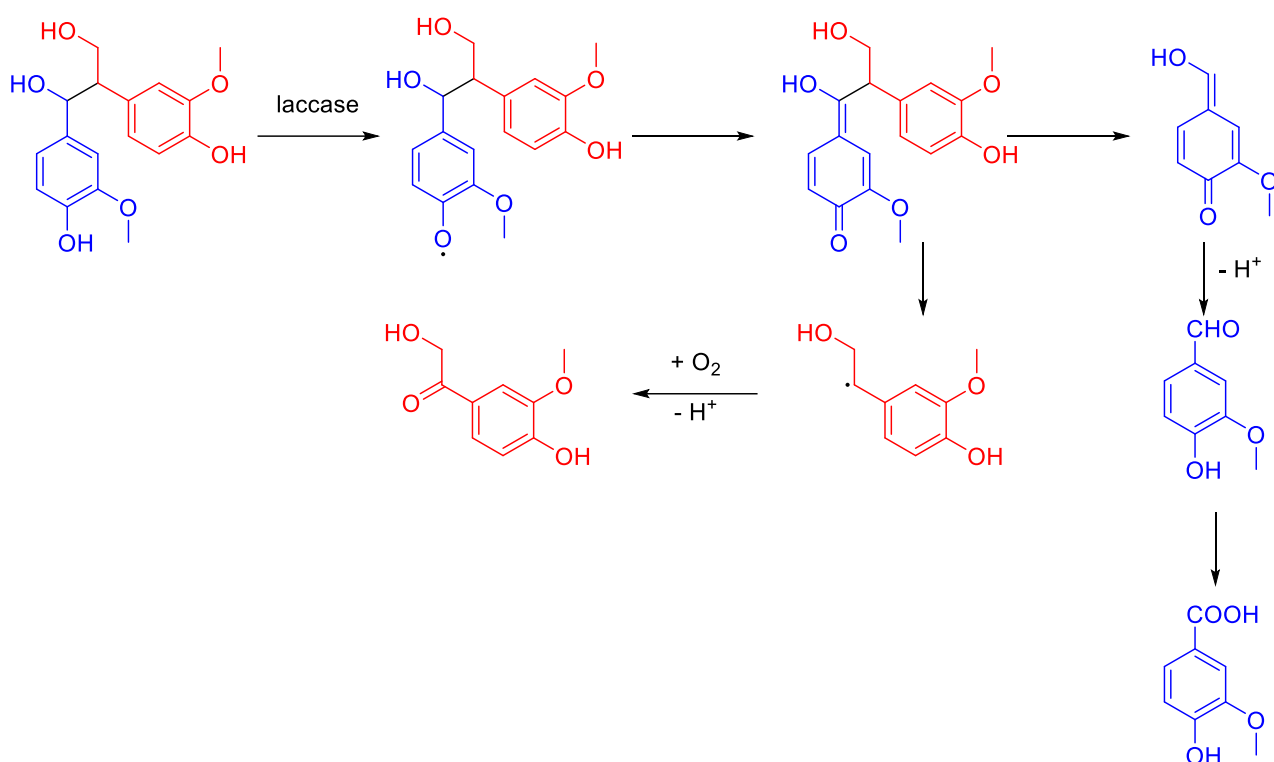


*Figure 3.8.* Mechanism for the laccase-catalysed oxidation of  $\beta$ -1' lignin structure resulting in the formation of vanillin, vanillic acid, and 2,4'-dihydroxy-3-methoxy-acetophenone.

The reaction starts with the conversion of a terminal hydroxyl group in an aryloxy radical via a single electron transfer process initiated by the enzyme. The so formed radical rearranges to a quinone methide intermediate. Then, quinone methide undergoes the homolytic cleavage of  $C_{\alpha} - C_{\beta}$  bond, resulting in a residual part preserving the  $C_{\beta}$  and  $C_{\gamma}$  (with an hydroxyl group), and a quinoidic structure corresponding to terminal aryloxy part of the substrate. As the quinoidic structure bears an enol hydroxyl group, its keto-enol tautomerisation results in the formation of the more stable corresponding ketone. This rearrangement restores the aromaticity of the ring forming also a terminal formyl group; the compound so obtained is vanillin. The laccase-catalysed oxidation of vanillin via the formation of an aryloxy radical allow the formation of vanillic acid.<sup>151</sup> The residual part of lignin, which bearing a secondary radical, reacts with molecular oxygen forming the corresponding carbonyl compound. The kinetics for the oxygen addition to the benzylic radical position are, in fact, much higher than those for the addition to the C-4 radical due to their different electron density. The result of that is the fast oxygen addition to the benzylic radical followed by the release of a superoxide anion forming the C- $\alpha$  carbonyl derivative. A compound related to this structure has been observed in some product mixtures (2,4'-dihydroxy-3-methoxy-acetophenone).

For the sake of completeness, by considering the oxidation of the residual  $\beta$ -O-4' units, the formation of vanillin can be attributed to the  $C_\alpha - C_\beta$  bond cleavage according to the mechanism depicted in Fig.3.9.

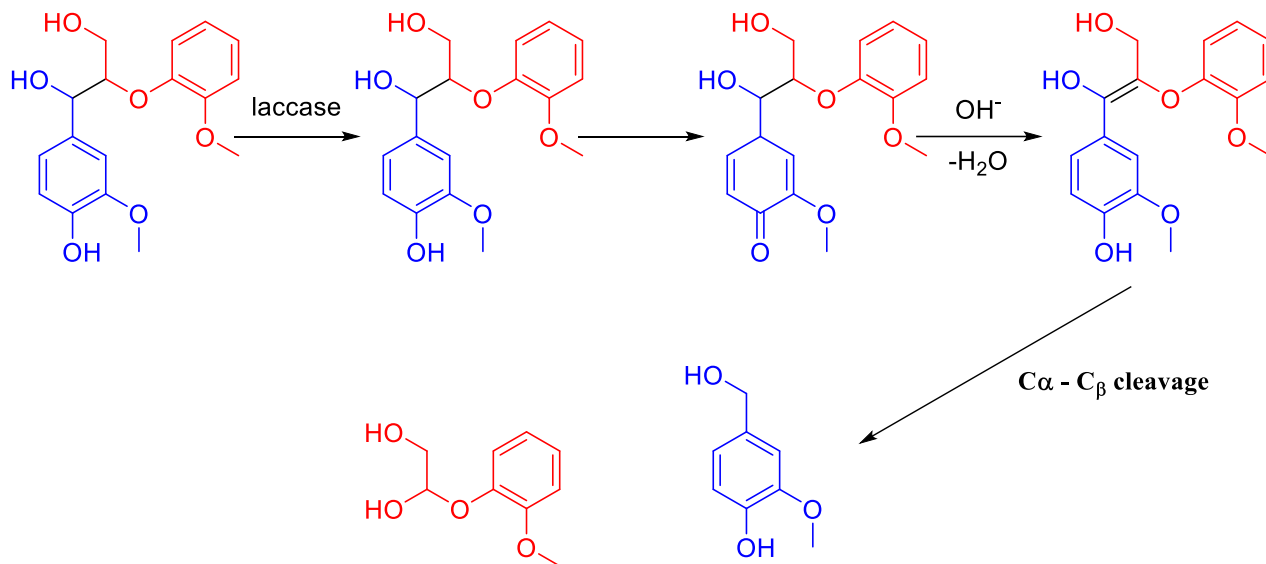


Figure 3.9. Mechanism for the laccase-catalysed oxidation of  $\beta$ -O-4' lignin structure resulting in the formation of vanillin.

Di-(4-hydroxy-3-methoxyphenyl)-ketone derives from the oxidation of stilbene units, as previously demonstrated by *Crestini*.<sup>140</sup> In fact, oxidation-transposition reactions allowing to obtain carbonyl compounds are known transformations of stilbene-like substrates in presence of hydroxy-radicals, as previously observed by *Caldwell*.<sup>169</sup>

The presence of seicoisolariciresinol and isoeugenol in the products mixture for the laccase-catalysed oxidation of technical lignins was demonstrated by *Vignali* and *Crestini*. In the case of seicoisolariciresinol, which commonly appears in wood extractives or as an absorbed compound in technical lignins, its enzymatic formation from the degradation of SKL was confirmed as the GC-MS analyses of the diethyl ether and toluene extracts of the starting material did not reveal any traces of the compound.

No catechol-like structures have been detected in the products mixtures; this fact was justified by considering that in the real samples the aryl substituents in  $\alpha$ -1' and  $\beta$ -1' disubstituted structures are linked to other lignin residues (e.g. via 5-5' or 4-O-5' linkages).

The formation of 2-(1-(4-hydroxy-3-methoxyphenyl))-acetic acid was attributed to the laccase-catalysed oxidation of a deformed  $\beta$ -1' structure. The alkyl-aryl cleavage mechanism allows the formation of a radical species on  $C_\beta$ . The oxygen addition followed by the hydrogen atom removal



causes the formation of the carboxyl group of 2-(1-(4-hydroxy-3-methoxyphenyl))-acetic acid, as described in Fig. 3.10.

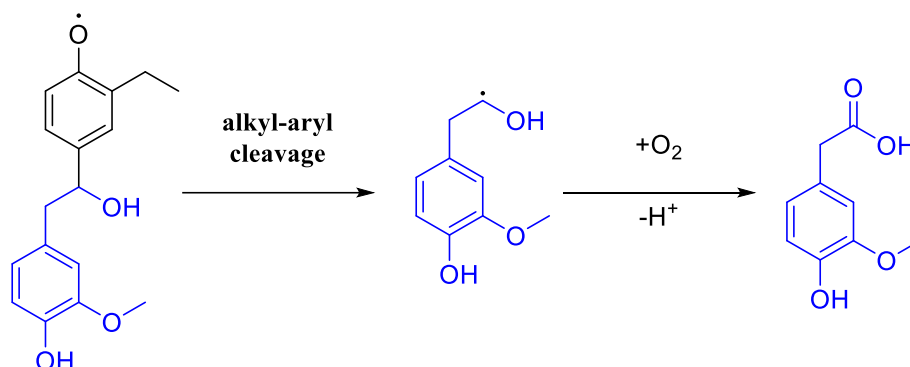


Figure 3.10. Mechanism for the laccase-catalysed oxidation of highly degraded (deformylated in C<sub>γ</sub> position) β-1' lignin structure resulting in the formation of 2-(1-(4-hydroxy-3-methoxyphenyl))-acetic acid .

As previously mentioned, the genesis of the dihydroxylated guaiacol-derivative is uncertain.

GC-MS analyses were performed also on WSL samples. The comparison of the composition of the reaction mixtures for all the samples is reported in Figure 3.7.B. Degradation patterns similar to those observed for SKL were noticed; in general, it can be observed that the overall effect of WSL fractionation is represented by an implementation of the selectivity against certain products. In addition, by considering the effect of the amount of the enzyme on the reaction mixture, it was noticed that in all cases the highest amount of enzyme favoured the formation of low molecular weight aldehydes at the expenses of other more substituted structures. For instance, by comparing samples WSLe1 and WSLe100, it was observed that the formation of vanillin and syringaldehyde are more tangible only in the case of WSLe100.

The presence of syringaldehyde from a softwood lignin is not surprising; in fact, *Gibbs* demonstrated in his taxonomical studies that certain types of gymnosperms contain relevant amounts of syringyl units.<sup>42</sup>

The mechanism for the formation of these aldehydes was rationalised according to the degradation pathways previously described for SKL. In particular, the C<sub>α</sub> - C<sub>β</sub> cleavage of terminal units seems the most plausible route. Differently from SKL and its fractions, in which β-O-4' structures were almost excluded as possible origin point for vanillin, in this case these bond pattern can be invoked, as their content in Organosolv lignin is unneglectable. This is particularly true in the case of the formation of syringaldehyde (Fig.3.11).<sup>136</sup>

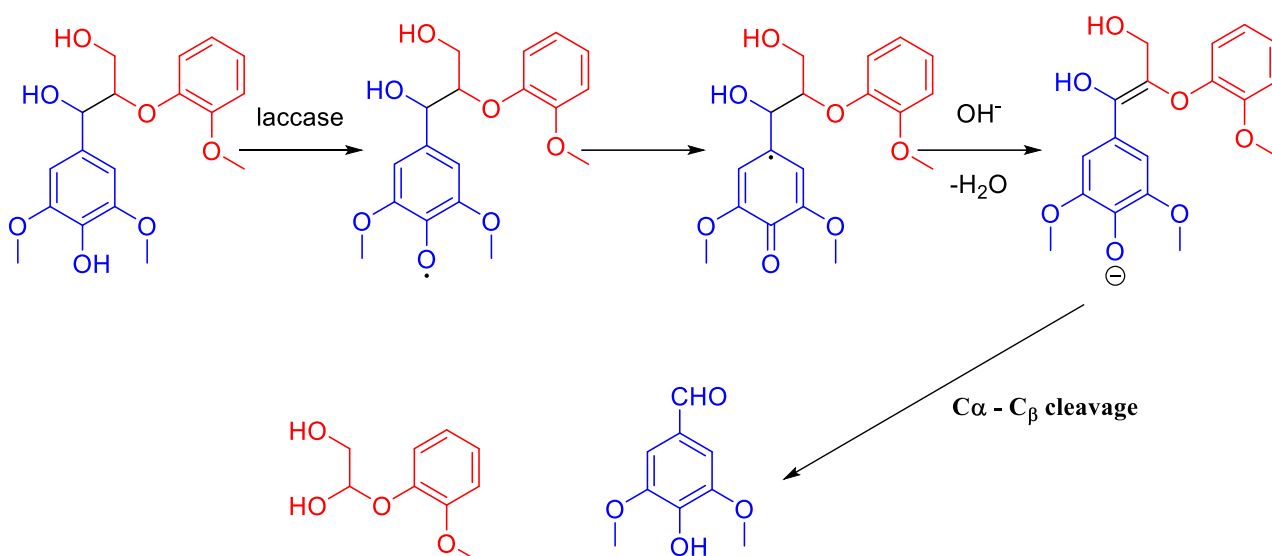


Figure 3.11. Mechanism for the laccase-catalysed oxidation of  $\beta$ -O-4' lignin structure resulting in the formation of syringaldehyde.

4-hydroxy-3-methoxy cinnamic acid (12) is formed when the stoichiometric amount of enzyme is used for the incubation of WSL; moreover, as the amount of the enzyme increased, the compound disappears from the products mixture. The determination of a reasonable reaction mechanism for its formation is still doubtful, moreover it is not excluded the possibility to relate it with the oxidation of isoeugenol.

Both AIWSL and ASWSL did not result in vanillin when the enzymatic oxidation was performed with the stoichiometric amount of enzyme; the use of an excess of enzyme allowed the obtention of that product. In addition, in the case of ASWSL, *p*-vinyl guaiacol became particularly relevant in the case of ASWLe1 and ASWLe10. As of now, the formation of *p*-vinyl guaiacol remains a phenomenon that requiring further investigations. Interestingly, the increase in the amount of laccase to treat the ASWSL samples resulted in a decrease in the content of *p*-vinyl guaiacol, favouring the formation of the previously mentioned low molecular weight aldehydes.

A cross comparison of the yields in monomeric compounds (YMC) was made. In the case of both technical lignins, the most recalcitrant fractions against the formation of monomeric compounds was the acetone insoluble. In fact, if SKLe100 is compared to AIKLe100, for instance the YMC resulting from the insoluble fractions represent only the 0.3% of that of the unfractionated lignin. Similarly, if WSKLe100 and AIWSKLe100 are compared, the YMC of latest represented only the 30% of the one of unfractionated lignin.

In addition, the comparison of SKLe100 and WSLe100 in terms of YMC demonstrated the higher reactivity of Kraft lignin if compared to the Organosolv counterpart (the YMC of WSL represents the 6.7% of the one of SKL). The nature of this difference was attributed to the different structural features of the two lignins; in fact, the highly dealkylated structure of SKL seemed to be more prone to be attacked by phenol-targeted enzymes.

In order to evaluate the validity of the method developed for the determination of the amount of enzyme to use as well as the pH conditions used, a comparison of the YMC with existing literature was performed. Moreover, at the best of the knowledge of the writer, poor literature exists on the estimation of low molecular weight compounds from the laccase-catalysed oxidation of technical lignins fractions. Tab. 3.9 compare the only available data recently reported by *Vignali* who only considered the acetone soluble fractions.<sup>157</sup>

*Table 3.9.* Comparison of YMC the obtained data in the present research with the existing literature.

	<i>SKL</i>	<i>ASKL</i>	<i>WSL</i>	<i>ASWSL</i>
<i>Vignali et al.</i> <sup>150</sup>	10.24	6.55	1.05	0.77
<i>YMC with optimised condition discussed</i>	17.19	6.56	1.16	1.98

With these results it becomes clear that the optimised conditions permitted to obtain higher yield in YMC, especially in the cases of SKL and ASWSL.

In conclusion, the GC-MS analyses of the oxidation mixtures demonstrated the efficacy of laccase to depolymerise terminal phenolic moieties of technical lignins. Depending on the amount of enzyme, different YMC were obtained depending on the treated fractions.

### **3.2.6 Residual lignin after laccase treatments: structural characterization**

GC-MS analyses of the laccase-catalysed oxidation of technical lignins demonstrated that low molecular weight compounds can be obtained according to various depolymerisation mechanisms previously elucidated in [Paragraph 3.2.5.](#)

Typical sites for the depolymerisation of laccase-catalysed oxidation of lignins are depicted in Fig.3.12.

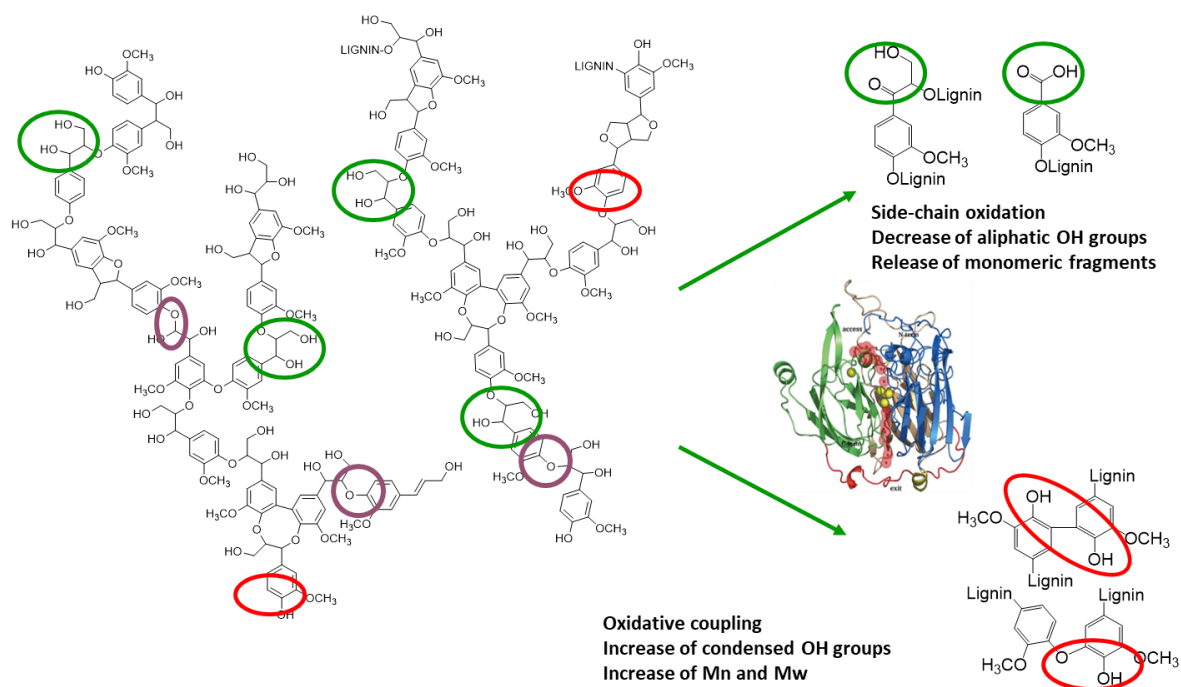


Figure 3.12. Typical sites for the laccase-catalysed oxidative depolymerisation (green) and polymerisation (red) of lignins. Ether phenolic substrate not undergoing laccase-catalysed oxidation are those highlighted in purple.

The production of low-molecular weight compounds is not the only possible reaction occurring on lignins when they are treated with laccase. In fact, as it was previously mentioned, the C $\alpha$  oxidation of lignin aliphatic chains as well as the demethylation results in the formation of new hydroxyl groups are two possible pathways that should be considered too.

At the same time, according to the existing literature, lignins can also undergo a laccase-catalysed polymerisation mechanism resulting in the formation of diaryl ether (4-O-5') and biphenyl (5-5') structures.<sup>23</sup> A confirmation of the validity of the hypothesis of the polymerising action of laccases can be found, for instance, in *Krisnagura* studies demonstrating that in his studies the incubation of lignins with laccases resulted in the incrementation in the content of condensed structures.<sup>170</sup> Diaryl ether patterns are the result of the radical coupling of aryloxy and semiquinone radicals, as depicted in Fig.3.13.

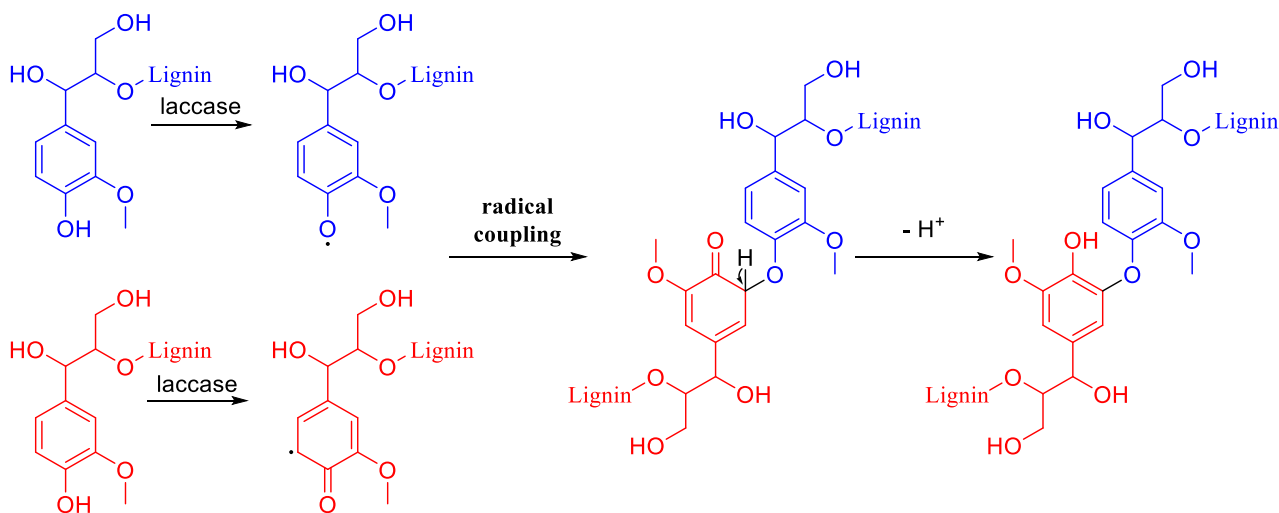


Figure 3.13. Laccase-catalysed formation of diaryl ethers via radical coupling.

A similar type of radical coupling is also at the base of the formation of biphenyls, whether two semiquinone radicals are involved. The mechanism is depicted in Fig.3.14.

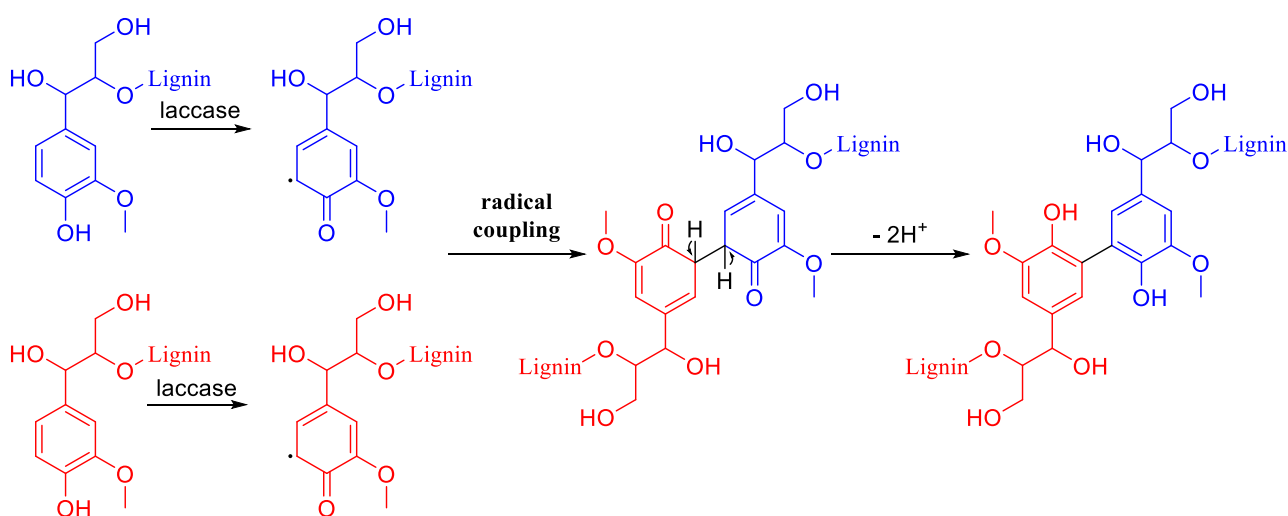


Figure 3.14. Laccase-catalysed formation of biphenyls via radical coupling.

Typical substrates for the laccase-catalysed polymerisation of lignins are highlighted in Fig.3.12. Of the polymerisation mechanisms depicted in Figg.3.13 and 3.14 increasing the degree of condensation of lignins, the formation of diaryl-ethers allow to reduce the content of phenolic hydroxyl groups. A confirmation of the validity of the hypothesis of the polymerising action of laccases can be found in the previously mentioned research by *Krisnagura* demonstrating that the incubation of lignins with laccases resulted in an incrementation in the content of condensed structures.

With these premises, in order to elucidate the action of the enzyme on the various lignin preparations,  $^{31}\text{P}$  NMR and GPC analyses were performed. Data for blank samples were considered as well with the aim to exclude the effect of the alkaline conditions on the modifications occurring on lignin during the enzymatic oxidation.  $^{31}\text{P}$  NMR data reported henceforth are the average of triplicate analyses of the samples; the percent error ranges between 3.7 and 5.8%.

In general, both SKL and WSL samples demonstrated a decrease in the content of the hydroxyl groups after the enzymatic oxidation. A visual comparison of the content of the hydroxyl groups in the samples before and after the enzymatic treatment with different loadings of enzymes is reported in Figure 3.15 for SKL-related samples. The corresponding numerical data are reported in Table 3.10.

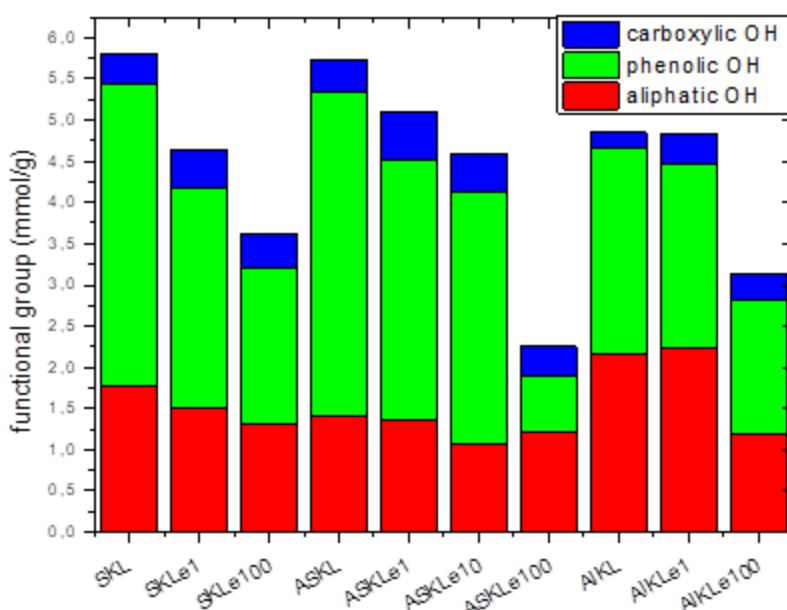


Figure 3.15. Hydroxyl groups content in SKL and its fractions before and after the enzymatic treatment with different amounts of laccase.

Table 3.10. Content of the various hydroxylated moieties per gramme of SKL-related lignin preparation, determined via <sup>31</sup>P NMR analyses.

Sample	Aliphatic OH (mmol/g)	Phenolic OH (mmol/g)				Aliphatic/phenolic OH	COOH (mmol/g)
		Condensed/S- Units	G- units	H- units	total		
SKL	1.77	1.63	1.88	0.18	3.68	0.48	0.36
SKLb	1.73	1.21	1.60	0	2.81	0.62	0.55
SKLe1	1.50	1.20	1.47	0	2.67	0.56	0.48
SKLe100	1.30	0.62	1.00	0.29	1.91	0.68	0.41
ASKL	1.41	1.76	1.86	0.11	3.93	0.36	0.39
ASKLb	1.33	1.46	1.64	0.11	3.21	0.41	0.56
ASKLe1	1.37	1.36	1.77	0	3.14	0.44	0.58
ASKLe10	1.06	1.20	1.74	0.12	3.07	0.35	0.47
ASKLe100	1.21	0.16	0.52	0	0.69	1.75	0.35
AIKL	2.17	1.30	0.99	0.09	2.50	0.87	0.18
AIKLb	2.06	1.20	0.96	0.12	2.28	0.90	0.35
AIKLe1	2.23	1.09	1.16	0	2.25	0.99	0.36
AIKLe100	1.19	0.56	0.83	0.23	1.63	0.73	0.32

The analyses of the trends evidenced that as the amount of the enzyme increases, the content in hydroxyl groups lignin decreases. More specifically, by considering phenolic hydroxyl groups, which are the standard substrate in laccase-mediated oxidation of lignin-substrates, it was observed that the higher variation was observed in the case of ASKLe100. In fact, their content decreased from 3.93 mmol/g to 0.69 mmol/g. This fact was justified according to the structure of ASKL, which is a polyphenolic condensed material deriving from the condensation of low molecular weight monomeric units deriving from the Kraft pulping.

The complete oxidation of *p*-hydroxyphenyl terminal units was noticed for ASKLe100. Owing to the high content in condensed and non G-related units of ASKL, not all of them were converted in the enzymatic decay, even if an excess of enzyme was used (e100).

Similar trends to those highlighted for ASKL were found for the phenolic hydroxyl groups in the case of SKL. In particular, even if the variation in the content was lower than that of ASKL, relevant variations in terms of either condensed or non-condensed structures were demonstrated via <sup>31</sup>P NMR. AIKL was the more recalcitrant SKL-related lignin preparation. Moreover, the beneficial effect of high loading of enzyme in the conversion of the substrates was highlighted.

The decrease in terms of aliphatic hydroxyl groups content in lignin is not directly related to the action of laccase on lignin, as described in [Paragraph 1.7.4](#). Moreover, it seemed reasonable to attribute to some of the low molecular weight compounds formed in situ from the depolymerisation of lignin the redox mediators. In fact, molecules like vanillin or apocynin, can be activated via laccase, resulting in aryloxy radicals which can easily diffuse across lignin structure permitting the hydrogen-atom abstraction on benzylic hydroxyl groups starting their oxidation.<sup>153,154</sup>

With respect to the variation in the content of aliphatic hydroxyl groups, the sample undergoing the most prominent variation was AIKL. In fact, due to its highly dealkylated structure, its degradation is favoured as the interaction with redox mediator is more probable than for SKL or ASKL. From the other side, ASKL, which has the lower content in aliphatic hydroxylated moieties, it seemed more recalcitrant to this type of oxidation. SKL displayed an intermediate behaviour between AIKL and ASKL.

Finally, the variation in terms of carboxylic groups content was not as relevant as the one in aliphatic and phenolic hydroxyl groups. In particular, only a slight increase was noticed in almost all the samples. Moreover, by comparing the samples oxidised with e1 to those with e100 amount of enzyme, it was possible to conclude that the content in carboxylic groups in the firsts (SKLe1, AIKLe1, and ASKLe1) is slightly higher than the same in the latter (SKLe100, AIKLe100, and ASKLe100). It seemed reasonable to assume that at the beginning of the catalytic action of laccase, carboxylic groups are formed; then, by the action of additional laccase, these groups are polymerised with the formation of diaryl ethers structures according to the mechanism suggested by *Ikeda*.<sup>171</sup>

The <sup>31</sup>P NMR data obtained from WSL and its fractions are summarised in Figure 3.16 and Table 3.11.



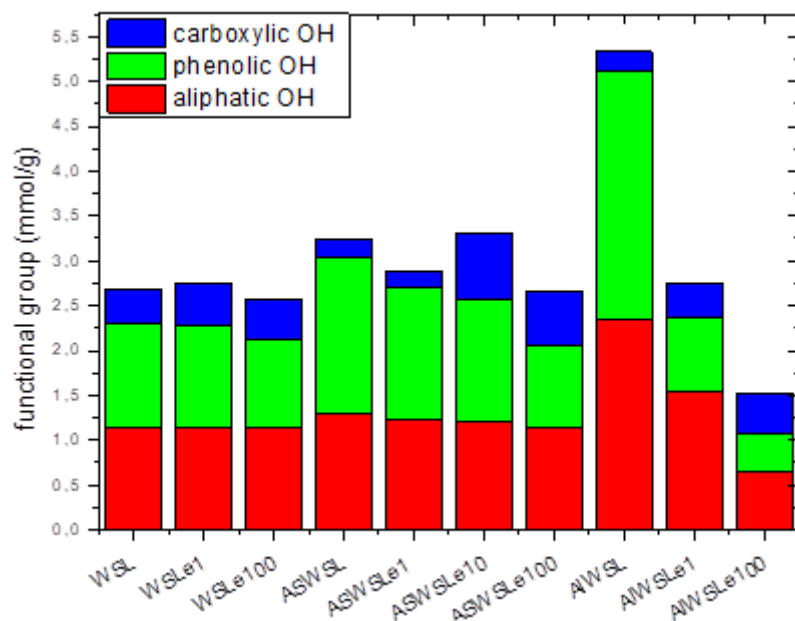


Figure 3.16. Hydroxyl groups content in WSL and its fractions before and after the enzymatic treatment with different amounts of laccase.

Table 3.11. Content of the various hydroxylated moieties per gramme of WSL-related lignin preparation, determined via  $^{31}\text{P}$  NMR analyses.

Sample	Aliphatic OH (mmol/g)	Phenolic OH (mmol/g)				Aliphatic/phenolic OH	COOH (mmol/g)
		Condensed/S-units	G-units	H-units	total		
WSL	1.13	0.52	0.44	0.14	1.18	0.96	0.37
WSLb	1.07	0.42	0.52	0.20	1.14	0.94	0.19
WSLe1	1.15	0.46	0.48	0.20	1.14	1.01	0.46
WSLe100	1.14	0.38	0.44	0.16	0.99	1.15	0.45
ASWSL	1.30	0.60	0.85	0.28	1.73	0.75	0.20
ASWSLb	1.45	0.55	0.69	0.26	1.49	0.97	0.10
ASWSLe1	1.22	0.53	0.71	0.24	1.48	0.82	0.19
ASWSLe10	1.20	0.48	0.68	0.19	1.36	0.88	0.74
ASWSLe100	1.15	0.37	0.39	0.15	0.91	1.26	0.60
AIWSL	2.35	1.43	1.12	0.12	2.76	0.85	0.22
AIWSLb	2.05	0.79	1.16	0.29	2.25	0.91	0.34
AIWSLe1	1.55	0.29	0.48	0.06	0.82	1.89	0.38
AIWSLe100	0.65	0.21	0.16	0.04	0.43	1.51	0.44

In the case of WSL, the unfractionated lignin was the most recalcitrant material against to the laccase catalysed oxidation. No relevant variation in terms of aliphatic hydroxyl groups content were highlighted even if the concentration of the enzyme was increased. The same observation was extended for either phenolic or carboxylic groups. The reactivity of WSL fractions was more relevant. From one side, the ASWSL underwent the oxidation of both phenolic and aliphatic hydroxyl groups. The beneficial effect of an increased concentration in the enzyme was discretely noticeable; if phenolic hydroxyl groups are considered, their content decreased from 1.73 mmol/g in ASKL to 1.48, 1.36 and 0.91 mmol/g respectively in ASKLe1, ASKLe10, and ASKLe100. The decrease in terms of aliphatic hydroxyl groups was less relevant; in fact only a variation of 0.15 mmol/g was quantified even if e100 laccase had been used. The variation in terms of carboxylic groups was more relevant, which controversially increases from 0.20 mmol/g in ASK to 0.60 mmol/g in ASWSLe100. From the other side, AIWSL resulted in a relevant the decay of the content of both aliphatic and phenolic hydroxyl groups. The decrease in aliphatic hydroxyl groups, from 2.35 mmol/g to 0.65 mmol/g in AIWSLe100 was related to the transformation occurring on AIKL. In particular, the role of vanillin was assumed as fundamental as redox-mediator for the oxidation of these substrates. The decrease in phenolic hydroxyl groups, from 1.73 mmol/g to 0.91 mmol/g in AIWSLe100 was attributed to the standard oxidation mechanism of laccase, while the increase of carboxylic groups was correlated to the formation of new acidic groups via the oxidation of terminal aliphatic hydroxyl groups.

In conclusion, <sup>31</sup>P NMR analyses demonstrated that both SKL and WSL were chemically modified by the enzyme; different reactivities between the fractions and the starting material were highlighted. These results demonstrated the beneficial effect of fractionation, resulting in materials which could be oxidatively functionalised more selectively and to higher extent if compared to pristine starting materials. With regards to the acetone soluble fractions, it was concluded that the polyphenolic nature of ASKL allowed the higher variation in phenolic hydroxyl groups if compared to the insoluble counterpart. The same reactivity was not extended to ASWSL, in which this variation of hydroxyl groups was more limited. The recalcitrancy of ASWSL was possibly attributed to the expected higher content in methoxylated structures, sterically obstructing the action of laccase. More interesting were the transformations occurring on the acetone insoluble fractions of both lignins. In fact, in either cases, these fractions are those characterised by the highest decrease in terms of non-phenolic hydroxyl groups.

GPC analyses. In the perspective of understanding the overall effect of laccase on technical lignins, proving eventually polymerisation and depolymerisation mechanisms, the enzymatically modified

samples were analysed via GPC in order to determine their molecular weight. The so determined molecular weights variations were then correlated with those of blanks, in order to exclude the effect of the alkaline buffer used during the enzymatic oxidation. Numerical data for the  $M_n$  and the PDI of SKL and WSL samples are reported in Tab. 3.12 and 3.13.

*Table 3.12.*  $M_n$  and PDI for SKL, its fractions, the blanks, and the enzymatically degraded samples with the stoichiometric amount of enzyme (e1) and one hundred times the stoichiometric amount of enzyme (e100). For ASKL, the enzymatically degraded samples have also been prepared with ten times the amount of stoichiometric enzyme (e10).

	$M_n$	PDI
SKL	1200	4.3
SKLb	2100	3.8
SKLe1	2300	4.0
SKLE100	4400	3.0
AIKL	5300	4.2
AIKLb	5800	5.3
AIKLE1	5500	4.3
AIKLE100	6200	3.7
ASKL	1000	2.4
ASKLb	1700	2.1
ASKLE1	1800	2.1
ASKLE10	2300	2.3
ASKLE100	3500	2.7

Table 3.13.  $M_n$  and PDI for WSL, its fractions, the blanks, and the enzymatically degraded samples with the stoichiometric amount of enzyme (e1) and one hundred times the stoichiometric amount of enzyme (e100). For ASWSL, the enzymatically degraded sample have been prepared also with ten times the amount of stoichiometric enzyme (e10).

	$M_n$	PDI
WSL	2800	14
WSLb	3500	13
WSLe1	3300	13
WSLe00	3400	7.4
AIWSL	5400	13
AIWSLb	5300	13
AIWSLe1	5700	12
AIWSLe100	5200	5.2
ASWSL	700	2.0
ASWSLb	1000	2.1
ASWSLe1	1000	2.0
ASWSLe10	1300	1.9
ASWSLe100	2000	2.1

Hereafter, when the variation of the molecular weight distribution ( $\Delta M_n$ ) is referred, the difference between  $M_n$  for the oxidatively modified lignin ( $M_n^{ox}$ ) and the one of the corresponding blank ( $M_n^{blank}$ ) is considered:

$$\Delta M_n = M_n^{ox} - M_n^{blank}$$

The chromatograms for laccase-oxidised SKL and its fractions are depicted in Figure 3.17. In all cases, the extent in the variation of the molecular weight of lignins was related to the amount of the enzyme used. Greater variations were obtained with the higher loadings of enzyme. The sample whose  $M_n$  increased the most was SKL, where  $\Delta M_n$  corresponded to 2300 u.m.a. (SKLe100). This evidence supported the hypothesis of a polymerisation process. Similar conclusions were extended to AIKL and ASKL, moreover none of them varied the  $M_n$  as much as SKL did. In fact, ASKL increased its molecular weight of 1800 u.m.a. after the enzymatic oxidation (ASKLe100), and AIKL followed the same trend resulting in a final variation of 400 u.m.a. (AIKLe100). Not only a variation in the molecular weight of lignins was observed; in fact, a decrease in the PDI was also found.

The decrease in the PDI index coupled with the increase of the molecular weight of the lignins and the formation of low molecular weight compounds permitted to speculate on the nature of the reactions occurring during the oxidation of SKL with laccase. In fact, it was hypothesized that the depolymerisation mechanisms resulting into the liberation of the low molecular weight compounds were at the basis of (a) the generation of radical species and (b) the oxidation of hydroxylated moieties.

The action of the laccase on lignins, favoured by the long reaction time as well as the alkaline conditions, permitted the radical coupling mechanisms described at the beginning of the paragraph. This fact justified the decrease in the PDI corresponding to an increase in the homogeneity of the oxidised lignins.

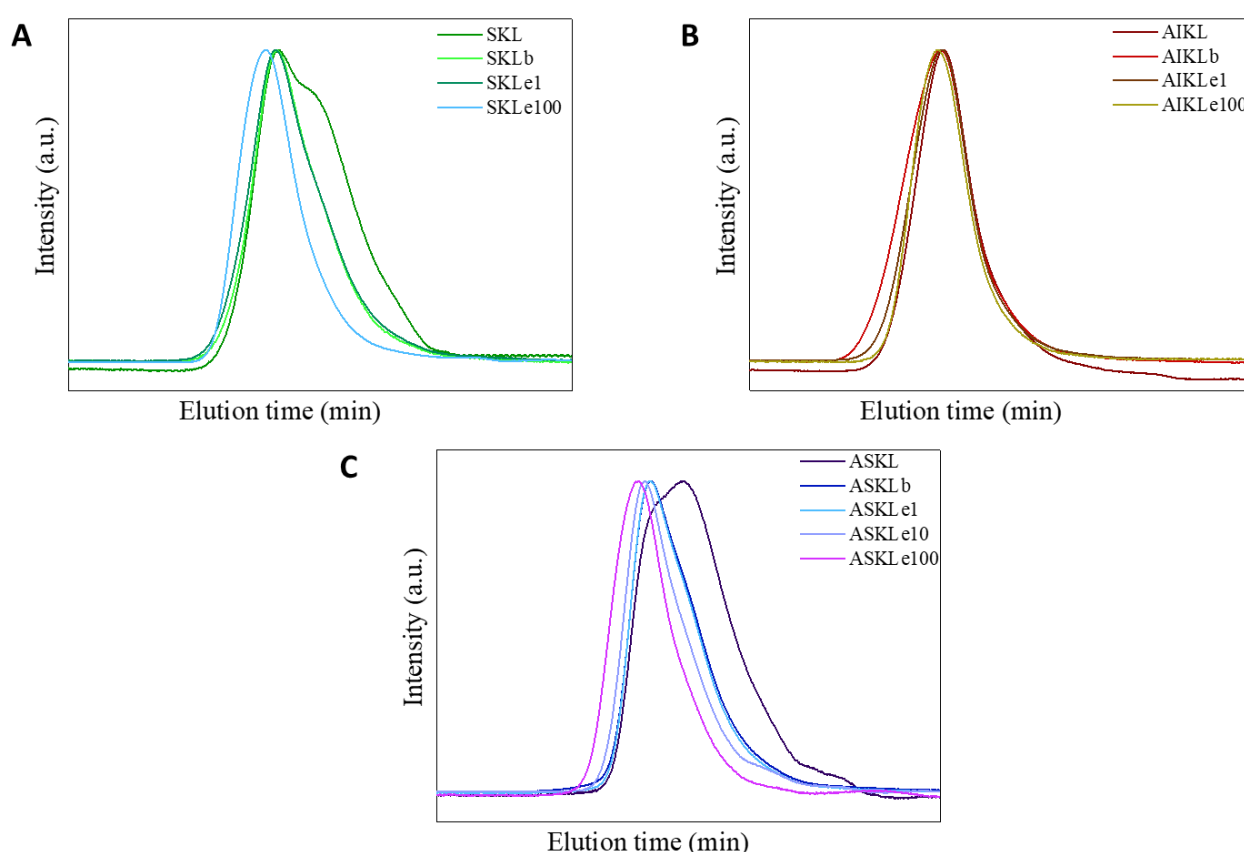


Figure 3.17, Comparison of the GPC analysis for precipitated lignin after the enzymatic incubation for (A) SKL, (B) AIKL, and (C) ASKL.

The GPC analyses for WSL-related lignin preparations are reported in Figure 3.18.

From one side, WSL and AIWSL decreased their molecular weight as the amount of the enzyme increased. In fact, both of them demonstrated a  $\Delta M_n$  of approximately 100 u.m.a. after the enzymatic

treatment (WSLe100 and AIWSLe100). This evidence demonstrated a depolymerising action of the enzyme on lignins.

From the other side, the laccase-catalysed oxidation of ASWSL allowed to observe an increase in its molecular weight (ASWSLe100,  $\Delta M_n = 1000$  u.m.a. ). Interestingly, even if the genesis of the lignin was the same, owing to the different structural features of the samples, a polymerisation mechanism was noticed here.

Similarly to the results obtained for SKL, WSL and its fractions decreased their PDI after the enzymatic oxidation. This evidence permitted to extend the considerations previously made on the polymerising/depolymerising action of laccases for SKL to WSL. In particular, in the case of WSL it was concluded that the depolymerisation mechanisms governing the oxidative modification WSL and AIWSL were balance by a polymerising counterpart permitting the homogenisation of the lignin chains and structures.

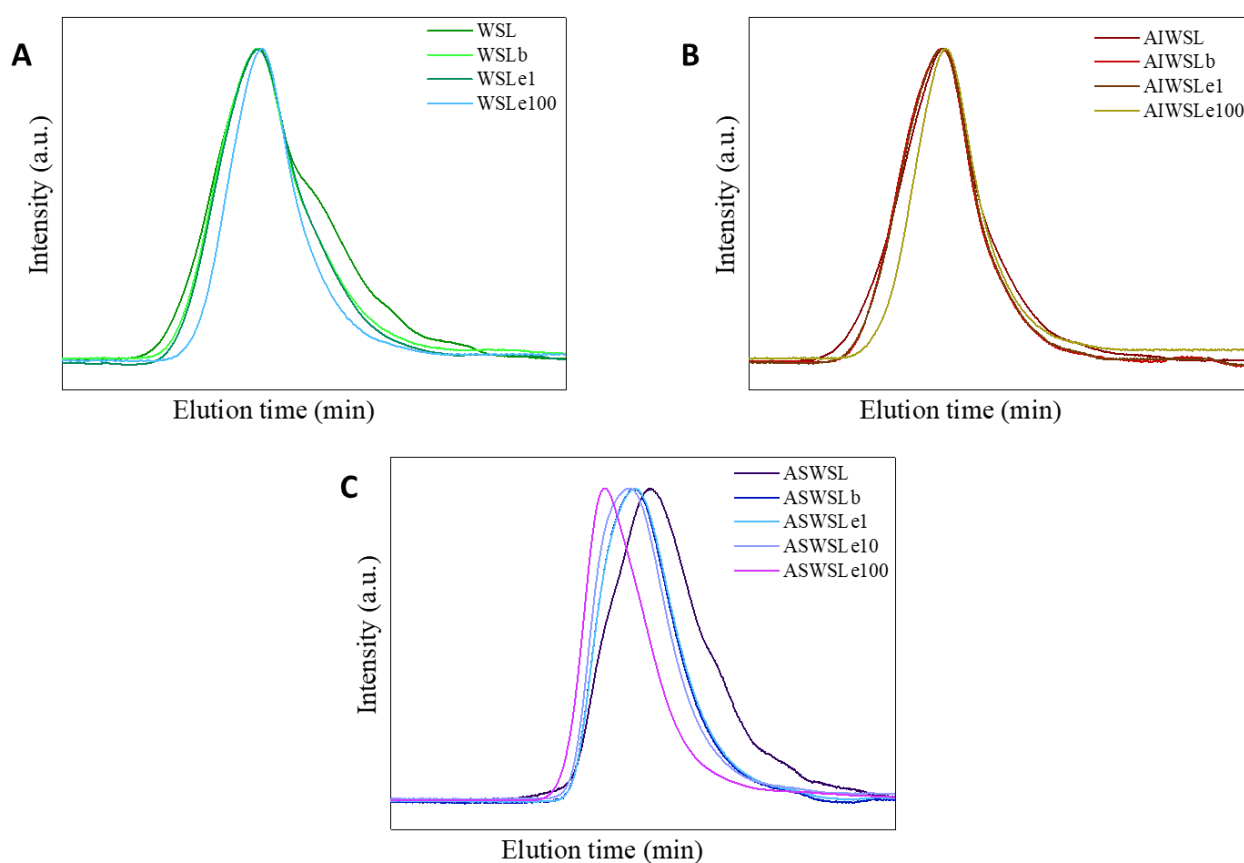


Figure 3.18. Comparison of the GPC analysis for precipitated lignin after the enzymatic incubation for (A) WSL, (B) AIWSL, and (C) ASWSL.

### 3.3. Experimental part

The laccase used in the research is a transgenic enzyme produced and kindly supplied by *Metgen* (Kaarina, Finland). Na<sub>2</sub>ABTS (97%) was purchased from *AlfaAesar*. Glycine, hydrochloric acid (37%), sodium acetate, acetic acid, citric acid, sodium citrate, sodium dihydrogenophosphate, disodium hydrogenophosphate, and sodium hydroxide were obtained in reagent grade from *Merck*. Acetovanillone, acetosyringone, and sodium borohydride were obtained from *TCI Chemicals*. Diethyl ether, ethyl acetate, and p-dioxane were purchased at *Merck*.

Technical lignins used for this research, were kindly supplied by *Stora Enso* (SKL) and *CIMV* (WSL),

#### 3.3.1 Lignin fractionation

Lignin fractionation is carried in accordance with the first step of the fractionation approach suggested by *Cui*.<sup>158</sup> Specifically, a 100 mg/mL lignin (either SKL or WSL) dispersion in acetone is stirred at room temperature for 12 h. Afterwards, the acetone insoluble fraction (AI) is isolated by filtration and dried in vacuum at 30°C, while the acetone soluble fraction (AS) is collected by rotary evaporation at 30°C. Four samples are thus obtained: acetone soluble SKL (ASKL), acetone insoluble SKL (AIKL), acetone soluble WSL (ASWL) and acetone insoluble WSL (AIWL).

#### 3.3.2 Spectrophotometric determinations of laccase activity via ABTS

Prior to the tests, laccase solution was diluted 1 : 100 with milliQ water.

In a 2 mL quartz cuvette 900 µL of buffer solution (50 mM) are mixed with 100 µL of 20 mM Na<sub>2</sub>ABTS solution in milliQ water. Then, 10 µL of diluted enzyme solution are added, the solution is rapidly and vigorously shaken, and the variation of absorbance was measured at 420 nm in with a *Shimadzu* UV-vis spectrometer during 1 minute.

The following formula was used to obtain the activity of the enzyme solution:

$$\text{enzyme activity} = \frac{\text{absorbance variation} \cdot 1000}{21.2 \frac{\text{cm}^2}{\mu\text{mol}} \cdot 10 \mu\text{L}}$$

### 3.3.3 Preparation of apocynol 4-(1-hydroxyethyl)-2-methoxyphenol

Apocynol was prepared according to the procedure described by *Adler* with some modifications.<sup>172</sup> 4 g of acetovanillone (24 mmol) are dissolved in 60 mL of an ethanol/water mixture (1/1), then the solution is alkalinised with 1 M sodium hydroxide solution. The reaction mixture is cooled in an ice bath; then 0.45 g (12 mmol) of sodium borohydride are added in small portions during 30 minutes. The mixture is stirred for an additional period of two hours. The completion of the reduction is checked via *Brady's test*<sup>1</sup> (dinitrophenylhydrazine test) on an aliquot of the reaction mixture. If a positive test results (formation of apocynin-dinitrophenylhydrazone, red precipitate), the reaction has to continue for a longer time. If negative test results the solution is acidified with 0.1 M hydrochloric acid and extracted with diethyl ether. A crude slightly yellow crystalline product is obtained with vacuum evaporation of sodium sulphate dried ether extracts. Apocynol purification was achieved via dissolution of the solid in ethyl acetate followed by the precipitation with the addition of hexane. 2.81 g (16.7 mmol) of pure product resulted, yield of 69.5%.

### 3.3.4 Preparation of 4-(1-hydroxyethyl)-2,6-dimethoxyphenol

4-(1-hydroxyethyl)-2,6-dimethoxyphenol was prepared similarly to apocynol. 2 g of acetosyringone (10 mmol) are dispersed in 200 mL of an methanol, then the solution is alkalinised with a sodium hydroxide 1 M solution. The reaction mixture is cooled in an ice bath; then 0.40 g (10mmol) of sodium borohydride are added in small portions during 30 minutes. The mixture is stirred for an additional period of two hours. The completion of the reduction is checked via *Brady's test*. If a positive test results (formation of acetosyringone-dinitrophenylhydrazone, red precipitate), the reaction has to continue for a longer time. If negative test results the solution is cooled in an ice/acetone bath, acidified with 0.1 M hydrochloric acid and extracted with diethyl ether. A slightly pink crystalline crude product is obtained with vacuum evaporation of sodium sulphate dried ether extracts. 4-(1-hydroxyethyl)-2,6-dimethoxyphenol purification was achieved via dissolution in the solid in ethyl

---

<sup>1</sup> *Brady's test* is performed by adding 10 drops of the reaction mixture in 1 mL of *Brady's reagent* solution and heating the resulting solution in a steam bath for 5 minutes. The reagent is prepared by dissolving 3 grammemes of 2,6-dinitrophenylhydrazine in 100 mL of water/ethanol (30/70), followed by the addition of 30 mL of concentrated (98%) sulphuric acid. The mixture is kept in an ice bath during the addition of the acid.



acetate followed by the precipitation with the addition of hexane. 0.95g (4.8 mmol) of pure product result, yield of 48.0%.

### 3.3.5 Laccase test of lignin model compounds

0.23 mmol of lignin model compound (40 mg of apocynol, 48 mg of 4-(1-hydroxyethyl)-2,6-dimethoxyphenol) are dissolved in a couple of millilitres of *p*-dioxane. Then, the solution is made up with the chosen buffer (which has been previously saturated with oxygen by extensive air bubbling over a period of time of 2 hours) up to the final concentration of 12 m M with respect to the starting model compound. Laccase is added to a final concentration of 0.5 U/mL according to the enzyme activity determined at pH 4; the solution is incubated overnight at room temperature with vigorous stirring. The day after, the reaction mixture is boiled for ten minutes and extracted with three aliquots of 20 mL each of ethyl acetate. The extract is dried over sodium sulphate, evaporated to dryness under reduced pressure, and analysed via GC after its dilution in 1 mL of diethyl ether.

An *Agilent 6890N* gas-chromatographer equipped with an HP-1 column and a flame ionisation detector is used in order to evaluate the conversion of the substrates. The heating ramp of the oven used for the separation of the constituents of the reaction mixture is the following: 5 minutes at 50°C, then 10°C/minutes up to 280°C; then, the temperature is then kept constant for 10 minutes before cooling down and terminating the acquisition data from the mixture.

### 3.3.6 Enzymatic treatments of lignins

Lignin samples are dissolved in a pH 10 sodium glycinate buffer (2 mg/mL). The pH is eventually adjusted with 0.1 M sodium hydroxide. The solution is transferred in a 40°C thermostatic reactor and mixed (100 rpm) with a mechanical overhead stirrer for 2 h under air bubbling. Afterwards, the calculated amount of laccase (see [Paragraph 3.2.4](#)) is added, and the mixture is incubated for 16 h.

At the end of the incubation time, the pH is adjusted to pH 1.5 with 0.1 M HCl to allow the precipitation of the oxidized lignin, which is subsequently isolated by centrifugation (10 min, 5000 rpm, MPW-351), washed with clean water and centrifuged again (3×). Lignin precipitates are dried under vacuum at 40°C to constant weight.

The supernatants from the washing operation are collected and extracted three times with ethyl acetate after the addition of 1 mL of ethyl acetate solution of veratraldehyde (1 mg/mL), used as internal standard for GC-MS analyses. Extracts are concentrated to dryness via vacuum evaporation; the residual oily product is diluted with acetone and analysed via GC-MS.

### 3.3.7 GC-MS analyses of low molecular weight compounds from lignin enzymatic oxidation

Qualitative and quantitative analyses of the ethyl acetate extracts from enzymatic incubation of lignins is performed via GC-MS analysis on a *Shimadzu* GCMS QP2010 Ultra equipped with an AOi20 autosampler unit. A SLB®-5ms Capillary GC Column (L × I.D. 30 m × 0.32 mm, df 0.50 μm) is used as the stationary phase, ultrapure helium as the mobile phase. The identification of metabolites is performed via comparison of their fragmentation patterns with the NIST library database. The quantification of metabolites referred per gramme of lignin is calculated according to the area obtained from the chromatograms using the following formula:

$$\text{metabolite}_i(\text{mg/g}) = \frac{\text{Area}_i \cdot \text{concentration}_{IS}(\text{mg/mL}) \cdot \text{volume}_{IS}(\text{mL})}{\text{Area}_{IS} \cdot m_{\text{lignin}}(\text{g})}$$

where  $\text{Area}_i$  and  $\text{Area}_{IS}$  are respectively the areas of the peaks of the considered metabolite and the internal standard (veratraldehyde), concentration IS is the concentration of the internal standard solution used (mg/mL), volume IS is the volume (mL) of internal standard solution added before the extraction, and  $m_{\text{lignin}}$  is the mass (g) of the lignin preparation treated with the enzyme.

### 3.3.8 $^{31}\text{P}$ NMR analyses of the laccase modified lignins

The determination of the hydroxyl group content in the lignin samples is carried out by  $^{31}\text{P}$  NMR, following the standard procedure developed by *Argyropoulos*.<sup>66,67</sup> Briefly, a precisely weighted amount of dry sample is dissolved in a pyridine/ $\text{CDCl}_3$  mixture (1.6:1) in the presence of an the internal standard (cholesterol). The resulting solution is then derivatized using 2-chloro-4,4,5,5-tetramethyl-1,3,2-dioxaphospholane and the spectra of the solution is recorded on a *Bruker* 300 MHz NMR spectrometer (nucleus  $^{31}\text{P}$ , zgig pulse programme, 256 scans, relaxation delay 10 s, acquisition delay 10 s).

### 3.3.9 GPC analyses of the enzymatically modified lignin

GPC analyses are carried out in accordance with *Crestini* procedures reported elsewhere.<sup>74,75,173</sup> In particular, samples are analysed on a *Shimadzu* HPLC system equipped with a UV-vis detector and a PLgel 5μm MiniMIX-C column (Agilent). HPLC grade DMSO containing 0.1% lithium chloride is

used as eluent (0.2 mL/min, 70°C). Polystyrene sulfonate standards (4.3 – 2600 kDa, Sigma Aldrich) and lignin model compounds (170 – 941 Da) are used to build the calibration curve.

### **3.4. Conclusions**

The overall effect of laccase on two different technical lignins was evaluated according to chromatographic (GC-MS and GPC) and spectroscopic (<sup>31</sup>P NMR) characterisation data. Differences in the reactivity of the enzyme were noticed depending on either the nature of the technical lignin or on the nature of the acetonic fraction.

Laccase resulted in an overall polymerisation on all the SKL-related samples coupled with the decrease in the content of the various hydroxylated moieties. From one side, the sample undergoing the highest extent of transformations was ASKL; this fact was attributed to the major content in hydroxylated moieties than the SKL and AIKL. From the other side, owing to the lesser amount of hydroxyl groups, the more recalcitrant sample to the oxidation was AIKL. The extent of the modification was directly correlated to the amount of the enzyme used during the incubation.

WSL related preparations exhibited a different reactivity. From one side, WSL and AIWSL demonstrated of being more recalcitrant to the oxidative polymerisation previously noticed for SKL-samples. From the other side, ASWSL has undergone into the same type of polymerisation demonstrated by SKL-samples. Even in this case, the variation in the molecular weight of the samples was accompanied with a decrease in the content of hydroxyl groups.

The mild depolymerising effect of laccase on terminal phenolics from both SKL and WSL was assessed via GC-MS; depending on the amount of the enzyme used as well as the sample treated, different products were revealed.

As general trends, from this research emerged that more soluble lignin fractions undergo significant polymerization processes, possibly triggered by low molecular weight components; insoluble fractions prefer a partial depolymerization at least.

GPC analyses overall demonstrated a decrease in the PDI of lignins after the enzymatic treatment. This fact, coupled with the data confirming the polymerising/depolymerising activity of laccase, as well as the GC-MS data showing the formation of phenolic monomeric compounds, permitted to conclude the tailoring effect of the enzyme on the treated lignin preparations.

Further analyses on the enzymatically modified lignins based on the use of quantitative <sup>13</sup>C NMR as well as bidimensional NMR techniques will be able to demonstrate more in depth the chemical modifications of the samples and permit to better elucidate the polymerisation mechanisms occurred.

In view of the results obtained, the enzymatic treatment seems a promising strategy for the modification of technical lignins properties resulting in more homogeneous materials, characterised by different molecular weights and tailored content in hydroxyl groups.

## 4. Combined lignin fractionation/laccase modification in the development of with tailored size and hydrophobicity.

*In this Chapter a tandem strategy for the tailoring of kraft lignin nanoparticles (KLNPs) properties was developed. More specifically, a sample of angiosperm dicotyledon kraft lignin (AKL) was submitted to sequential fractionation/laccase treatments to modulate the content of polar hydrophilic functional groups and the molecular weight distribution. The array of samples obtained from the different treatments was in turn used in the synthesis of KLNPs. The colloidal dispersion obtained showed predictable trends in hydrophobicity and size as a function of phenolic groups content and molecular weight distributions.*

### 4.1 Introduction

Burning kraft lignin is a common practice for pulping industry as in this way energy can be recollect and used to supply the process. Moreover, owing to its aromatic and polymeric structure, lignin is nowadays considered as a potential starting point for the preparation of high-value chemicals and materials.

Among the materials which can nowadays be prepared from kraft lignin, particular relevance has recently been given to the production of lignin nanoparticles (LNPs), after their initial discovery by *Frangville*.<sup>87</sup> The size of these nanomaterials coupled with their aromatic nature permits to use these nanomaterials for a wide class of applications, limited not only to UV-vis shielding barriers, drug delivery systems, and antibacterials.<sup>100</sup>

As it has been discussed in Paragraph 1.6, different strategies are nowadays available for the preparation of LNPs.<sup>174</sup> Precipitation methods are the most convenient as they do not require the utilisation of expensive instrumentation (e.g. homogenisers) nor reticulating agents. Among them, the *anti-solvent strategy*, based on the dissolution of lignins in organic solvents followed by their precipitation via dilution in water, allows to obtain nanostructured lignins in high yields.<sup>175</sup> The reason for the high yields resides on the good solvating properties of the solvent used for the dissolution of lignins.

Size and hydrophobicity constitute two crucial characteristics that dictate the ranges of applicability of LNPs. LNPs size, that was demonstrated to vary depending on the system used for their isolation, is directly correlated with their biocompatibility and UV-vis absorption. In particular, the bigger the particles are, the better their biocompatibility is. Hydrophobicity can instead affect the LNPs

compatibility not only in the preparation of composite materials but also in the active uptake and release kinetics in active controlled delivery systems. In fact, the active upload in LNPs is strongly affected by the relative hydrophobicity of the active and the lignin itself. Therefore, by increasing lignin hydrophobicity, the range of actives possibly uploaded in LNPs can be conveniently widened. Furthermore, the kinetics of release can also be tuned by such modifications due to the occurrence of different aggregation/disaggregation dynamics.

In view of that, in this *Chapter* the development of a strategy for tailoring LNPs in terms of size and hydrophobicity is described with the aim to pave the way for the development of a new family of LNPs with improved performances and wide applicability.

## ***4.2 Results and discussion***

### **4.2.1 Design of a stream for tailoring lignin nanoparticles properties**

In the present study a protocol for the sequential lignin fractionation/laccase modification has been designed in order to obtain lignin samples with an array of different amounts of functional groups and molecular weight distributions. A first fractionation step was carried out on the starting AKL to yield acetone insoluble and soluble fractions, AIAKL and ASAKL respectively. Laccase treatment of both AKL and its fractions yielded lignin oxidized samples, AKLox, AIAKLox, and ASAKLox respectively. This array of samples was fully characterized by GPC and <sup>31</sup>P NMR analysis.

From the different lignin samples obtained KLNPs colloidal dispersions were obtained by the hydrotropic approach based on the dissolution of lignin into a *p*-toluene sulfonic acid sodium salt solution at a concentration higher than that of its critical micellar concentration, followed by nanoprecipitation with water. The obtained KLNPs were then characterized in size and ζ-potential.

KLNPs were obtained from the various lignin preparations resulting from the different steps of the valorisation stream reported in Fig. 4.1 and cross-compared to evaluate the effect of each treatment on the chemical-physical properties of the final product.

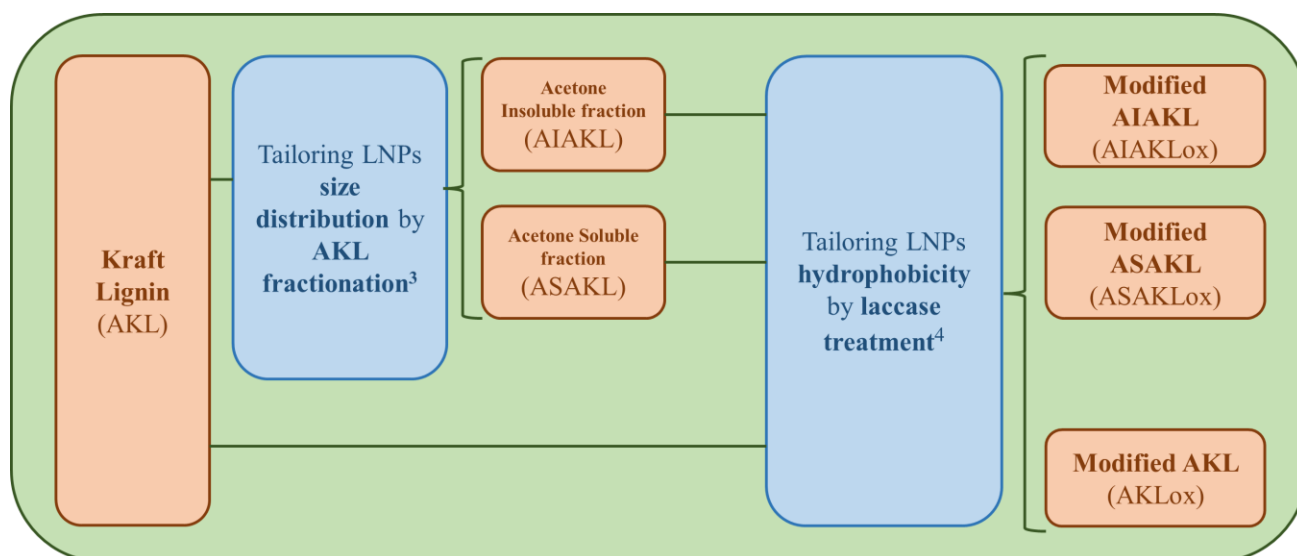


Figure 4.1. Tandem system coupling a fractionation step with the enzymatic incubation of AKL-derived preparations.

#### 4.2.2 Lignin fractionation

The use of a fractionation step permitted the isolation of the two AKL different constituents. The isolation of AIAKL and ASAKL was performed according to the fractionation protocol described in *Chapter 3*.<sup>158</sup> The composition of the AKL in its fractions is schematised in Fig. 4.2, while the chemical and physical properties of the fractions (the content of the various hydroxylated moieties and the molecular weight distribution) are reported in Fig.4.3. The numerical data are reported in Tab.4.1. This AKL is characterized by a high content (70,6 %) in the soluble fraction. ASKL showed a lower  $M_n$  than the insoluble one. As expected, ASAKL contains a higher amount of phenolic groups, while the AIAKL shows a higher amount of aliphatic OH groups. Carboxylic acids are also more abundant in the ASAKL fraction than the others. Noteworthy, the technical lignin used in this study was characterised by a high content in carboxylic moieties which was attributed to the presence of aliphatic or aromatic carboxylic groups in lignin structures as well as muconic acids, deriving from the oxidation of lignin via oxygen addition in the bleaching step after kraft pulping.

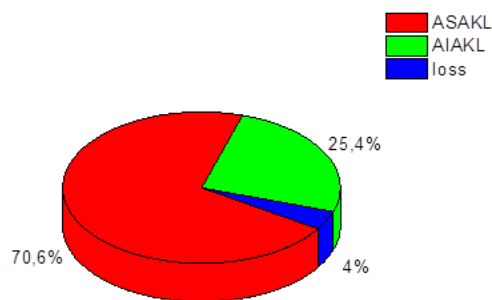


Figure 4.2. Composition in terms of fractions of AKL. Acetone soluble fraction (ASAKL) is the prominent constituent of AKL.

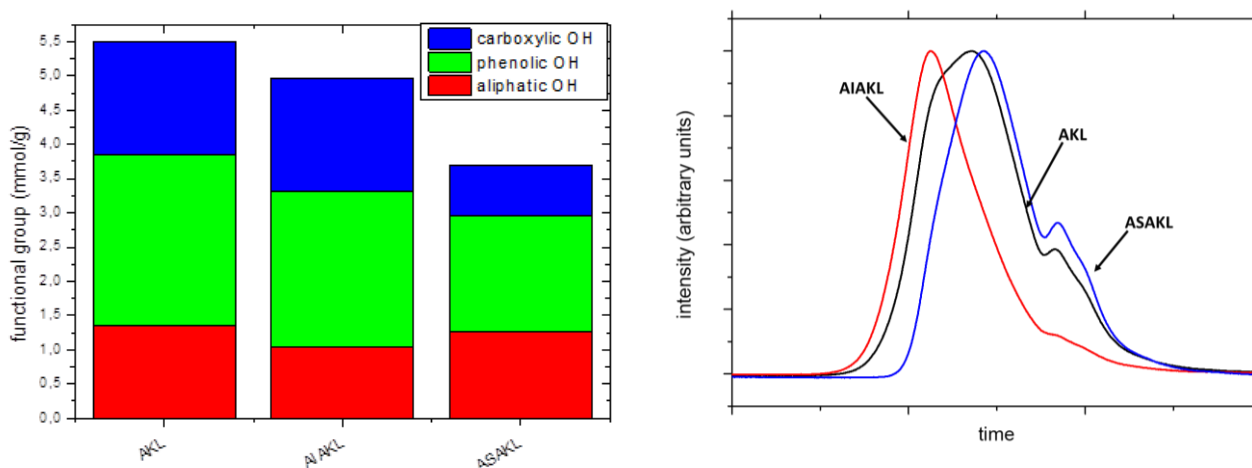


Figure 4.3. (left) Composition in terms of various hydroxylated moieties for AKL and its fractions determined via  $^{31}\text{P}$  NMR analyses. (right) Molecular weight distribution for AKL and its fractions.

ASAKL is characterised by a lower molecular weight, while AIAKL has a higher one.

Table 4.1. Molecular weight distribution from GPC analysis, functional groups occurrence on AKL, and its fractions.

Sample	$M_n$	PDI	Aliphatic OH (mmol/g)	Phenolic OH (mmol/g)	Carboxylic OH (mmol/g)
AKL	1300	6.6	1.36	2.48	1.66
ASAKL	3900	6.3	1.03	2.29	1.65
AIAKL	950	2.8	1.26	1.69	1.11



The laccase-catalysed oxidation of the different lignin samples was carried out via the methodology previously developed and extensively described in *Chapter 3*. One-hundred-fold excess of laccase, calculated accordingly to enzymatic activity of laccase solution and the content of the various hydroxylated moieties per gramme of lignin, was used in these experiments; the reaction time was set to 16 hours to favour the complete oxidation of the treated substrates.

Table 4.2 shows the structural characteristics of the oxidized lignin samples. GPC analyses demonstrated an increase in the molecular weight in all the cases (AKLox, AIAKLox, and ASAKLox); this increase was coupled with a decrease, after oxidation, in the PDI for both AKL and AIAKL, while ASAKL did not show any relevant variations. The peak shoulders appearing in the chromatograms of both AKL and ASAKL disappeared in the chromatograms of their oxidised counterpart. This fact testified the removal of a low molecular weight fraction by the use of alkaline conditions of the buffer.  $^{31}\text{P}$  NMR analyses revealed the efficacy of laccase as the content of all the hydroxylated moieties decreased at different extents, as reported in Tab.4.2.  $^{31}\text{P}$  NMR data reported henceforth are the average of triplicate analyses of the samples; the percent error ranges between 4.3 and 6.2%.

*Table 4.2. Functional groups distribution and Mn/PDI of AKL and its fractions before and after the enzymatic treatment determined via  $^{31}\text{P}$  NMR and GPC analyses.*

Sample	Aliphatic OH (mmol/g)	Phenolic OH (mmol/g)			aliphatic/ phenolic OH	COOH (mmol/g)	$M_n$	PDI
		Condens ed/Syrin gyl	Non condensed	Total				
AKL	1.36	0.50	1.98	2.48	0.55	1.66	1300	6.6
AKLblank	1.18	0.21	0.77	1.04	1.13	1.35	2000	6.2
AKLox	0.93	0	0.50	0.50	1.86	0.56	2700	3.5
ASAKL	1.03	0.38	1.91	2.29	0.89	1.65	950	2.8
ASAKLblank	0.85	0.29	0.87	1.16	0.73	1.20	1500	2.4
ASAKLox	0.72	0.19	0.47	0.66	1.09	0.89	2800	2.8
AIAKL	1.26	0.28	1.41	1.69	0.75	1.11	3900	6.3
AIAKLblank	1.07	0.14	0.58	0.72	1.49	0.95	4100	3.8
AIAKLox	0.91	0.24	0.56	0.80	1.14	0.80	4400	4.7

Of particular relevance was the unexpected variation in content of carboxylic groups. In order to rationalise this experimental evidence, two situations were considered. With regards to the aromatic acids, it was supposed that laccase would have polymerised them resulting in the formation of new

4-O-1' units in combination with the decarboxylation of the system. This reaction mechanism was demonstrated by *Ikeda* when studying the action of laccase in the presence of syringic acid in acidic buffered conditions.<sup>171</sup> The reaction is schematised in Fig.4.4.

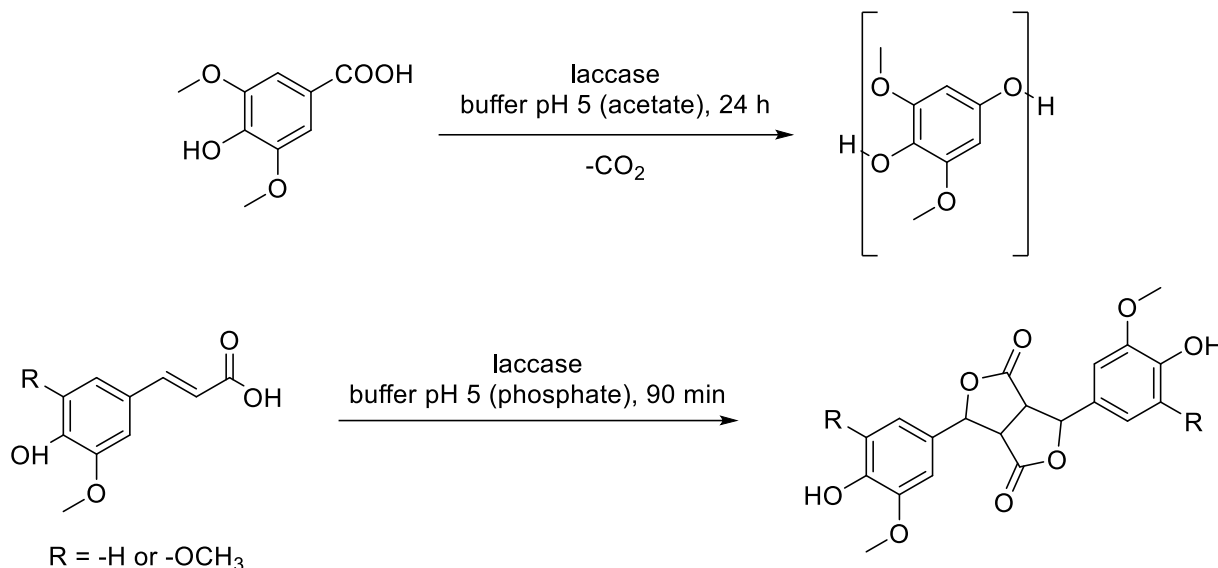


Figure 4.4. Laccase-catalysed oxidation of carboxylic groups according to *Ikeda* and *Tranchimand*.<sup>171,176</sup>

A different coupling mechanism, which does not involve the decarboxylation, was invoked to rationalise the decrease of aliphatic carboxylic groups, especially those on C<sub>γ</sub>. In fact, according to *Tranchimand*, ferulic acid as well as sinapic acid can couple with laccase treatment in mild acidic conditions resulting in the formation of a pinosresinol-like structure in which both C<sub>γ</sub> bear a carbonyl groups<sup>176</sup>, as reported in the second mechanism of Fig.4.4. <sup>19</sup>F NMR analyses of the so oxidised lignins, after the appropriate functionalisation, would be an interesting strategy to evaluate the eventual formation of pinosresinol-like structures.<sup>177</sup>

The decrease of carboxylic groups was not only related to the action of laccase. In fact, the analyses of blanks demonstrated that a slight decrease in their content resulted from the alkaline treatment of lignin preparations. This experimental fact was related to the presence of some carbohydrate-like species, like glucuronic acids, which were formed in pulping conditions and remained trapped on AKL in the precipitation step. Reasonably, their neutralisation in sodium glycinate buffer would result in the formation of glucuronates which are solubilised and removed during the washing steps.

AKL, ASAKL, and AIAKL as well as their enzymatically modified counterparts, were then used for the preparation of KLNPs via the hydrotropic method.

### 4.2.3 Preparation of AKL KLNPs

Among the various methods to prepare LNPs, solvent/antisolvent methods represent a promising way.<sup>178</sup> As previously mentioned, the obtention of nanoparticles relies on the fast change of the solvent system environment surrounding lignin, resulting in the aggregate of lignin. Unfortunately, the most commonly used solvent to dissolve lignin prior to the solvent exchange, like tetrahydrofuran, dimethyl sulfoxide, and ethanol, results in low yields of KLNPs because of the poor solubility of lignin in them.<sup>179–181</sup> In addition, the anti-solvent methodologies deal with the use of solvents which are difficultly recollected after the nanosizing operation, resulting in a limited applicability of the method on the large scale if the economic factor as well as the sustainability of the process are considered.

An interesting innovation on the preparation of LNPs via a methodology close to the antisolvent is represented by the hydrotropic method.<sup>182,183</sup> This methodology relies on the dissolution of lignin in hydrotropic mixtures, which are concentrated solutions of deprotonated aromatic acids; the dilution of the resulting lignin solutions drive to the precipitation of the nanoparticles, which can be conveniently isolated from the dispersion via extended centrifugation. The physical phenomenon behind the dissolution of lignin in hydrotropic solutions resides on the formation of  $\pi$ - $\pi'$  interactions between the aromatic rings of the neutralised acids and the aromatic rings on lignin; these interactions unfold lignin, resulting in its dissolution. The dilution of lignin hydrotropic solutions causes the permeation of water molecules in the  $\pi$ - $\pi'$  systems resulting in the precipitation of the nanoparticles. Various salts from aromatic acids have been studied for the realisation of lignin hydrotropic solutions as well as convenient way to pulp wood since the Forties of the Last Century.<sup>184</sup> Particularly relevant were the studies on sodium benzoate made by *Traynard* in the Fifties, as well as the more extensive screening on various sodium salts of benzenesulfonic acids (benzenesulfonate, tosylate, xylenesulfonate, ethyl-benzene sulfonate, butyl-benzene sulfonate, and cymene sulfonate) of *Migita*.<sup>185–187</sup> Moreover, the most commonly used hydrotropic salt for the preparation of KLNPs is, as of now, sodium tosylate.<sup>175</sup>

Theoretically, hydrotropic method can be seen as anti-solvent systems if the hydrotropic solution is considered as solvent. Moreover, the most relevant advantage of the use of solutions of salts is represented by their possibility to be easily and quantitatively recollect via evaporation the spent mixtures used for the preparation of KLNPs. Additionally, it was demonstrated that the use of hydrotropic mixtures permits to obtain solutions with higher concentrations in lignin, resulting in higher yields in nanoparticles.<sup>175</sup>

Anti-solvent methods as well as the hydrotropic method share a pivotal parameter that has to be carefully evaluated during the nanosizing of lignins: the dilution step. In fact, dilution step has to be performed by dispersing the lignin solution in water and not vice-versa. This observation has a direct correlation with the size of the resulting nanoparticles, as they would result bigger if water is added into the lignin solution. In fact, in that way lignin would initially find an environment slightly diluted which would result in a higher degree of aggregation.

According to these observations, KLNPs were prepared from AKL, its fractions, and their enzymatically modified counterpart according to the methodology described by *Cailotto* with slight modifications.<sup>175</sup> In order to evaluate the yield in KLNPs, after their precipitation from the hydrotropic solutions and the washing operations, aiming to remove the residual traces of sodium *p*-toluene sulfonate, the resulting nanoparticles were dispersed in an tared flask and diluted to the mark on the flask (50 mL). A 10 mL aliquot of the resulting dispersion were then sampled and freeze-dried for three days. Then, the weight of the resulting freeze-dried KLNPs was related to the weight of the treated lignin ( $m_{\text{lignin, solution}}$ ) with sodium *p*-toluen sulfonate, resulting in the effective yield:

$$KLNPS_{\text{yield}}(\%) = \frac{KLNPS_{\text{freeze-dried}} \cdot 5(\text{mg})}{m_{\text{lignin}}(\text{mg})} \cdot 100$$

KLNPs yields are reported in Tab.4.3.

*Table 4.3.* Yields and DLS analyses for KLNPs from AKL, its fractions, and the enzymatically modified counterpart. DLS analyses were repeated in triplicate for every KLNPs dispersion.

<i>Sample</i>	<i>Yield</i> (%)	<i>Average</i> <i>diameter (nm)</i>	<i>Pdl</i>
<i>AKL</i>	73.5	506 ± 24	0.475
<i>AKLox</i>	76.8	740 ± 1	0.602
<i>AIACL</i>	88.6	598 ± 25	0.220
<i>AIAKLox</i>	97.1	766 ± 65	0.544
<i>ASAKL</i>	63.2	492 ± 2	0.362
<i>ASAKLox</i>	59.4	617 ± 28	0.542

For both AKL and AIACL the yields in nanoparticles slightly increase when enzymatically modified lignins were used. This fact was related with a higher solubility of these preparations in hydrotropic mixtures. Different results were obtained for ASAKL preparations, where lower yields were obtained if compared to those of the other samples.

In order to determine the size of KLNPs as well as their colloidal stability, DLS and  $\zeta$ -potential analyses were performed. Prior to these analyses, KLNPs dispersions were diluted resulting in 0.01% m/V solutions that were further characterised. This step was pivotal to obtain reliable results. DLS and  $\zeta$ -potential measures data are summarised in Tab.4.3 and 4.4 respectively.

*Table 4.4.*  $\zeta$ -potential determination for KLNPs from AKL, its fractions, and the enzymatically modified counterpart. The analyses were performed in aqueous dispersion with a solid content of 0.01%.  $\zeta$ -potential determinations were repeated in triplicate on the samples.

<i>Sample</i>	<i><math>\zeta</math>potential (mV)</i>	<i>ionic mobility (<math>\mu\text{m}\cdot\text{cm}</math>)/(V<math>\cdot</math>s)</i>	<i>conductivity (mS/cm)</i>
<i>AKL</i>	$-30 \pm 1$	$-2.3 \pm 0.1$	$0.018 \pm 0.006$
<i>AKLox</i>	$-32.7 \pm 0.8$	$-2.56 \pm 0.06$	$0.007 \pm 0.001$
<i>AIACL</i>	$-34 \pm 2$	$-2.0 \pm 0.2$	$0.0053 \pm 0.0001$
<i>AIAKLox</i>	$-42 \pm 2$	$-2.6 \pm 0.3$	$0.0062 \pm 0.0007$
<i>ASAKL</i>	$-30.7 \pm 0.6$	$-2.40 \pm 0.04$	$0.007 \pm 0.002$
<i>ASAKLox</i>	$-30.8 \pm 0.9$	$-2.42 \pm 0.07$	$0.012 \pm 0.006$

Good colloidal stability for the so prepared KLNPs was demonstrated in all cases with  $\zeta$ -potential values ranging from -29.0 to -44 mV, as reported in Tab.4.4.

#### **4.2.3 On the effect of the tandem system on KLNPs size**

The molecular weight of KLNPs as well as the content of the various hydroxylated moieties were then correlated with the DLS analyses. Fig. 4.5, .4.6, and 4.7 summarise the observations further described.

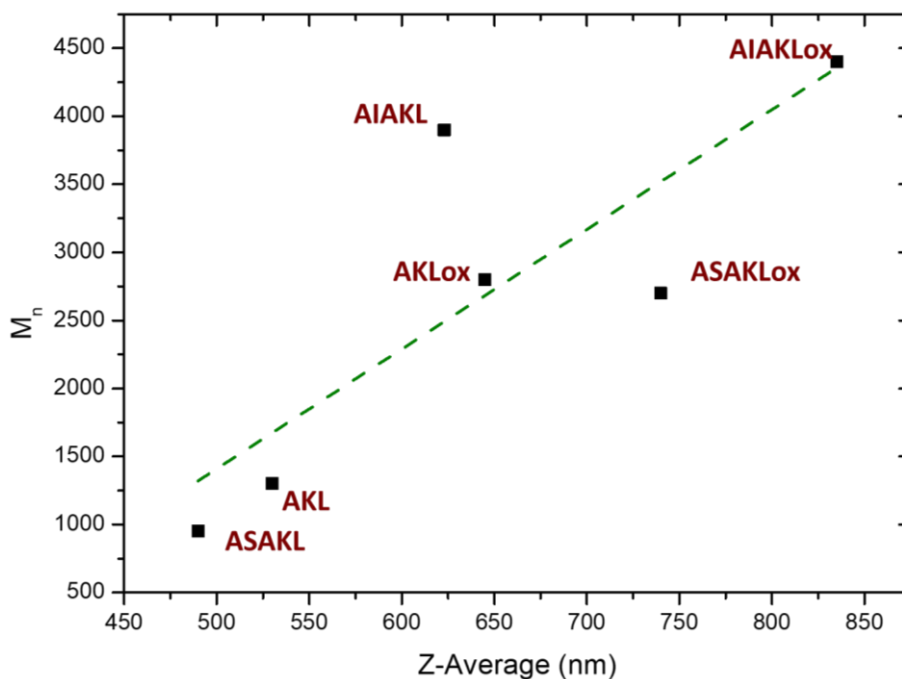


Figure 4.5. Correlation of the molecular weight of lignin preparations with the size of the resulting KLNPs via the hydrotropic method.

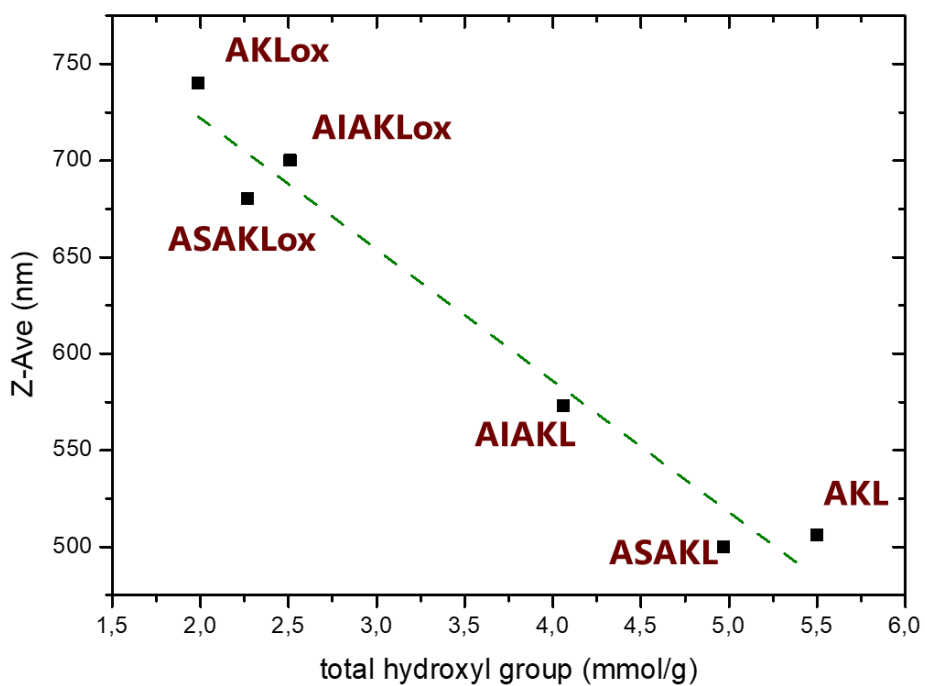


Figure 4.6. Correlation of the hydroxyl group content of lignin preparations with the size of the resulting KLNPs via the hydrotropic method.

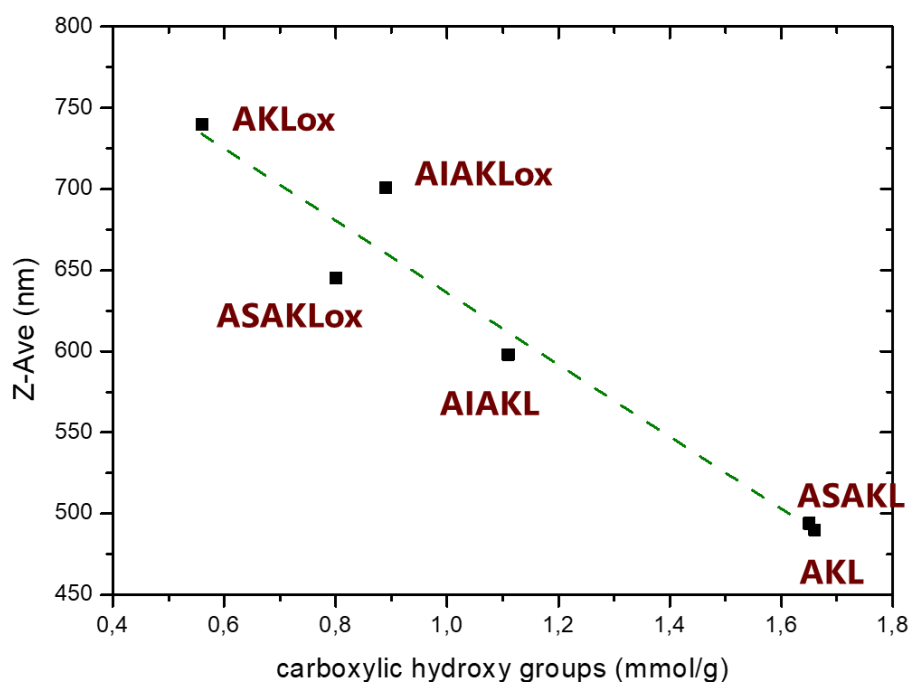


Figure 4.7. Correlation of the carboxylic group content of lignin preparations with the size of the resulting KLNPs via the hydrotropic method.

Firstly, a direct correlation between the molecular weight of lignins with the particles size was demonstrated, as depicted in Fig. 4.5. In particular, lignin preparations characterised by low molecular weights resulted in KLNPs with smaller average diametres than those deriving from lignin with higher molecular weight. This experimental evidence demonstrates the validity of the fractionation as a pre-treatment useful to process technical lignins to tailor the size of the resulting KLNPs. With that respect, a similar effect was extended to the enzymatically modified lignins; in fact, all the laccase-treated lignin preparations revealed higher average diametres than the non-enzymatically modified counterpart. These data were in line with the demonstrated polymerising effect of laccase on lignin. These findings were particularly interesting as, at the best of the knowledge of the writer, no direct correlation with the molecular weight of lignin preparations with the particle size have been reported before.

Secondly, a linear trend was also noticed when the content of carboxylic group had been plotted against the size of KLNPs (Fig. 4.6). The correlation between these two parametres is supported by early results from *Lindström*, demonstrating that the aggregation phenomena of kraft lignin are under control of the degree of deprotonation of carboxylic groups.<sup>111</sup> In fact, at the time, the *Author* claimed that as the degree of deprotonation of carboxylic acids increases, the aggregation of kraft lignin decreases. This correlation was further extended to all the hydroxylated moieties.

Finally, an increasing linear trend relating the content of hydroxylated moieties with the size of the KLNPs was observed (Fig. 4.7). This trend is not surprising since it is now known that the phenomena dominating the aggregation of lignin nanoparticles are mostly related to the weak interactions between lignin domains, the hydrogen bonds deriving from the interactions of hydroxyl groups, and the  $\pi,\pi'$  interactions occurring between aromatic rings.<sup>188,189</sup> Consequently, as unmodified lignin preparations (AKL, AIAKL, and ASAKL) were characterised by higher content of carboxylic acids, they were expected to provide particles with lower average diameters than the modified counterpart. These observations suggested that the rationalisation of the experimental data could not be limited to the intramolecular interactions, but the consideration of the lignin weight should also be taken into consideration. In view of that, an attempt to describe the aggregation mechanism of the samples was made on the basis of the two experimental results:

- The diameter of the LNPs increases with the decrease of the hydroxyl groups content;
- The diameter of the LNPs increases with the molecular weight of the lignin;

The first point depicts a scenario in which, owing to the interactions deriving from hydroxylated moieties, it seems logical that as high the amount of these functional group is, as more packed the lignin molecules in nanoparticles are, resulting in smaller particles. Consequently, this operation is the result of both intermolecular and intramolecular attractions.

The second experimental result can be explained taking into account the polymeric nature of lignin. It is known that kraft lignin is characterised by a folded-branched structure. Moreover, when the lignin is dissolved, the polymeric chains tend to unfold, resulting in a unfolding process in which the single chains interact within each other or with the solvent via intermolecular interactions.

In this context, as lignin preparations used differed for both the molecular weight and the content of hydroxyl groups, it appeared logical that those with lower amounts of hydroxyl groups were less prone to generate interactions. In addition, because of the steric hindrance of lignins, especially of those with high molecular weight, even in the unfolded status in solution, the tendency to re-aggregate was discouraged. In order to consider both these effects, a new parameter, the “*density of hydroxyl groups per chain*” ( $d_{OH}$ ) was introduced. This new variable was calculated as the ratio of the content of total hydroxyl groups per gramme of lignin ( $n_{OH}$ ) and the molecular weight of the lignin sample ( $M_n$ ):

$$d_{OH} = \frac{n_{OH}(\text{mmol/g})}{M_n(\text{u. m. a.})}$$

Calculated  $d_{OH}$  values for the nanosized lignin preparations are reported in Tab.4.5.



Table 4.5.. Calculated density of hydroxyl groups per chain ( $d_{OH}$ ) for the AKL-related lignins used for the preparation of KLNPs.

<i>Sample</i>	<i>dOH</i> ( $\text{mmol}\cdot\text{g}^{-1}\cdot\text{u.m.a.}^{-1}$ )
<i>AKL</i>	$4.2\cdot 10^{-3}$
<i>AKLox</i>	$7.4\cdot 10^{-4}$
<i>AIACL</i>	$1.0\cdot 10^{-3}$
<i>AIAKLox</i>	$5.7\cdot 10^{-4}$
<i>ASAKL</i>	$5.2\cdot 10^{-3}$
<i>ASAKLox</i>	$8.1\cdot 10^{-4}$

Even if linear trends were not denoted while plotting the  $d_{OH}$  versus the average diameter, it was noticed that as high this ratio was, as smaller the size of the particles resulted. For instance, in the case of AKL,  $d_{OH}$  corresponded to  $4.2 \cdot 10^{-3} \text{ mmol}\cdot\text{g}^{-1}\cdot\text{u.m.a.}^{-1}$  (480 nm) while for the enzymatic modified counterpart, AKLox, the value was reduced of almost one order ( $7.4 \cdot 10^{-4} \text{ mmol}\cdot\text{g}^{-1}\cdot\text{u.m.a.}^{-1}$ , 740 nm).

In view of that, it was concluded that as low the amount of hydroxyl group per chain of lignin is, as reduced the amount of possible interactions between chains would result. Consequently, as the number of interactions is correlated with aggregation of lignin to generate nanoparticles, it seemed logical to highlight that when only limited interactions are possible, the compactness as well as the size of the resulting structure would suffer of that. In particular, the less compact the aggregate structure is, the bigger the gap between the interacting lignin chain is, resulting in bigger particles.

### 4.3. Experimental part

Angiosperm Kraft lignin used for this research was supplied by *WestRock Company*, Florence (South Carolina). Sodium tosylate >98% was purchased from *ThermoFisher*. Reagents used for the fractionation of AKL and the enzymatic modifications (reagent grade acetone, glycine puriss. p.a. grade, sodium hydroxide puriss. p.a., hydrochloric acid 37%) were purchased from *ThermoFischer U.S.*. Reagents used for the  $^{31}\text{P}$  NMR characterisation of lignins (N-hydroxy-5-norbornene-2,3-dicarboximide 97%, chromium (III) acetylacetonate 98%, 1-chloro-4,4',5,5'-tetramethyl-1,3,2-dioxaphospholane, deuteriated chloroform, and anhydrous pyridine) were purchased from *Merck*

U.S., while those required for GPC analyses were obtained from *Macron* (dimethylsulphoxide, HPLC grade) and *Merck* (lithium chloride, 98%).

#### ***4.3.1 Isolation of lignin fractions***

Lignin fractions are obtained accordingly to the protocol reported in *Chapter 4* which results in the isolation of acetone soluble and acetone insoluble lignin fractions.

#### ***4.3.2 Enzymatic modification of lignin preparations***

The laccase-catalysed modification of SKL and its fractions is performed using the same experimental protocol reported in *Chapter 4*. The amount of the enzyme is calculated in the same way, according to the content of phenolic hydroxyl groups per gramme of lignin, and by multiplying this value x100.

#### ***4.3.3 Characterisation of lignin preparations***

The characterisation of lignin preparations via  $^{31}\text{P}$  NMR and GPC is performed according to the experimental details reported in *Chapter 4*. For  $^{31}\text{P}$  NMR analyses a 500 MHz nuclear magnetic spectrometre is used (Department of Forest Biomaterials facilities, North Carolina State University, Raleigh, NC, U.S.A.), while GPC analyses are performed with a Shimadzu chromatographer, as previously mentioned in *Chapter 4*.

#### ***4.3.4 Preparation of KLNPs via the hydrotropic method***

KLNPs from KL and its fractions are prepared according to the method reported in *Cailotto* with small modifications.<sup>175</sup> 0.21 g of lignin preparations are dispersed in 10 mL of 2 M sodium tosylate, and the dispersion is stirred overnight in order to implement the solubilisation process in the hydrotropic mixture. The day after, the dispersion is centrifuged (15 minutes, 8000 rpm) and the supernatant is filtrated through a 0.24  $\mu\text{m}$  syringe-filtre. Then, the resulting clear solution is dispersed by dripping in vigorously stirred water, resulting in a 0.5 M final concentration of sodium tosylate. The resulting nanoparticles dispersion is then centrifuged in and the supernatant discharged; the precipitate, which is constituted by nanosized lignin, is washed three times with distilled water. The resulting nanoparticles are then dispersed in distilled water for further characterisations as reported above.

#### ***4.3.5 Characterisation of lignins after fractionation and enzymatic modification***

AKL and its fractions are characterised via  $^{31}\text{P}$  NMR in order to determine the content of the various hydroxylated moieties before and after the enzymatic modification using Argyropoulos' protocol. (see Chapter 4 for experimental details). In order to determine the molecular weight of lignin preparations GPC analyses are performed; the use of a calibration curve made of sulphonated polystyrene permits to correlated the eluograms with the molecular weights. (see Chapter 4 for experimental details).

#### ***4.3.6 Dynamic light scattering analyses (DLS)***

Lignin nanoparticles sizes and distributions determinations are performed using a *Malvern Zetasizer* nanosystem. In particular, after determining the yield of nanoparticles and the concentration of the nanoparticles dispersions, the last are diluted with distilled water in order to obtain a 0.01% m/V dispersion of lignin nanoparticles in water. The DLS analyses of the resulting dispersions are performed in a 1 mL polyethylene cuvettes suitable for the use in UV-vis spectroscopy. The scanning parametres for the instrument are set in the way that the analyses beging after 120 seconds of sample thermosetting at 25°C; the dispersing medium for the nanoparticles is set as “distilled water” and the refractive index for the particles is set as 1.511. Three sets of thirteen scans each are performed per each sample; for each set an average value is automatically calculated by the instrument. Finally, an average value considering the average data for each of the three sets is calculated obtain the average diametre for the nanoparticles as well as their polydispersity index.

#### ***4.3.7 Zeta-potential analyses ( $\zeta$ -potential)***

Nanoparticles colloidal stability in water is estimated via the determination of their  $\zeta$ -potential. As previously described for DLS, even in this case the determinations are performed using a *Malvern Zetasizer* nanosystem. The same dispersions prepared for DLS analyses are used for the  $\zeta$ -potential analyses; distilled water is selected as dispersing medium and the lignin refractive index (1.511) is set for the measurements. Three sets of ten scans per each nanoparticles dispersion are performed after a thermosetting step at 25°C for 120 seconds; the resulting values represent an average value for each data set. Then, an average value considering the three set is calculated in order to estimate more accurately the  $\zeta$ -potential of the colloidal lignins dispersions.

#### ***4.4 Conclusions***

In this research a strategy permitting to tailor AKL KLNPs properties via the coupling of a series of pre-treatments on AKL prior to the nanosizing step was developed. In particular, a tandem system coupling a fractionation operation with a laccase-based modification of lignin samples was developed. This approach resulted in the isolation of five lignin preparations from AKL (AIAKL, ASAKL, AKLox, AIAKLox, and ASAKLox) which were then nanosized according to the hydrotropic method, a green and sustainable anti-solvent strategy for the preparation of KLNPs. Resulting KLNPs from different AKL preparations differed each from the others in terms of size and hydrophobicity.

From one side, it was demonstrated that by controlling the molecular weight of AKL as well as the content of hydroxylated moieties, it was possible to control the size of KLNPs. With this respect, the effect of laccases was particularly relevant, as it implemented the degree of polymerisation of AKL as well as it reduced the content of hydroxylated moieties. The coupling of the variation of these two factors directly affected the nanoparticles size, which increased if compared to the non-enzymatically modified counterpart.

From the other side, the isolation of lignin preparations characterised by different content in hydroxylated moieties permitted to tailor KLNPs hydrophobicity.

Further morphological analyses of the resulting KLNPs are needed to understand the shape and the real distribution in size of them.

## 5. Creating new networks with laccase: enzymatic deposition of angiosperm Kraft lignin nanoparticles on lignin-rich nanofibrillated cellulose

*In this chapter a strategy to modify the mechanical and the thermal properties of nanofibrillated cellulose-based films (CNFs) with the use of KLNPs was described. CNFs were prepared from a lignin-rich pulp (unbleached pulp) via ultra-grinding. The deposition of KLNPs on CNFs was assisted by the use of laccase, who activated lignin domains in both materials. The casting operation of the films was performed in optimised conditions of consistency, pH, and volume. The resulting films were then characterised via tensile test and thermogravimetric analyses. Implemented plasticity of the CNFs films with enzymatically-deposited KLNPs as well as an enhanced thermal degradability were observed in comparison with the counterpart in which no-enzyme had been used in the casting operations.*

### 5.1. Introduction

Cellulose nanofibrils (CNFs) and lignin nanoparticles (LNPs) are interesting wood-deriving nanosized products finding high-value applications in different fields, from the preparation of advanced films for packaging properties and biomedical applications (for CNFs)<sup>190,191</sup> to the UV-shielding as well as antibacterial properties and as a drug delivery system (for LNPs)<sup>95,178</sup>. In view of these interesting properties, their coupling in new materials could be particularly relevant for various technological applications. In particular, the good filming properties of CNFs with the highly hydrophobic barrier that well dispersed LNPs can create if they are properly dispersed on them, seems in the candidate point of view an interesting starting point for the preparation of new films that can find for packaging applications.

The preparation of advanced composite materials from CNFs with lignin (either residual lignin or colloidal) has been recently reviewed.<sup>192</sup> Moreover, the approaches commonly followed do not involve the formation of additional chemical bonds between cellulose CNFs from bleached pulp with the additional lignin. Only a successful attempt for the creation of a chemical cellulose-lignin network has been recently reported by *Hambardzumyan*. In particular, the creation of a the bond between cellulose and lignin has been achieved via radical coupling profiting of the action of the well-known *Fenton* chemistry.<sup>193</sup>

The possibility to create a cellulose-lignin network via coupling opens the possibility to investigate different strategies, more sustainable than the use of *Fenton* reagent, deriving from the use of different reagents inducing the formation of radicals. Among the various radicals generating species for lignin, the use of laccases is a promising approach. In fact, the reactivity of this class of enzymes against lignin and lignin model compounds has been extensively studied, and it is nowadays well-established their mechanism of generating radicals via a two electron transfer mechanism, resulting in the formation of two types of radicals: one on the phenolic position, or on the benzylic carbon.<sup>154,194</sup> The genesis of these laccase-induced radicals is their repolymerization via cross-coupling.<sup>130</sup>

In view of that, in this chapter the possibility of using laccase to graft ween LNPs onto a CNFs matrix via radical coupling is investigated in order to modulate the properties of the final CNFs-based films. In particular, with the aim of facilitate the creation of the network between LNPs and CNFs, CNFs from unbleached pulp (hereafter referred as “CNFs”) have been used because of the presence of residual lignin. The last has been used as a possible bridge between LNPs and the cellulose domain. LNPs arising from different lignin fractions have been studied in the grafting efficiency and the final properties of the LNPs-CNf films.

<sup>31</sup>P NMR as well as GPC have been applied to study the properties of LNPs during the grafting conditions as well as those of the starting materials used for the preparation of CNFs films. DLS and measurement of  $\zeta$ -potential have been considered for the evaluation of the stability of either the LNPs prepared as well as their stability in the casting conditions. Finally, the mechanical and thermal properties of the films have been evaluated.

## **5.2. Results and discussion**

### **5.2.1 Evaluation of KLNPs pH-stability**

Prior to the preparation of CNFs, in order to determine in which pH-range KLNPs could be dispersed with CNFs in order to prevent nanoparticles coalescence or re-dissolution, their pH stability was qualitatively estimated.

The pH stability was determined by comparing the UV-vis spectra of KLNPs dispersions in various buffers. In particular, the base-line of the dispersions in the range between 500 to 700 nm, in which neither lignin nor buffers absorb, was compared. A scattered base, deriving from the existence of undissolved material finely dispersed, was attributed to the presence of KLNPs confirming the stability of the colloidal system at the buffer pH-conditions. The pH range investigated spread from

2 to 10 and allowed to conclude that KLNPs exhibit their greatest stability in acidic conditions (pH<3); these pH-conditions were obtained using a glycine hydrochloride buffer.

### **5.2.2 Preparation of CNFs from unbleached pulp and optimisation of the casting process for the preparation of films**

CNFs from unbleached pulp were used as starting substrate for the deposition of KLNPs in order to profit of the residual lignin linked with the cellulosic fibres. In principle, these lignin domains could interact with the nanosized lignin, after their laccase-catalysed activation, resulting in the generation of the network between the two.

The pulp used to produce CNFs was a technical one, provided by *Westwaco*; the pulp was characterised by a *Klason* lignin content of 21.4% and a Kappa number of 122. These parameters were determined according to standard protocols (Kappa number of pulp, Test Method TAPPI/ANSI T 236 om-13 and *Klason* determination<sup>195</sup>). The mechanical procedure used to shred the cellulosic material was previously reported by *Lavoine* for bleached pulps, and was extended to unbleached pulp.<sup>192</sup> Briefly, the pulp was firstly refined and then nanosized by processing it fifteen times using an ultra-grinder. The content of lignin in the resulting CNFs was re-determined after the nanosizing. With that regard, the *Klason* value remained almost unchanged at 21.2% while, on the other side, Kappa number slightly increased, reaching a value of 134.3. The observed increment was attributed to the nanosizing effect which reasonably implements the ratio of available superficial lignin after the shredding operation. The resulting CNFs, a white gel, were characterised by a solid content, determined by heating at 120°C of 0.98%.

The optimisation of the casting of CNFs films containing KLNPs was then evaluated. In view of that, three parameters were considered: (a) the consistency, (b) the amount of CNFs dispersed to obtain a peelable film, and (c) the casting time.

Owing to the pH stability of KLNPs, which tend to dissolve in mildly acidic medium and above (pH 4), the casting mixture was prepared dispersing the CNFs in a pH 3 glycine hydrochloride buffer. In general, it was observed that films can be obtained from CNFs dispersions with various consistencies; moreover, the concentration of CNFs in the casting mixture plays a pivotal role in the quality of the films. In fact, by casting the same volume of CNFs dispersions with different consistency, it was noticed that films deriving from casting mixtures with consistency higher than 0.37% wt. were wrinkled; however, when consistencies lower than 0.17% wt. were used, the resulting films were

fragile and difficult to peel. Therefore, the optimum consistency for the casting was identified in 0.27% wt..

In order to optimise the amount of CNFs dispersions to cast films that can be conveniently peeled, different volumes of a 0.27% consistency casting mixture were poured in 9 cm diameter *Petri*-dishes and the quality of the films was compared after 48 hours of casting. With that regard, it was found that a film which could be peeled required a ratio volume of casting mixture/surface area of the *Petri*-dish of approximately of 0.78 mL/cm<sup>2</sup>. Lower ratios resulted in films difficult to peel.

Lastly, the casting time was critically considered. In particular, by comparing the preparation of films with the same consistency, it was concluded that the optimal casting time ranged between 48 to 72 hours depending on if the sample was cast in a fume hood or not.

### **5.2.3 Preparation of CNFs from unbleached pulp and optimisation of the casting process for the preparation of films**

The previously optimised parameters were then successfully used for the preparation of CNFs films with deposited KLNPs. Loading of KLNPs on CNFs films ranged from 1 to 10% wt. with respect to the solid content in CNFs of the casting mixture. To deposit KLNPs on CNFs, KLNPs from hydrotropic solutions were diluted using a pH 3 glycine hydrochloride buffer solution resulting in dispersions with a final solid content of 5 mg/mL, and then added, in appropriate volume according to the desired final load to the casting mixture. Then, the volume was adjusted, and the resulting mixtures was casted in Plexi-glass *Petri*-dishes in a fume-hood for 48 hours; the resulting films were easily peeled and stored before further characterisations.

To elucidate the phenomena governing the casting of the films, the measurement of the  $\zeta$ -potential of the casting mixture was performed. An aliquot of the casting mixture before and after the addition of KLNPs (10% wt. load) was diluted with distilled water (to a 0.01% wt. concentration) and then analysed. The colloidal stability of the system varied after the addition of LNPs; in particular, an increase of the  $\zeta$ -potential was observed (from -27mV to -17 mV). This variation was attributed to the presence of different types of electrostatic interactions between the additional KLNPs, the residual lignin, and the cellulose nanofibrils. These interactions were considered as primarily responsible for the deposition of LNPs on the CNFs matrix.

In an attempt to characterise the mechanical and thermal properties of the films with deposited LNPs from KL, tensile test and thermogravimetric analyses (TGA) were performed on the films. The



numerical data for the tensile tests are reported in Table 5.1, while in Fig. 5.1 A a comparison of the stress/strain curves for CNFs with increasing loadings of KLNPs is depicted.

In order to plot the stress versus strain curves, the percentage strain was calculated by dividing the elongation of the sample (mm) for its initial length (mm) according to the following formula:

$$\text{strain (\%)} = \frac{\text{elongation (mm)} - \text{sample length (mm)}}{\text{sample length (mm)}} \cdot 100$$

While the stress (MPa) was determined dividing the load (kN) applied for the cross-sectional area ( $\text{m}^2$ ) of the sample according to the following formula:

$$\text{stress (MPa)} = \frac{\text{load (kN)} \cdot 1000}{\text{cross - sectional area (m}^2\text{)}} \cdot 100$$

These data were plotted and the *Young* moduli for the films were determined as the slope of the initial linear step of the curve. Their values were normalised by the basis-weight, obtaining the specific *Young* moduli (SYM). From each sample three specimens were analysed and the average value as well as the standard deviation were calculated, as reported in Tab.5.1. The determination of the tensile strength (TS) was also performed on the films according to the following equation:

$$\text{tensile strength (MPa/m}^2\text{)} = \frac{\text{maximum load applied (MPa)}}{\text{cross - sectional area (m}^2\text{)}} \cdot 100$$

where the maximum load applied corresponds to the force applied to the sample at the breaking point (MPa).

*Table 5.1.* Tensile properties for the CNFs films with deposited KLNPs from AKL and its acetone insoluble (AIAKL) and soluble (ASAKL) fractions.

<i>Sample</i>	<b>Specific Young Modulus (GPa·m<sup>2</sup>/kg)</b>	<b>Standard deviation</b>	<b>Tensile strength (MPa/m<sup>2</sup>)</b>	<b>Standard deviation</b>
<b>CNFs</b>	1.6	0.2	42	8
<b>CNFs+AKL1%</b>	1.15	0.03	46	3
<b>CNFs+AKL2%</b>	1.7	0.5	38	7
<b>CNFs+AKL4%</b>	1.3	0.2	50	3
<b>CNFs+AKL5%</b>	1.18	0.02	47	4
<b>CNFs+AKL10%</b>	1.4	0.5	48.3	0.3
<b>CNFs+AIAKL1%</b>	1.4	0.4	30	5
<b>CNFs+AIAKL2%</b>	0.8	0.2	45	15
<b>CNFs+AIAKL4%</b>	1.4	0.2	37	10
<b>CNFs+AIAKL5%</b>	0.73	0.06	27	8
<b>CNFs+AIAKL10%</b>	1.7	0.5	35	12
<b>CNFs+ASAKL1%</b>	1.3	0.2	33	3
<b>CNFs+ASAKL2%</b>	1.90	0.05	32	1
<b>CNFs+ASAKL4%</b>	1.5	0.4	39	7
<b>CNFs+ASAKL5%</b>	1.2	0.3	36	3
<b>CNFs+ASAKL10%</b>	0.02	0.01	4	3

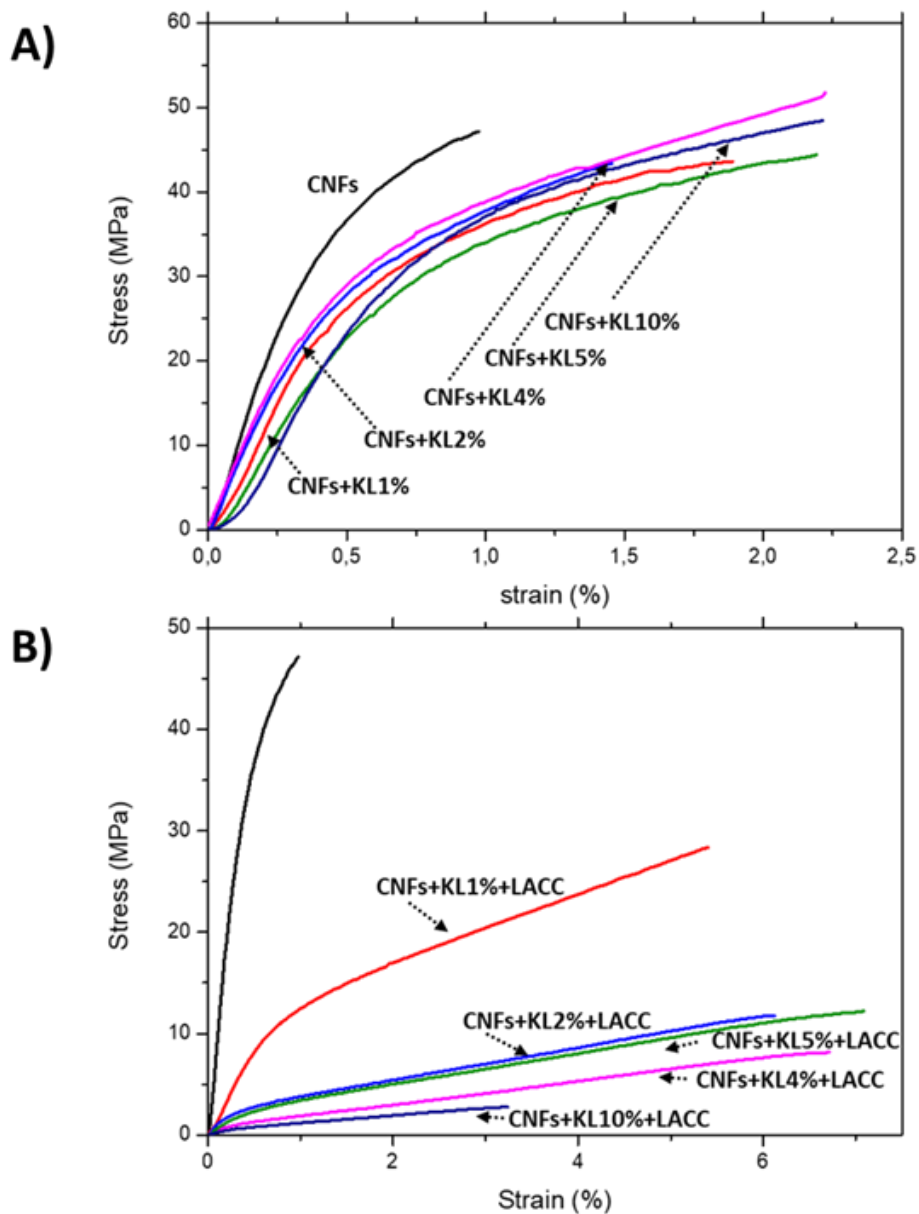


Figure 5.1. Strain vs. stress curves for the CNFs films with (A) deposited, and (B) enzymatically deposited AKL KLNPs.

The SYM for the prepared composites varied between 1.15 and 1.7 GPa·m<sup>2</sup>/kg; by comparing these value with the SYM of a film made of pristine CNFs (1.6 GPa·m<sup>2</sup>/kg) it can be concluded that the addition of KLNPs modify the SYM. The same conclusion was extended to the TS of the samples; in fact, their values oscillated between 38 and 50 MPa/m<sup>2</sup> (for pristine CNFs, 42 MPa/m<sup>2</sup>). To rationalise the variation of the mechanical properties of the films, the effect of intramolecular forces between the various domains in the films was considered. In particular, aggregation phenomena, due to hydrogen bonds as well as *van der Waals* forces and  $\pi$ - $\pi$ ' interactions are believed to favour the interaction of

KLNPs with residual lignin. The latter is represented by a deposit on cellulose fibrils of unbleached pulp as micro- and nano-globules.<sup>196</sup> In view of that, these lignin globules can be seen as *germination seeds* on which additional lignin nanoparticles deposit.

An attempt to find a correlation between these properties with the content of KLNPs was made via the plot of either SYM or TS versus the content of KLNPs; unfortunately, no linear trends were noticed. In general, by considering the trends for the data sets, it could be argued that the lack of linearity for the samples would derive from an intrinsic lack of homogeneity in the casted polymeric material; however, this option was excluded by repeating the measurements in triplicate. Therefore, it was concluded that the load of KLNPs did not linearly modify the properties of the films.

TGA analyses of for the films were performed in nitrogen-inert atmosphere allowing to study the thermal properties of the films. Thermal data for CNFs films with deposited AKL KLNPs are reported on Tab. 5.2.

*Table. 5.2.* Thermal properties for the CNFs films with deposited KLNPs from AKL and its acetone insoluble (AIAKL) and soluble (ASAKL) fractions.

<i>Sample</i>	<b>T<sub>onset</sub> (°C)</b>	<b>DTG (°C)</b>	<b>T(10%) (°C)</b>	<b>char (%)</b>
<b>CNFs+AKL1%</b>	183.3	214.3	203.4	26.9
		237.7		
		314.1		
<b>CNFs+AKL2%</b>	191.8	224.3	209.0	28.0
		245.6		
		323.6		
<b>CNFs+AKL5%</b>	182.8	214.6	202.5	26.4
		235.7		
		318.9		
<b>CNFs+AKL10%</b>	185.9	220.4	211.8	29.3
		246.1		
		324.6		
<b>CNFs+AIAKL1%</b>	185.6	217.2	209.3	26.1
		245.2		
<b>CNFs+AIAKL2%</b>	188.3	219.7	213.5	30.7
		246.0		

<b>CNFs+AIAKL5%</b>	174.5	217.4	216.1	30.4
		240.0		
<b>CNFs+AIAKL10%</b>	188.8	217.9	209.9	30.8
		240.5		
<b>CNFs+ASAKL1%</b>	185.8	214.3	207.5	32.1
		241.5		
		319.3		
<b>CNFs+ASAKL2%</b>	180.6	213.2	206.7	27.4
		234.1		
		321.9		
<b>CNFs+ASAKL5%</b>	191.3	219.0	205.9	33.0
		320.1		
<b>CNFs+ASAKL10%</b>	189.9	232.7	213.4	27.3
		323.0		
<b>CNFs</b>	191.3	213.1	198.9	31.3
		236.5		
<b>AKL</b>	194.0	324.9	230.0	21.8
<b>ASAKL</b>	187.7	327.7	219.8	27.7
<b>AIAKL</b>	192.4	315.4	226.7	25.5
<b>glycine hydrochloride</b>	238.4	257.9	238.8	15.4
<b>laccase</b>	178.3	189.5	177.5	5.8
		218.7		
		238.5		

The onset temperature ( $T_{\text{onset}}$ ) for pristine CNFs and AKL KLNPs corresponded to 191°C and 194°C respectively, while  $T_{\text{onset}}$  for CNFs + AKL KLNPs films ranged between 184 and 191°C, depending on the content of LNPs. These results were unexpectedly not in accordance with the *rule of mixture*, advising that the theoretical  $T_{\text{onset}}$  of the films should range between those of CNFs and AKL KLNP, depending on the composition of the film. Initially, this fact had been attributed to the presence of residual traces of the buffer used to cast the films (glycine hydrochloride); moreover, this hypothesis was excluded after recording the thermogram of glycine hydrochloride. The  $T_{\text{onset}}$  of the amino-acid hydrochloride corresponded to 238°C. Consequently, its contribution was excluded, as it would have

expectedly favoured and incrementation of the  $T_{\text{onset}}$  of the film. Future analyses are still needed to justify this fact.

From the TGA thermograms the ashes content of the samples was also evaluated. This value, corresponding to the residual weight of the sample at 600°C, was used to make correlations with the thermal stability of the sample. With that regard, it can be generally stated that as low the coal content is, as lower the thermal stability of the film is. The ashes content in pristine CNFs was assessed as the 31% wt., while in the case of AKL KLNPs this value corresponded to the 21% wt.. Intermediate values were obtained for CNFs composites with AKL KLNPs, as reported in Tab.5.2. Even if a direct correlation between the stability of the films and the content of added KLNPs was not evident, the decrease in the coal content testified a variation in the thermal stability of the films resulting from the addition of a material less thermally stable. This fact was seen as a confirmed the effective presence of KLNPs on the films and their interaction with the CNFs matrix.

With regard to the obtained results, an attempt to implement the properties of the films via the use of AKL KLNPs from AKL fractions was evaluated. Attempts were made in view of the results previously obtained on KLNPs from AKL fractions, demonstrating the different properties in terms of particles size and the surficial functional groups. CNFs films casted with AIAKL and ASAKL KLNPs were prepared with the same loadings previously considered using AKL KLNPs. pH buffer as well as the casting time remained unvariated. The mechanical and thermal properties of the films were then determined via tensile test and TGA, and the characterisation data are reported in Tab. 5.1 and 5.2. Unfortunately, even if different chemical and physical properties were previously highlighted for the KLNPs deriving from AKL fractions, no relevant beneficial effect on their use was demonstrated for the preparation of CNFs films with KLNPs.

#### **5.2.4 Laccase-mediated deposition of KLNPs**

The bond-creating effect resulting from the laccase incubation of lignin was previously demonstrated in *Chapter 3*. In that context, condensation reactions involving the formation of new *biphenyl* or *diaryl* structures (5-5' and 4-O-5' units) were suggested as the most probable mechanisms resulting in the polymerisation of the lignin preparations. Consequently, it seemed logical to believe that the deposition of AKL KLNPs could be promoted by the use of laccase resulting the formation of a networks.

To evaluate this possibility, the same protocol used for the preparation of previous CNFs films with KLNPs was considered with the addition of the enzyme. Fig.5.2 summarise the protocol.

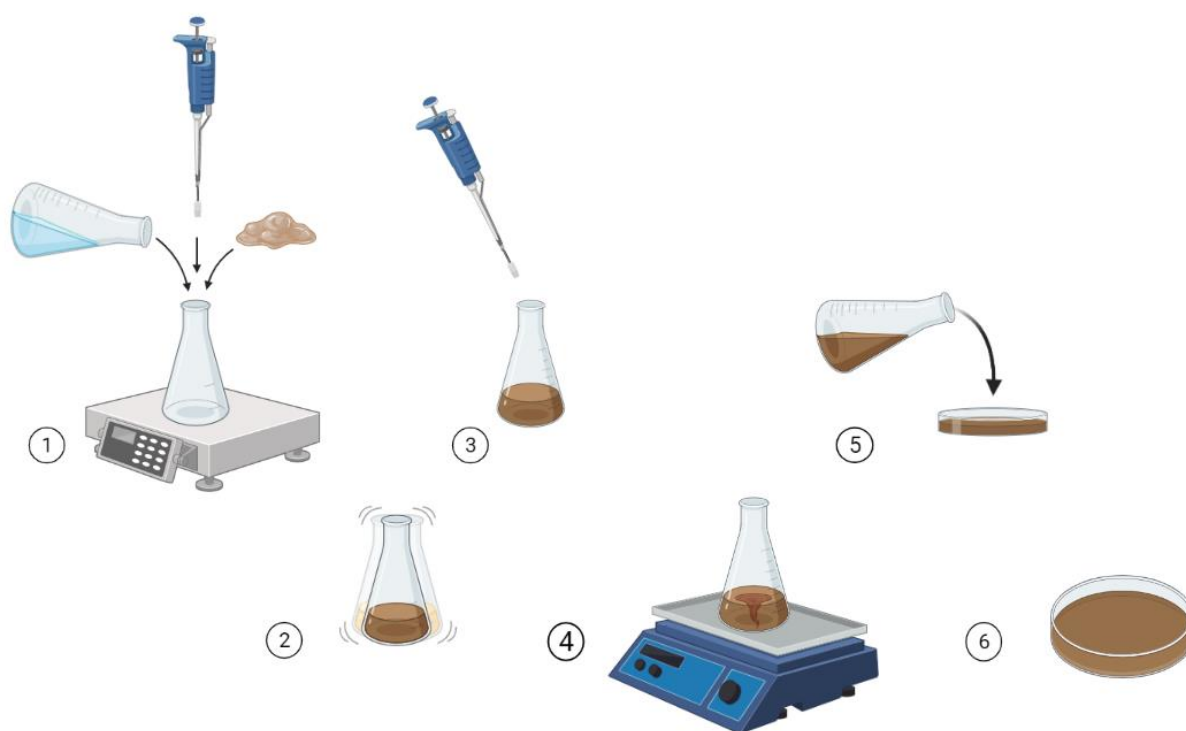


*Figure 5.2.* Casting protocol for CNFs films with enzymatically-deposited AKL KLNPs consisting of: (1) dispersion of CNFs and AKL KLNPs in the buffer solution, (2) mixing, (3) addition of the enzyme, (4) extensive aeration of the casting mixture, (5) transfer of the casting mixture in a *Petri-dish*, and (6) casting at room temperature for 48 hours.

Moreover, due to the statical condition at which casting process occurs, as well as the long time required to obtain films from CNFs mixtures, which can result in the enzyme deactivation, the amount of enzyme to introduce in the system was carefully considered. In fact, to ensure the highest reactivity for the enzyme during the casting operation, a volume of laccase solution equivalent to that of AKL KLNPs was used while preparing the casting mixture. In order to maximise the laccase activity, the buffer solution used was saturated with oxygen (air bubbling for 4 hours at room temperature) and, prior to the casting, the casting mixture was stirred at room temperature for 1 hour favouring the formation of the reactive species on both AKL KLNPs and residual lignin (aryloxy radicals and the corresponding mesomeric forms) that can later interact.

### 5.2.5 Preparation of CNFs from unbleached pulp with enzymatically deposited KLNPs

The casting of films with enzymatically deposited KLNPs was studied by evaluating the colloidal stability (via  $\zeta$ -potential measurement) of the casting mixture before and after the addition of the enzyme. Practically, an aliquot of CNFs casting mixture with 10% wt. AKL KLNPs was diluted with distilled water and then the  $\zeta$ -potential of the mixture was determined before and after the addition of the enzyme. Interestingly, and differently from what had been previously observed for the casting of CNFs films with deposited AKL KLNPs, the enzymatic deposition of AKL KLNPs resulted in a decrease of the  $\zeta$ -potential. In particular, the numerical values changed from -27 mV for just the CNFs, to -16 mV for the CNFs with KL LNPs, and -29 mV for CNFs with KL LNPs and laccase. This evidence testified an incrementation in the colloidal stability of the casting mixture. The observed increase in colloidal stability deriving from the addition of laccase to the casting mixture suggested to exclude the presence of electrostatic interactions favouring the deposition of AKL KLNPs on the CNFs matrix, leading to the enzyme the pivotal role of favouring the deposition of the nanoparticles.

The mechanical properties of the so prepared films were evaluated via tensile test. SYM lied between 0.18 and 0.017 GPa·m<sup>2</sup>/kg, while for the TS varied between 22 and 5 MPa/m<sup>2</sup>; full numerical data are reported in Tab. 5.3.

Table 5.3. Tensile properties for the CNFs films with laccase-mediated deposited KLNPs from

<i>Sample</i>	AKL.			
	<b>Specific Young Modulus (GPa·m<sup>2</sup>/kg)</b>	<b>Standard deviation</b>	<b>Tensile strength (MPa/m<sup>2</sup>)</b>	<b>Standard deviation</b>
<b>CNFs</b>	1,6	0,2	42	8
<b>CNFs+AKL1%+LAC</b>	0,180	0,004	22,0	8
<b>CNFs+AKL2%+LAC</b>	0,038	0,008	10,0	2
<b>CNFs+AKL4%+LAC</b>	0,05	0,03	7	1
<b>CNFs+AKL5%+LAC</b>	0,041	0,004	10	3
<b>CNFs+AKL10%+LAC</b>	0,017	0,003	5	2



The comparison of the data reported in Tab.5.3 with those in Tab.5.1 demonstrates that the action of the enzyme results in a difference up to two orders of magnitude in the mechanical properties of the films. These findings are in accordance with previous observations made by *Rojo* demonstrating that CNFs with high content in residual lignin are characterised by lower mechanical properties if compared to CNFs from bleached pulp.<sup>196</sup>

In order to rationalise these results, the effect of laccase on either cellulose (from CNFs) or lignin (from both CNFs or residual lignin) was considered.

With respect to the cellulosic domains, their partial enzyme-mediated degradation seemed reasonable; in fact, it was previously reported that laccases, in presence of a redox mediator, can cause chemical modification of cellulosic fibres.<sup>197–199</sup> Even if no redox mediators were introduced on purpose in the casting mixture, apocynin and vanillin, which have been confirmed as metabolites of laccase-based KL digestion, are expected to be present in the casting environment. Reasonably, these compounds are expected to act as radical mediators. The alterations of cellulose fibres caused by laccase has been critically considered by *Quintana*, who recently demonstrated that these modifications do not affect cellulose fibres strength; in fact, in the opinion of the *Author*, the formation of hemiacetalic structures (from aldehydic carbonyls and hydroxylated cellulose moieties) restores their networks.<sup>199</sup> Moreover, this pathway seemed to be less reasonable during the enzymatic deposition of LNPs, especially if the acidity conditions of the casting as well as the static at which the operation occurs.

With respect to the cellulosic domains modification, owing to the large amount of laccase used during the enzymatic deposition of LNPs, the activation of cellulose resulting in the formation of secondary carbon-radicals cannot be excluded. In fact, *Hüttermann* demonstrated that cellulose can be activated in presence of large excess of laccase.<sup>200</sup> In particular, it was supposed that the resulting cellulose radical species deriving from the enzymatic activation can, in presence of radicalised lignin, resulted in the formation of new types of chemical bond between the two domains. Even if the nature of the bond between cellulose and lignin was not discussed by the *Author*, in the point of view of the writer it is reasonable that the activation of cellulose occurred especially on C2 position, via an hydrogen-atom abstraction. The so formed secondary radical can further interact with activated phenolic moieties of LNPs allowing the grafting via the formation of alkyl-aryl ether bonds. Further analyses of the casting mixture via the use of electron paramagnetic resonance would be able to confirm the formation of radicals on the matrix. In fact, by distinguish those species deriving from cellulose from the lignin-related ones, as well as performing their quantification in time, it would be possible to properly demonstrate the activation of the substrate.

With respect to the effect of laccase on the lignin domains, clear evidence of the transformations occurring on AKL were extensively described on *Chapter 4*, where its enzymatic incubation was carried out prior to the nanosizing operation. Even if in that case the laccase-treatment was applied on dissolved lignin, it is reasonable to expect that a similar effect would result on the surficial hydroxylated moieties on AKL KLNPs because of the laccase specificity for hydroxylated moieties. As these functional groups represent the most relevant sources of hydrogen-bond interactions, which by consequence favour also the compacting of CNFs fibres, their drastic decrease was considered as resulting in a possible weaker structure, driving to a reduction of the mechanical properties of the films.

Attenuated total reflectance (ATR) analyses of films was performed to confirm the described chemical modification deriving from the enzymatic deposition of AKL KLNPs on unbleached CNFs. Moreover, even if the characteristic bands attributed to hydroxyl ( $\sim 3300\text{ cm}^{-1}$ ), methine ( $\sim 2900\text{ cm}^{-1}$ ), and carbonyls ( $\sim 1600 - \sim 1700\text{ cm}^{-1}$ ) groups were clearly noticed in all the spectra, no significant changes could be highlighted from the different samples. Even if ATR data were negative, this fact was not surprising; in fact, the chemical bonds arising from the action of laccase on AKL KLNPs, residual lignin, and cellulose fibres do not differ from those characteristics for lignin which were already available on CNFs from unbleached pulp. In view of implementing the pool of characterisation data for the prepared films future analyses via scanning electron microscopy (SEM) as well x-ray photoelectronic spectroscopy (XPS) would be considered. In particular, SEM would give the possibility to distinguish the structural changes on CNFs fibres as well as the effective deposition of AKL KLNPs, while XPS would provide structural information on the surficial properties of enzymatically modified AKL KLNPs, confirming the possibility of a reduced tendency to form hydrogen bonds.

The TGA analyses of the films was performed accordingly to the approach previously used for CNFs films with deposited AKL KLNPs. A comparison of the thermograms for samples with AKL KLNPs deposited with or without the aid of laccases and the derived counterparts is reported in Fig. 5.3. The numerical data are reported in Tab. 5.4.

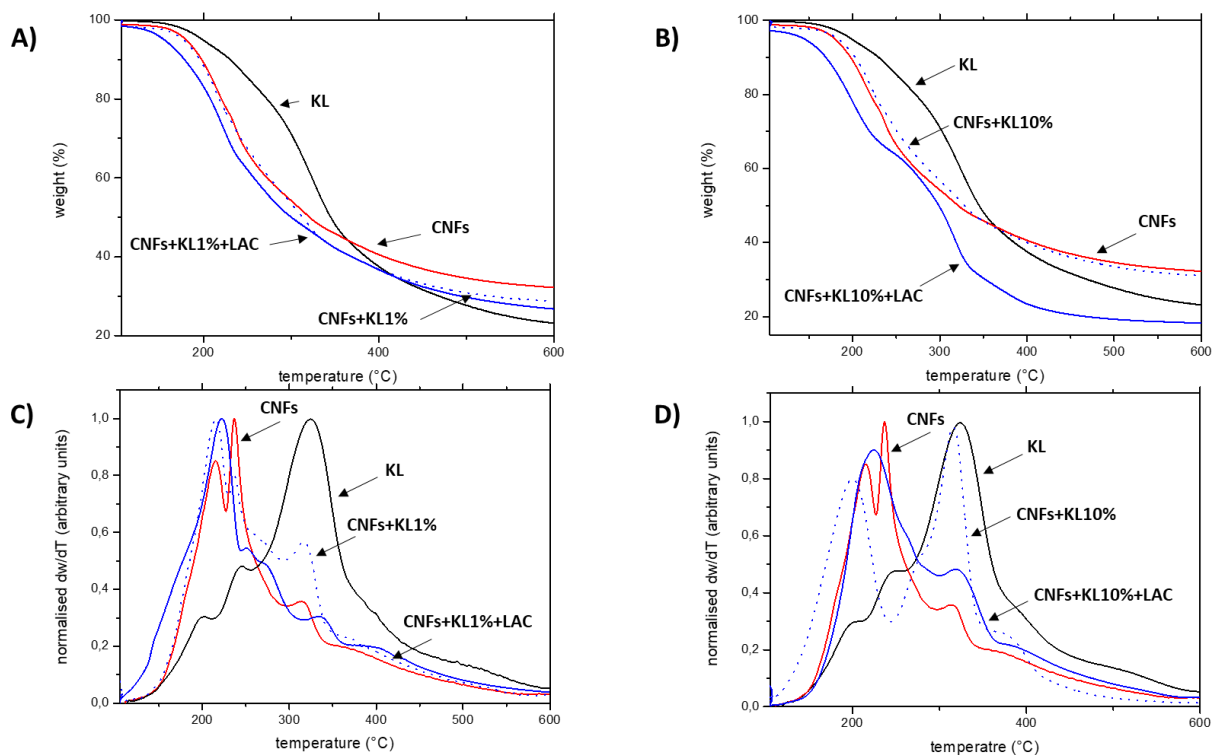


Figure 5.3. Thermograms for CNFs films with 1% wt. and 10% wt. of AKL KLNPs casted with and without laccase and the corresponding derivatives.

Derivatives have been normalised to the maximum of each curve.

Table 5.4. Thermal properties for the CNFs films with deposited KLNPs from AKL and its acetone insoluble (AIAKL) and soluble (ASAKL) fractions.

Sample	$T_{\text{onset}}$ (°C)	DTG (°C)	$T(10\%)$ (°C)	char (%)
<b>CNFs+AKL1%+LAC</b>	171.9	222	185.0	25.8
<b>CNFs+AKL2%+LAC</b>	177.3	221.4	191.0	24.7
		291.7		
<b>CNFs+AKL5%+LAC</b>	168.9	212.9	177.8	19.2
		311.2		
<b>CNFs+AKL10%+LAC</b>	161.4	199.4	183.7	16.0
		317.0		

The ashes content of the samples decreases from 25.8% wt., for the CNFs film loaded with 1% wt. AKL KLNPs, to 16.0% wt. in the case of CNFs film loaded with 10% wt. AKL KLNPs. Interestingly, a decreasing trend was highlighted also for the  $T_{\text{onset}}$ , whose values were respectively 171.9°C and

161.4°C for 1 and 10% wt. KL LNPs. To rule out the possibility that such variation could derive from the presence of residual traces of the enzyme in the films, the  $T_{\text{onset}}$  of laccase was considered. Moreover, owing to the incrementation lack of a distinct peak in the derivative curves corresponding to the degradation of the enzyme, laccase contribution was excluded. In view of that, it was concluded that these data confirmed that a chemical modification occurred in the system. Further analyses are required to better elucidate the effective modifications.

### **5.2.6 On the plasticity of unbleached CNFs films with enzymatically deposited KLNPs**

Interesting considerations can be point out by analysing the elongation to break of the curves plotted in Fig.5.1.A and Fig.5.1.B. In particular, it was observed that if the elongation to break of films casted AKL KLNPs lied between the 1.7 to the 2.1% of the initial length of the samples, the values for the counterparts casted with the enzyme-mediated deposition of KLNPs resulted in elongation to break values ranging from the 5 to the 7% of the initial length. In order to rationalise this enhancement of more than two-times of the plasticity of the films, a self-healing mechanism promoted by the action of laccase was hypothesized. In fact, among the various types of network-restoring interactions, a coupling of mechanical and chemical self-healing seems to be reasonable in this case. Specifically, the lignin-modified CNFs align in an ordered network after the application of the initial strain, and then, the homolytic cleavage of C-C bond in newly formed lignin domains occurs. The regeneration, in this way, is induced via the interaction of radicals already available in the matrix.

The cleavage of the bonds in the films was attributed to the breaking of additional condensed structures deriving from the enzymatic deposition of AKL KLNPs on the CNFs matrix. In particular, due to the expected higher content of 5-5' units in the films with enzymatically deposited AKL KLNPs, the formation of C5 radicals in lignin aromatic rings seemed to the most reasonable hypothesis. In fact, once these radicals are formed, they surrounded by an environment rich in other lignin radicals of different types: (a) radicals already existing in kraft lignin, (b) radicals generated by the mechanical action of CNFs shredding, (c) radicals deriving from the action of laccase stabilised by the surrounding lignin environment. The first type or radicals are of semi-quinone, ortho-quinone and quinone-methide nature and derive from either chemical pulping operations or mechanical treatments on AKL KLNPs.<sup>201-203</sup> The existence of the second type of radical was reported by *Solala*, who demonstrated that the mechanical action of ultra-grinding, used to obtain the CNFs, results also in the formation of cellulose radicals which are stabilised by radical transfer to lignin with the generation of new additional aryloxy radicals.<sup>204</sup> Finally, for the last type of radicals it seems

reasonable to believe that owing to the high amount of laccase used; it was also possible to confirm the existence of other type of aryloxy radicals on terminal units of lignin, which are stabilised via their resonance forms. In general, the majority of these radical is stable and they remain trapped in lignin for long periods of time.<sup>203</sup> In the view of that, in the elongation conditions, the formation of a self-healing via radical coupling of vicinal lignin radicals is expected to occur. The mechanism is schematised in Fig. 5.4, starting from a for a *biphenyl* unit.

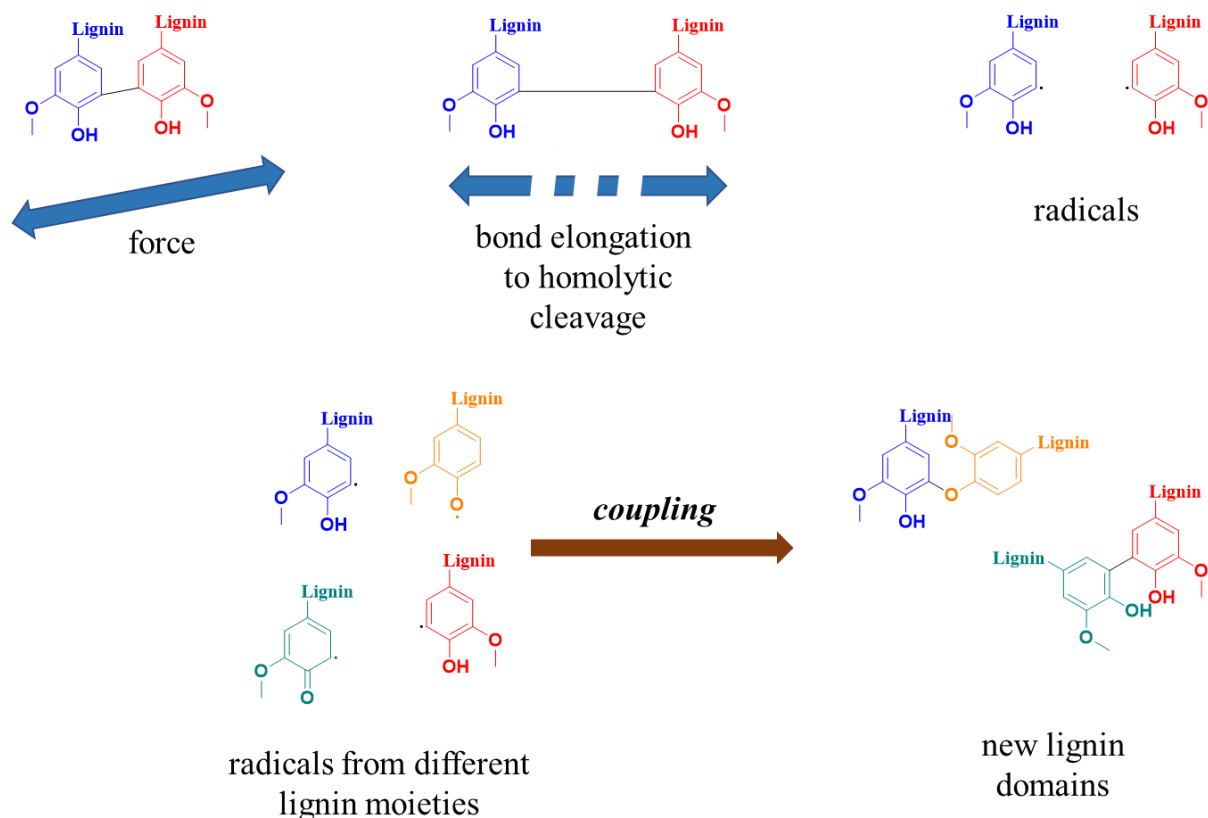


*Figure 5.4.* Suggested self-healing mechanism for a biphenyl unit. The application of a strain alongside the C-C bond of a biphenyl (5,5' unit) results in the formation of two radicals which undergo in a radical coupling mechanism with other vicinal radicals.

In conclusion, the reorganization of the network after the break of the bonds results in a higher elongation of the films, as demonstrated by the elongated plastic-deformation area of the stress vs. strain curves. The same type of mechanism cannot take place for the counterpart of samples casted with no enzyme, as no radicals would appear in the system. Further computational determinations would be necessary to demonstrate the reactivity of the mentioned radicals.

### **5.3. Experimental part**

Hydrochloric acid, glycine, sodium p-toluene sulfonate were purchased from *ThermoFischer*. Angiosperm Kraft Lignin was the same used for Chapter five. Unbleached gymnosperm pulp was kindly supplied by *WestRock Company*, Florence (South Carolina); laccase has been kindly provided by *MetGen*, Kaarina, Finland.

#### **5.3.1 Preparation of AKL KLNPs**

Nanoparticles from AKL and its fractions are prepared according to the hydrotropic mixture previously described in *Chapter 4*. Differently from that, once AKL KLNPs are obtained after the washing operations, they are made up to volume with pH 3 glycine hydrochloride buffer and are stored in dark bottles in a refrigerator prior to their incorporation in CNFs films.

#### **5.3.2 Preparation of CNFs from unbleached pulp via ultra-grinding**

The experimental procedure followed for the preparation of CNFs is in accordance with a protocol previously optimised in *Lavoine's group* with small modifications.<sup>192</sup> In brief, 240 g of never dried gymnosperm unbleached pulp (K number 122, *Klason* content of lignin 21.4%, consistency 18.2%) are refined following TAPPI-248 standard procedure. The beating equipment employed for the operation is a *PFI-MILL beating machine No. 312* (performances adjusted by the *Norwegian Pulp and Paper Institute*). Refining is performed at 5000 revolutions. The resulting refined pulp is diluted with distilled water to a final consistency of 0.67% using a *Durant blender* and grinded using an ultra-fine friction grinder (MKCA6-5J, *Masuko Sangyo Co. Ltd.*, Japan). Nanosizing shredding is achieved using silicon carbide based non-porous grinding stones with a rotation speed of 1200 rpm; during the operation the gap clearance between the stones varies between -50 to -250  $\mu\text{m}$ . The total energy consumption has been 0.18kWh/kg.

#### **5.3.3 Casting operation of CNFs films with deposited AKL KLNPs**

The following procedure is used for each of CNFs films with deposited LNPs. In a 100 mL beaker 7.44 g of CNFs dispersion are mixed with 20 mL of 50 mF glycine hydrochloride buffer (pH 3) and the mixture is stirred up to the obtention of a homogeneous CNFs dispersion. Then, the suitable amount of LNPs is added followed by additional glycine hydrochloride buffer up to 50 mL. Finally,

after stirring at room temperature using a magnetic stirrer, the mixture is poured in a polyacrylate *Petri* dish with internal diameter of 9 cm and is casted in a fume-hood for 72 hours. The resulting films are peeled and stored in plastic bags up to the moment of further analyses.

#### **5.3.4 Casting operation of CNFs films with enzymatically deposited AKL KLNPs**

The following procedure is used for each of CNFs films with enzymatically deposited LNPs. In a 100 mL beaker 7.44 g of CNFs dispersion are mixed with 20 mL of air-saturated 50 mF glycine hydrochloride buffer (pH 3) and the mixture is stirred up to the obtention of an homogeneous CNFs dispersion. Then, the suitable amount of KLNPs is added followed by laccase and additional glycine hydrochloride buffer up to 50 mL. The mixture is stirred at room temperature in order to favour the activation of lignin. Finally, the mixture is poured in a polyacrylate *Petri* dish with internal diameter of 9 cm and casted in a fume-hood for 72 hours. The resulting films are peeled and stored in plastic bags up to the moment of further analyses.

#### **5.3.5 Thermogravimetric analyses of CNFs films with AKL KLNPs**

Thermogravimetric analyses of the films are performed using a *TGAQ500* thermobalance. 8-10 mg aliquots of each films are analysed under a continuous 60 mL/min flow of nitrogen. The samples are heated from 35 to 600°C with a 10°C/min ramp. Weight-temperature curves are plotted and the corresponding  $T_{\text{onset}}$ , temperature for weight loss of 10%, and the coal content are determined from them. Derivative curves are calculated by deriving the weight with respect to the temperature.

#### **5.3.6 Tensile tests for CNFs films with AKL KLNPs**

Tensile tests are performed on the CNFs films (samples were cut in rectangular shape of 10 x 40 mm with thickness varying between 20 to 120  $\mu\text{m}$ ) using an *Instron 4443* machine. Before the analyses, the samples are set for 48 h in a humidity and temperature controlled environment (23°C, 50% of humidity). The tests are performed at the same conditions of humidity and temperature using a load cell of 0.5 kN with crosshead speed of 2.54 mm/min.

Strain vs. stress curves are plotted and the corresponding elongation moduli are determined in the initial elastic region (at low strain values). Three samples per film are analysed per sample.

## 5.4. Conclusions

In this study a protocol to link AKL KLNPs on lignin-rich CNFs was designed and developed in order to obtain peelable films in relatively short casting times. In particular, the deposition was studied with and without laccase, an enzyme capable to activate lignin moieties via the formation of aryloxy radicals. The formation of these radical species was supposed to drive to radical-coupling mechanisms, as previously demonstrated in *Chapter three*, resulting into the creation of new lignin-lignin domains.

The characterisation of the resulting films was performed in order to elucidate the differences between the deposition of KLNPs with and without laccase.  $\zeta$ -potential determination of the casting mixtures demonstrated that electrostatic interactions were the most reasonable phenomena occurring during the casting of CNFs films with AKL KLNPs without laccase; differently, in the case of films casted with laccase, the higher colloidal stability of the dispersions testified that these interactions were less probable. These results supported the hypothesis of the radical-coupling mechanism.

The determination of the mechanical properties of the films demonstrated that the presence of AKL KLNPs decreased both SYM and TI for the CNFs films; however, an implementation in the plasticity of the was observed. Finally, thermogravimetric analyses highlighted the role of the enzymatic deposition of LNPs on the implementation of the thermal degradability of the films.

All in one, it was demonstrated the beneficial effect of enzymatic deposition of AKL KLNPs on lignin-rich CNFs films, with respect to the possibility to modify the film properties. Moreover, further investigation elucidating both the nanostructure of these films, as well as the enzymatic deposition of AKL KLNPs, are required.





## References

- (1) Freudenberg, K.; Neish, A. C. *Constitution and Biosynthesis of Lignin*; Molecular Biology, Biochemistry, and Biophysics; Springer-Verlag: New York, 1968; Vol. 2.
- (2) Pettersen, R. C. *The Chemical Composition of Wood in "The Chemistry of Solid Wood"*; Advances in Chemistry; American Chemical Society: Washington D. C., 1984; Vol. 207.
- (3) Wilkie, J. S. Carl Nägeli, The Fine Structure of Living Matter, *Nature* 1961, 190 (4782), 1145–1150.
- (4) Meyer, H. K.; Misch, L., *Helvetica Chimica Acta* 1937, 20 (1), 232–244.
- (5) Zugenmaier, P., *Crystalline Cellulose and Derivatives*; Springer, Berlin, Heidelberg: Berlin, Heidelberg, 2008.
- (6) Malm, C. J. *Svensk Papperstid.* 1961, pp 740–743.
- (7) V.F. Volkov; Kuznetsova, E. P.; Kornilova, Y. I. *Tr. Sev.-Zapad. Zaoch. Politekh. Inst.* 1969, p 84.
- (8) de Carvalho Oliveira, G.; Filho, G. R.; Vieira, J. G.; De Assunção, R. M. N.; da Silva Meireles, C.; Cerqueira, D. A.; de Oliveira, R. J.; Silva, W. G.; de Castro Motta, L. A., *Journal of Applied Polymer Science* 2010, 118 (3), 1380–1385. <https://doi.org/10.1002/app.32477>.
- (9) Nasatto, P. L.; Pignon, F.; Silveira, J. L. M.; Duarte, M. E. R.; Nosedá, M. D.; Rinaudo, M., *Polymers* 2015, 7 (5), 777–803.
- (10) *Handbook of Wood Chemistry and Wood Composites*, 2nd ed.; Rowell, R. M., Ed.; CRC Press: Boca Raton, 2012.
- (11) Sjostrom, E. *Wood Chemistry: Fundamentals and Applications*, II.; Academic Press: New York, 1993.
- (12) Klason, P. Beitrag Zur Kenntnis Der Konstitution Des Fichtenholz-Lignins. *Berichte der deutschen chemischen Gesellschaft (A and B Series)* 1920, 53 (9), 1864–1873.
- (13) Brauns, F. E., *Journal of the American Chemical Society*, 1939, 61 (8), 2120–2127.
- (14) Buchanan, M. A.; Brauns, F. E.; Leaf, R. L., *Journal of the American Chemical Society* 1949, 71 (4), 1297–1299.
- (15) Adler, E.; Pepper, J. M.; Eriksoo, E., *Industrial and Engineering Chemistry*, 1957, 49 (9), 1391–1392.
- (16) Pepper, J. M.; Baylis, P. E. T.; Adler, E., *Canadian Journal of Chemistry* 1959, 37, 1241–12448.
- (17) Freudenberg, K. *Pure and Applied Chemistry* 1962, 5 (1–2), 9–20.
- (18) Freudenberg, K., *Science* 1965, 148 (3670), 595–600.

- (19) Karhunen, P.; Rummakko, P.; Sipilä, J.; Brunow, G.; Kilpeläinen, *Tetrahedron Letters* 1995, 36 (1), 169–170.
- (20) Karhunen, P.; Rummakko, P.; Sipilä, J.; Brunow, G.; Kilpeläinen, *Tetrahedron Letters* 1995, 36 (25), 4501–4504.
- (21) Karhunen, P.; Rummakko, P.; Pajunen, A.; Brunow, G. Synthesis and Crystal Structure Determination of Model Compounds for the Dibenzodioxocine Structure Occurring in Wood Lignins. *Journal of Chemical Society, Perkin Transactions 1* 1996, No. 18, 2303–2308.
- (22) Crestini, C.; Melone, F.; Sette, M.; Saladino, R., *Biomacromolecules* 2011, 12 (11), 3928–3935.
- (23) Browning, B. L. *Methods of Wood Chemistry*, Interscience.; New York, 1967; Vol. 2.
- (24) Willstätter, R.; Zechmeister, L., *Berichte der deutschen chemischen Gesellschaft* 1913, 46 (2), 2401–2412.
- (25) Wald, W. J.; Ritchie, P. F.; Purves, C. B., *Journal of the American Chemical Society*, 1947, 69 (6), 1371–1377.
- (26) Freudenberg, K.; Zocher, H.; Dürr, W. Weitere, *Berichte der deutschen chemischen Gesellschaft (A and B Series)* 1929, 62 (7), 1814–1823.
- (27) Freudenberg, K.; Zechmeister, L., *Progress in the Chemistry of Organic Natural Products*; Springer-Verlag: Wien, 1954; Vol. 11.
- (28) Wise, L. E.; Peterson, F. C.; Harlow, W. M., *Industrial and Engineering Chemistry Anal. Ed.* 1939, 11 (1).
- (29) Bjorkman, A., *Svensk Pappersit.* 1956, pp 477–485.
- (30) Bjorkman, A., *Svensk Pappersit.* 1957, pp 243–251.
- (31) Kirk, T. K.; Chang, H., *Holtzforschung* 1974, 28 (6), 217–222.
- (32) Kirk, T. K., *Holtzforschung* 1975, 29 (3).
- (33) Sjostrom, E. *Wood Chemistry: Fundamentals and Applications*, II.; Academic Press: New York, 1993.
- (34) Willstätter, R.; Kalb, L., *Berichte der deutschen chemischen Gesellschaft (A and B Series)* 1922, 55 (8), 2637–2652.
- (35) Pearl, I. A. *Chemistry of Lignin*; Marcel Dekker: New York, 1967.
- (36) Bjorkman, A., *Svensk Pappersit.* 1957, pp 329–335.
- (37) S. Y. Lin; Carlton, W. D. *Methods in Lignin Chemistry*; Springer Series in Wood Science; Springer, Berlin, Heidelberg, 1992.
- (38) Freudenberg, K., *Angewandte Chemie* 1939, 52 (20), 362–363.

- (39) Freudenberg, K.; Lautsch, W., *Naturwissenschaften* 1939, 27 (14), 227–228.
- (40) Freudenberg, K.; Lautsch, W.; Engler, K., *Berichte der deutschen chemischen Gesellschaft (A and B Series)* 1940, 73 (3), 167–171.
- (41) Creighton, R. H. J.; Hibbert, H., *Journal of the American Chemical Society* 1944, 66 (1), 37–38.
- (42) Creighton, R. H. J.; Gibbs, R. D.; Hibbert, H., *Journal of the American Chemical Society* 1944, 66 (1), 32–37.
- (43) Higuchi, T.; Ito, Y.; Shimada, M.; Kawamura, I., *Phytochemistry* 1967, 6 (11), 1551–1556.
- (44) Freudenberg, K.; Janson, A.; Knopf, E.; Haag, A., *Berichte der deutschen chemischen Gesellschaft (A and B Series)* 1936, 69 (6), 1415–1425.
- (45) Larsson, S.; Miksche, G. E., *Acta Chemica Scandinavica* 21, 1970, 1970.
- (46) Sjostrom, E.; Raimo, A. *Analytical Methods in Wood Chemistry, Pulping, and Papermaking*; Springer Series in Wood Science; Springer-Verlag: Berlin, Heidelberg, 1999.
- (47) Lapiere, C.; Monties, B.; Rolando, C., *Holtzforschung* 1986, 40 (2), 113–118.
- (48) Lapiere, C.; Monties, B.; Rolando, C., *Holtzforschung* 1986, 40 (1), 47–50.
- (49) Lapiere, C.; Rolando, C., *Holtzforschung* 1988, 42 (1), 1–4.
- (50) Lundquist, K. Proton (1H) NMR Spectroscopy. In *Methods in Lignin Chemistry*; Lin, S. Y., Dence, C. W., Eds.; Springer Series in Wood Science; Springer: Berlin, Heidelberg, 1992; pp 242–249.
- (51) Robert, D. Carbon-13 Nuclear Magnetic Resonance Spectrometry. In *Methods in Lignin Chemistry*; Lin, S. Y., Dence, C. W., Eds.; Springer Series in Wood Science; Springer: Berlin, Heidelberg, 1992; pp 250–273.
- (52) Chen, C.-L.; Robert, D. Characterization of Lignin by 1H and 13C NMR Spectroscopy. In *Methods in Enzymology*; Biomass Part B: Lignin, Pectin, and Chitin; Academic Press, 1988; Vol. 161, pp 137–174.
- (53) Kim, H.; Ralph, J., *Organic and Biomolecular Chemistry* 2010, 8 (3), 576–591.
- (54) Ralph, J. NMR of Lignins in *“Lignin and Lignans”* Ed. Heitner C., Dimmel D., and Schmidt J.; CRC Press, 2010.
- (55) Ede, R. M.; Brunow, G., *Journal of Organic Chemistry* 1992, 57 (5), 1477–1480.
- (56) Kilpelainen, I.; Sipilae, J.; Brunow, G.; Lundquist, K.; Ede, R. M., *Journal of Agricultural and Food Chem.* 1994, 42 (12), 2790–2794.
- (57) Ede, R. M.; Ralph, J.; Torr, K. M.; Watson, B., *Holtzforschung* 1996, 50 (2), 161–164.

- (58) Ralph, J.; Hatfield, R. D.; Grabber, J. H.; Jung, H.-J. G.; Quideau, S.; Helm, R. F. Cell Wall Cross-Linking in Grasses by Ferulates and Diferulates. In *Lignin and Lignan Biosynthesis*; ACS Symposium Series; American Chemical Society, Washington, D.C., 1998; Vol. 697 209–236.
- (59) Lapiere, C.; Guittet, E., *Holtzforschung* 1983, 37 (5), 217–224.
- (60) Lapiere, C.; Monties, B.; Guittet, E.; Lallemand, J.-Y., *Holtzforschung* 1987, 41 (1), 51–58.
- (61) Archipov, Y.; Argyropoulos, D. S.; Bolker, H. I.; Heitner, C., *Journal of Wood Chemistry and Technology* 1991, 11 (2), 137–157.
- (62) Argyropoulos, D. S.; Heitner, C.; Morin, F. G., *Holtzforschung* 1992, 46 (3), 211–218.
- (63) Argyropoulos, D. S.; Bolker, H. I.; Heitner, C.; Archipov, Y., *Journal of Wood Chemistry and Technology* 1993, 13 (2), 187–212.
- (64) Argyropoulos, D. S.; Heitner, C., *Holtzforschung* 1994, 48 (s1), 112–116.
- (65) Granata, A.; Argyropoulos, D. S., *Journal of Agricultural and Food Chemistry* 1995, 43 (6), 1538–1544.
- (66) Meng, X.; Crestini, C.; Ben, H.; Hao, N.; Pu, Y.; Ragauskas, A. J.; Argyropoulos, D. S., *Nature Protocols* 2019, 14 (9), 2627–2647.
- (67) Argyropoulos, D. S.; Pajer, N.; Crestini, C., *Journal of Visualized Experiments* 2021, No. 174, e62696.
- (68) Gierer, J., *Journal of Wood Science and Technology* 1985, 19 (4), 289–312.
- (69) Gierer, J., *Journal of Wood Science and Technology*. 1986, 20 (1), 1–33.
- (70) Gratzl, J. S.; Chen, C.-L. Chemistry of Pulping: Lignin Reactions. In *Lignin: Historical, Biological, and Materials Perspectives*; ACS Symposium Series; American Chemical Society, Washington, D.C., 1999; Vol. 742, pp 392–421.
- (71) Gierer, J., *Svensk Papperstidn* 74, 117–127.
- (72) Marton, J., Reactions in Alkaline Pulp. In “*Lignins: occurrence, formation, structure and reactions*” edited by Sarkanen K.V. and Ludwig C.H.; Wiley-Interscience: New York, 1971; pp 639–694.
- (73) Falkehag, S. I.; Marton, J.; Adler, E. Chromophores in Kraft Lignin. In *Lignin Structure and Reactions*; Marton, J., Ed.; American Chemical Society: Washington, D.C., 1966; Vol. 59, pp 75–89.
- (74) Crestini, C.; Lange, H.; Sette, M.; Argyropoulos, D. S., *Green Chem.* 2017, 19 (17), 4104–4121.

- (75) Lange, H.; Rulli, F.; Crestini, C., *ACS Sustainable Chemistry and Engineering* 2016, 4 (10), 5167–5180.
- (76) Keyoumu, A.; Sjö Dahl, R.; Henriksson, G.; Ek, M.; Gellerstedt, G.; Lindström, M. E., *Industrial Crops and Products* 2004, 20 (2), 143–150.
- (77) Nadányi, R.; Ház, A.; Lisý, A.; Jablonský, M.; Šurina, I.; Majová, V.; Baco, A., *Energies* 2022, 15 (18), 6520.
- (78) Väisänen, T.; Das, O.; Tomppo, L., *Journal of Cleaner Production* 2017, 149, 582–596.
- (79) Collard, F.-X.; Blin, J., *Renewable and Sustainable Energy Reviews* 2014, 38, 594–608.
- (80) Weissermel, K.; Arpe, H. J. Benzene Derivatives in “Industrial Organic Chemistry.” In *Industrial Organic Chemistry*; John Wiley & Sons, Ltd, 2003; pp 337–385.
- (81) Zakzeski, J.; Bruijninx, P. C. A.; Jongerius, A. L.; Weckhuysen, B. M., *Chemical Reviews* 2010, 110 (6), 3552–3599.
- (82) Wang, Y.-Y.; Wyman, C. E.; Cai, C. M.; Ragauskas, A. J., *ACS Applied Polymer Materials* 2019, 1 (7), 1672–1679.
- (83) Mahmood, N.; Yuan, Z.; Schmidt, J.; (Charles) Xu, C., *Bioresource Technology* 2013, 139, 13–20.
- (84) Kumar, M.; Hietala, M.; Oksman, K., *Frontiers in Materials* 2019, 6.
- (85) Svinterikos, E.; Zuburtikudis, I.; Al-Marzouqi, M. Electrospun Lignin-Derived Carbon Micro- and Nanofibers: A Review on Precursors, Properties, and Applications. *ACS Sustainable Chemistry and Engineering* 2020, 8 (37), 13868–13893.
- (86) Rezanowich, A.; Yean, W. Q.; Goring, D. A., *Journal of Applied Polymer Science* 1964, 8 (4), 1801–1812.
- (87) Frangville, C.; Rutkevičius, M.; Richter, A. P.; Velev, O. D.; Stoyanov, S. D.; Paunov, V. N., *ChemPhysChem* 2012, 13 (18), 4235–4243.
- (88) Richter, A. P.; Brown, J. S.; Bharti, B.; Wang, A.; Gangwal, S.; Houck, K.; Cohen Hubal, E. A.; Paunov, V. N.; Stoyanov, S. D.; Velev, O. D., *Nature Nanotechnology* 2015, 10 (9), 817–823.
- (89) Yang, W.; Owczarek, J. S.; Fortunati, E.; Kozanecki, M.; Mazzaglia, A.; Balestra, G. M.; Kenny, J. M.; Torre, L.; Puglia, D., *Industrial Crops and Products* 2016, 94, 800–811.
- (90) Yang, W.; Fortunati, E.; Bertoglio, F.; Owczarek, J. S.; Bruni, G.; Kozanecki, M.; Kenny, J. M.; Torre, L.; Visai, L.; Puglia, D., *Carbohydrate Polymers* 2018, 181, 275–284.
- (91) Domenek, S.; Louaifi, A.; Guinault, A.; Baumberger, S., *Journal of Polymers and the Environment* 2013, 21 (3), 692–701.

- (92) Tian, D.; Hu, J.; Bao, J.; Chandra, R. P.; Saddler, J. N.; Lu, C., *Biotechnology for Biofuels* 2017, *10* (1), 192.
- (93) Figueiredo, P.; Lintinen, K.; Kiriazis, A.; Hynninen, V.; Liu, Z.; Bauleth-Ramos, T.; Rahikkala, A.; Correia, A.; Kohout, T.; Sarmiento, B.; Yli-Kauhaluoma, J.; Hirvonen, J.; Ikkala, O.; Kostiaainen, M. A.; Santos, H. A., *Biomaterials* 2017, *121*, 97–108.
- (94) Lievonen, M.; José Valle-Delgado, J.; Mattinen, M.-L.; Hult, E.-L.; Lintinen, K.; A. Kostiaainen, M.; Paananen, A.; R. Szilvay, G.; Setälä, H.; Österberg, M., *Green Chemistry* 2016, *18* (5), 1416–1422.
- (95) Sipponen, M. H.; Lange, H.; Crestini, C.; Henn, A.; Österberg, M., *ChemSusChem* 2019, *12* (10), 2039–2054.
- (96) Feldman, D., *Journal of Macromolecular Science, Part A* 2016, *53* (6), 382–387.
- (97) Xing, Q.; Buono, P.; Ruch, D.; Dubois, P.; Wu, L.; Wang, W.-J., *ACS Sustainable Chemistry and Engineering* 2019, *7* (4), 4147–4157.
- (98) Zhao, W.; Simmons, B.; Singh, S.; Ragauskas, A.; Cheng, G., *Green Chemistry* 2016, *18* (21), 5693–5700.
- (99) Beisl, S.; Miltner, A.; Friedl, A., *International Journal of Molecular Sciences* 2017, *18* (6), 1244.
- (100) Iravani, S.; Varma, R. S., *Green Chemistry* 2020, *22* (3), 612–636.
- (101) Richter, A. P.; Bharti, B.; Armstrong, H. B.; Brown, J. S.; Plemmons, D.; Paunov, V. N.; Stoyanov, S. D.; Velev, O. D., *Langmuir* 2016, *32* (25), 6468–6477.
- (102) Qian, Y.; Deng, Y.; Qiu, X.; Li, H.; Yang, D., *Green Chemistry* 2014, *16* (4), 2156–2163.
- (103) Gigli, M.; Cailotto, S.; Crestini, C. 9 New Perspectives in Lignin Valorization: Lignin-Derived Nanostructures. In *Biorefinery: From Biomass to Chemicals and Fuels*; De Gruyter, 2021; pp 265–320.
- (104) Lu, Q.; Zhu, M.; Zu, Y.; Liu, W.; Yang, L.; Zhang, Y.; Zhao, X.; Zhang, X.; Zhang, X.; Li, W., *Food Chemistry* 2012, *135* (1), 63–67.
- (105) Nair, S. S.; Sharma, S.; Pu, Y.; Sun, Q.; Pan, S.; Zhu, J. Y.; Deng, Y.; Ragauskas, A. J., *ChemSusChem* 2014, *7* (12), 3513–3520.
- (106) E. Nypelö, T.; A. Carrillo, C.; J. Rojas, O., *Soft Matter* 2015, *11* (10), 2046–2054.
- (107) Gilca, I. A.; Popa, V. I.; Crestini, C., *Ultrasonics Sonochemistry* 2015, *23*, 369–375.
- (108) Gonugunta, P.; Vivekanandhan, S.; Mohanty, A. K.; Misra, M., *World Journal of Nano Science and Engineering* 2012, *02* (03), 148–153.

- (109) Li, H.; Deng, Y.; Liu, B.; Ren, Y.; Liang, J.; Qian, Y.; Qiu, X.; Li, C.; Zheng, D., *ACS Sustainable Chemistry and Engineering* 2016, 4 (4), 1946–1953.
- (110) Rangan, A.; Manchiganti, M. V.; Thilaividankan, R. M.; Kestur, S. G.; Menon, R., *Industrial Crops and Products* 2017, 103, 152–160.
- (111) Lindströmn, T., *Colloid & Polymer Sci* 1979, 257 (3), 277–285.
- (112) Käärik, A. A., 5 - Decomposition of Wood. In *Biology of Plant Litter Decomposition*; Dickinson, C. H., Pugh, G. J. F., Eds.; Academic Press, 1974; pp 129–174.
- (113) Kirk, T. K.; Moore, W. E., *Wood and fibre* 1972, 4, 72–79.
- (114) Kirk, T. K.; Highley, L., *Phytopathology* 1973, 63, 1338–1342.
- (115) Ander, P.; Eriksson, K. E. Selective Degradation of Wood Components by White-Rot Fungi, *Physiologia Plantarum* 1977, 41, 239–248.
- (116) Ishikawa, H. W.; Schubert, W. F.; Nord, F. F., *Archives of Biochemistry and Biophysics* 1963, 100, 131–139.
- (117) Ishikawa, H. W.; Schubert, W. F.; Nord, F. F., *Archives of Biochemistry and Biophysics* 1963, 100, 140–149.
- (118) Kirk, T. K.; Chang, H., *Holtzforschung* 1975, 29 (2), 56–64.
- (119) Kirk, T. K.; Adler, E., *Acta Chimica Scandinavica* 1970, 24, 3379–3390.
- (120) Ander, P.; Eriksson, K. E., *Progresses in Industrial Microbiology* 1978, 14, 1–58.
- (121) Kawakami, H., *Mokuzai Gakkaishi* 1976, 22, 252–257.
- (122) Odier, E.; Monties, B., *Annales de Microbiologie de l'Institut Pasteur* 1978, 129A, 361–377.
- (123) Deschamps, A. M.; Mahoudeau, G.; Lebeault, J. M. Fast, *European Journal of Applied Microbiology and Biotechnology* 1980, 9, 45–51.
- (124) Baldrian, P., *FEMS Microbiology Reviews* 2006, 30 (2), 215–242.
- (125) Agrawal, K.; Chaturvedi, V.; Verma, P., *Bioresources and Bioprocessing* 2018, 5 (1), 4.
- (126) Nakamura, T. *Biochimica et Biophysica Acta* 1958, 30, 44–52.
- (127) Solomon, E. I.; Sundaram, U. M.; Machonkin, T. E., *Chemical Reviews* 1996, 96 (7), 2563–2606.
- (128) Shleev, S. V.; Morozova, O. V.; Nikitina, O. V.; Gorshina, E. S.; Rusinova, T. V.; Serezhenkov, V. A.; Burbaev, D. S.; Gazaryan, I. G.; Yaropolov, A. I., *Biochimie* 2004, 86 (9), 693–703.
- (129) Thurston, C. F. Y., *Microbiology* 1994 140 (1), 19–26.
- (130) Munk, L.; Sitarz, A. K.; Kalyani, D. C.; Mikkelsen, J. D.; Meyer, A. S., *Biotechnology Advances* 2015, 33 (1), 13–24. <https://doi.org/10.1016/j.biotechadv.2014.12.008>.



- (131) Becconsall, S.; Clough, S.; Scott, G. Electron Magnetic Resonance Study of Free Phenoxy-Radicals. *Proc. Chem. Soc.* 1959, 3, 308–309.
- (132) Benfield, G.; Bocks, S. M.; Bromley, K.; Brown, B. R., *Phytochemistry* 1964, 3 (1), 79–88.
- (133) Fahraeus, G.; Junggren, H. *Biochimica et Biophysica Acta* 1959, 46, 22–32.
- (134) Kirk, T. K.; Harkin, J. M.; Cowling, E. B., *Biochimica et Biophysica Acta* 1968, 165, 145–163.
- (135) Kawai, S.; Umezawa, T.; Higuchi, T., *Archives of Biochemistry and Biophysics* 1988, 262 (1), 111–117.
- (136) Kawai, S.; Ohashi, H.; Hirai, T.; Okuyama, H.; Higuchi, T., *Mokuzai Gakkaishi* 1993, 39 (1), 98–102.
- (137) Gierer, J., *Journal of Wood Science and Technology* 1980, 14 (4), 241–266.
- (138) Gellerstedt, G.; Lindfors, E.-L., *Holtzforschung* 1984, 38 (3), 151–158.
- (139) Eriksson, T.; Gierer, J., *Journal of Wood Chemistry and Technology* 1985, 5 (1), 53–84.
- (140) Crestini, C.; Argyropoulos, D. S., *Bioorganic & Medicinal Chemistry* 1998, 6 (11), 2161–2169.
- (141) Lundquist, K.; Kristersson, P., *Biochemical Journal* 1985, 229 (1), 277–279.
- (142) Kersten, P. J.; Kalyanaraman, B.; Hammel, K. E.; Reinhammar, B.; Kirk, T. K., *Biochemical Journal* 1990, 268 (2), 475–480.
- (143) Bao, W.; O'Malley, D. M.; Whetten, R.; Sederoff, R. R., *Science* 1993, 260 (5108), 672–674.
- (144) Kondo, R.; Iimori, T.; Imamura, H.; Nishida, T., *Journal of Biotechnology* 1990, 13 (2), 181–188.
- (145) Xia, Z.; Yoshida, T.; Funaoka, M., *Biotechnology Letters* 2003, 25 (1), 9–12.
- (146) Bourbonnais, R.; Paice, M. G., *FEBS Letters* 1990, 267 (1), 99–102.
- (147) Rochefort, D.; Leech, D.; Bourbonnais, R., *Green Chemistry* 2004, 6 (1), 14–24.
- (148) Camarero, S.; Ibarra, D.; Martínez, M. J.; Martínez, Á. T., *Applied and Environmental Microbiology* 2005, 71 (4), 1775–1784.
- (149) Bourbonnais, R.; Paice, M. G., *Applied Microbiology and Biotechnology* 1992, 36 (6), 823–827.
- (150) Bourbonnais, R.; Leech, D.; Paice, M. G., *Biochimica et Biophysica Acta (BBA) - General Subjects* 1998, 1379 (3), 381–390.
- (151) Potthast, A.; Rosenau, T.; Chen, C.-L.; Gratzl, J. S., *Journal of Organic Chemistry* 1995, 60 (14), 4320–4321.
- (152) Fabbrini, M.; Galli, C.; Gentili, P.; Macchitella, D., *Tetrahedron Letters* 2001, 42 (43), 7551–7553.

- (153) Fabbrini, M.; Galli, C.; Gentili, P., *Journal of Molecular Catalysis B: Enzymatic* 2002, 16 (5), 231–240.
- (154) Crestini, C.; Jurasek, L.; Argyropoulos, D. S., *Chemistry – A European Journal* 2003, 9 (21), 5371–5378.
- (155) Kawai, S.; Umezawa, T.; Shimada, M.; Higuchi, T.; Koide, K.; Nishida, T.; Morohoshi, N.; Haraguchi, T. *Mokuzai Gakkaishi* 1987, 33, 792–797.
- (156) Lahive, C. W.; Kamer, P. C. J.; Lancefield, C. S.; Deuss, P. J., *ChemSusChem* 2020, 13 (17), 4238–4265.
- (157) Vignali, E.; Gigli, M.; Cailotto, S.; Pollegioni, L.; Rosini, E.; Crestini, C., *ChemSusChem* 2022, 15 (20), e202201147.
- (158) Cui, C.; Sun, R.; Argyropoulos, D.S., *ACS Sustainable Chemistry & Engineering* 2014, 2 (4), 959–968.
- (159) Merle, G.; Brunel, L.; Tingry, S.; Cretin, M.; Rolland, M.; Servat, K.; Jolival, C.; Innocent, C.; Seta, P., *Materials Science and Engineering: C* 2008, 28 (5), 932–938.
- (160) Hassan, M. M.; Elshafei, A. M.; Haroun, B. M.; Elsayed, M. A.; Othman, A. M., 2012, 12.
- (161) Ike, P. T. L.; Moreira, A. C.; de Almeida, F. G.; Ferreira, D.; Birolli, W. G.; Porto, A. L. M.; Souza, D. H. F., *SpringerPlus* 2015, 4 (1), 654.
- (162) Christopher, L. P.; Yao, B.; Ji, Y., *Frontiers in Energy Research* 2014, 2.
- (163) Sun, Y.; Liu, Z.-L.; Hu, B.-Y.; Chen, Q.-J.; Yang, A.-Z.; Wang, Q.-Y.; Li, X.-F.; Zhang, J.-Y.; Zhang, G.-Q.; Zhao, Y.-C., *Frontiers in Microbiology* 2021, 12.
- (164) Johannes, C.; Majcherczyk, A., *Journal of Biotechnology* 2000, 78 (2), 193–199.
- (165) Childs, R. E.; Bardsley, W. G., *Biochemical Journal* 1975, 145 (1), 93–103.
- (166) Ishihara, T.; Miyazaki, M., *Mokuzai Gakkaishi* 1974, 20 (1), 39–41.
- (167) Koetsier, M. J.; Visser, J.; Iancu, S. L.; Kabel, M. A.; Frommhagen, M.; Gruppen, H.; Lange, H.; Crestini, C.; Benjelloun-Mlayah, B. Polypeptides Having Demethylating Activity, December 29, 2016. <https://patentscope.wipo.int/search/en/detail.jsf?docId=WO2016207351> (accessed 2022-11-25).
- (168) Ragnar, M.; Lindgren, C. T.; Nilvebrant, N.-O., *Journal of Wood Chemistry and Technology* 2000, 20 (3), 277–305.
- (169) Caldwell, E. S.; Steelink, C., *Biochimica et Biophysica Acta (BBA) - General Subjects* 1969, 184 (2), 420–431.
- (170) Krisnangkura, K.; Gold, M. H., *Holtzforschung* 1979, 33 (5), 174–176.

- (171) Ikeda, R.; Sugihara, J.; Uyama, H.; Kobayashi, S., *Polymer International* 1998, 47 (3), 295–301.
- (172) Adler, E.; Hernestam, S., *Acta Chemica Scandinavica* 1955, 9, 319–334.
- (173) Guerra, A.; Gaspar, A. R.; Contreras, S.; Lucia, L. A.; Crestini, C.; Argyropoulos, D. S., *Phytochemistry* 2007, 68 (20), 2570–2583.
- (174) Low, L. E.; Teh, K. C.; Siva, S. P.; Chew, I. M. L.; Mwangi, W. W.; Chew, C. L.; Goh, B.-H.; Chan, E. S.; Tey, B. T., *Environmental Nanotechnology, Monitoring & Management* 2021, 15, 100398.
- (175) Cailotto, S.; Gigli, M.; Bonini, M.; Rigoni, F.; Crestini, C., *ChemSusChem* 2020, 13 (17), 4759–4767.
- (176) Tranchimand, S.; Tron, T.; Gaudin, C.; Iacazio, G., *Synthetic Communications* 2006, 36 (5), 587–597.
- (177) Ahvazi, B. C.; Crestini, C.; Argyropoulos, D. S., *Journal of Agricultural and Food Chemistry* 1999, 47 (1), 190–201.
- (178) Tang, Q.; Qian, Y.; Yang, D.; Qiu, X.; Qin, Y.; Zhou, M., *Polymers* 2020, 12 (11), 2471.
- (179) Qian, Y.; Zhong, X.; Li, Y.; Qiu, X., *Industrial Crops and Products* 2017, 101, 54–60.
- (180) Yearla, S. R.; Padmasree, K., *Journal of Experimental Nanoscience* 2016, 11 (4), 289–302.
- (181) Leskinen, T.; Smyth, M.; Xiao, Y.; Lintinen, K.; Mattinen, M.-L.; Kostianen, M. A.; Oinas, P.; Österberg, M., *Nordic Pulp & Paper Research Journal* 2017, 32 (4), 586–596.
- (182) Ma, Q.; Chen, L.; Wang, R.; Yang, R.; Zhu, J. Y., *Holzforschung* 2018, 72 (11), 933–942.
- (183) Ma, Q.; Zhu, J.; Gleisner, R.; Yang, R.; Zhu, J. Y., *ACS Sustainable Chemistry and Engineering* 2018, 6 (11), 14480–14489.
- (184) Brauns, F. E. *The Chemistry of Lignin*, I.; Academic Press: New York, 1952.
- (185) Traynard, P.; Eymery, A., *Holzforschung* 1955, 9 (6), 172–177.
- (186) Migita, N.; Nakano, J.; Ito, Y., *Journal of the Japanese Forestry Society* 1954, 36 (11), 343–
- (187) Migita, N.; Nakano, J.; Hirai, S.; Takatsuka, C., *Sen'i Gakkaishi* 1956, 12 (9), 632–638.
- (188) Qiu, X.; Kong, Q.; Zhou, M.; Yang, D., *Journal of Physical Chemistry B* 2010, 114 (48), 15857–15861.
- (189) Deng, Y.; Feng, X.; Zhou, M.; Qian, Y.; Yu, H.; Qiu, X., *Biomacromolecules* 2011, 12 (4), 1116–1125.
- (190) Boufi, S.; González, I.; Delgado-Aguilar, M.; Tarrès, Q.; Pèlach, M. À.; Mutjé, P., *Carbohydrate Polymers* 2016, 154, 151–166.

- (191) Du, H.; Liu, W.; Zhang, M.; Si, C.; Zhang, X.; Li, B., *Carbohydrate Polymers* 2019, 209, 130–144.
- (192) Trovagunta, R.; Kelley, S. S.; Lavoine, N., *Cellulose* 2021, 28 (18), 11329–11344.
- (193) Hambardzumyan, A.; Foulon, L.; Bercu, N. B.; Pernes, M.; Maigret, J. E.; Molinari, M.; Chabbert, B.; Aguié-Béghin, V., *Chemical Engineering Journal* 2015, 264, 780–788.
- (194) Dean, J. F. D.; Eriksson, K.-E. L., *Holtzforschung* 1994, 48 (s1), 21–33.
- (195) Kirk, T. K.; Obst, J. R. Lignin Determination. In *Methods in Enzymology; Biomass Part B: Lignin, Pectin, and Chitin*; Academic Press, 1988; Vol. 161, pp 87–101.
- (196) Rojo, E.; Peresin, M. S.; Sampson, W. W.; Hoeger, I. C.; Vartiainen, J.; Laine, J.; Rojas, O. J., *Green Chemistry* 2015, 17 (3), 1853–1866.
- (197) Patel, I.; Ludwig, R.; Haltrich, D.; Rosenau, T.; Potthast, A., 11th EWLP, Hamburg, Germany, August 16–19, 2010. 2011, 65 (4), 475–481.
- (198) Jaušovec, D.; Vogrinčič, R.; Kokol, V., *Carbohydrate Polymers* 2015, 116, 74–85.
- (199) Quintana, E.; Roncero, M. B.; Vidal, T.; Valls, C., *Carbohydrate Polymers* 2017, 157, 1488–1495.
- (200) Hüttermann, A.; Majcherczyk, A.; Braun-Lüllemann, A.; Mai, C.; Fastenrath, M.; Kharazipour, A.; Hüttermann, J.; Hüttermann, A. H., *Naturwissenschaften* 2000, 87 (12), 539–541.
- (201) Steelink, C.; Reid, T.; Tollin, G., *Journal of the American Chemical Society* 1963, 85 (24), 4048–4049.
- (202) Steelink, C. Stable Free Radicals in Lignin and Lignin Oxidation Products. In *Lignin Structure and Reactions*; Advances in Chemistry; American Chemical Society, Washington, D.C., 1966; Vol. 59, pp 51–64.
- (203) Patil, S. V.; Argyropoulos, D. S., *ChemSusChem* 2017, 10 (17), 3284–3303.
- (204) Solala, I.; Volperts, A.; Andersone, A.; Dizhbite, T.; Mironova-Ulmane, N.; Vehniäinen, A.; Pere, J.; Vuorinen, T., *Holtzforschung* 2012, 66 (4), 477–483.



## Acknowledgements

At the end of this journey, I feel the need to say “thank you” to all of those who supported my research activities of the last three years.

First of all, I would like to thank my supervisor, Prof. *Claudia Crestini*. Her patience, teachings, and continuous encouragement to be critical showed me the way for growing up as a good chemist. In addition, her support to my personal interests helped me carrying on with my PhD. I am grateful for her being a continuous source of inspirations during the last years.

My gratitude goes also to Prof. *Dimitris S. Argyropoulos*, who supervised me during my one-year stay in Raleigh at the North Carolina State University Raleigh. His *Wood and Pulping Chemistry* class (and the passion he conveys to his students) opened my eyes on various aspects of Wood Science I had never considered before; in this way, I had the chance to learn a lot. In addition, his wise approach to Science and support of my interests (even if outdated!), made the last year of my PhD way better.

I am also grateful for the help Dr. *Nathalie Lavoine* and her group (*RK, Mirela, Joseph, Emily, and Lisandra*) gave me during my stay at North Carolina State University. In particular, I am especially thankful for Dr. *Lavoine*'s professionalism and continuous incitation to make good Science.

An acknowledgement to Prof. *Stefano Paganelli* and Mrs. *Barbara Vicentini* (Ca' Foscari University of Venice) is also needed. Their being there all the time for sharing good and bad times added an incredible value to my PhD experience.

In addition, I would like to thank all my colleagues at Ca' Foscari University of Venice, who shared with me the pleasures and pains of the PhD life.

I also would like to thank my family: my mother, father and brother. Their support, especially when I thought I could not make it, pushed me through these years to reach this meaningful accomplishment.

During my stay in the United States, I realised that being alone on the other side of the world was not that easy. However, I had the chance to meet so many nice people who made my stay there a nice experience. I will never be able to show them all my gratitude for all I learnt from them and for the way they (maybe unintentionally) helped me growing up as a better person, a better chemist and a better friend. Being away from home helped me put in perspective my professional and personal life and for that I would like to say a general thank you, once again, for the chance.

Last but not least, a well-deserved “thank you” goes also to all close friends, who have always been there when their support was needed and that, I am sure, will be there when I will need support in the future.

